To the Graduate Council:

I am submitting herewith a thesis written by James Edward Doss entitled "Direct Location of Closed-Loop Singular Values in the Linear Quadratic Servo." I have examined the final copy of this thesis for form and content and recommend that it be accepted in partial fulfillment of the requirements for the degree of Master of Science, with a major in Electrical Engineering.

Walter L. Green

Walter L. Green, Major Professor

We have read this thesis and recommend its acceptance:

J Chung

Charles F. Moore

Accepted for the Council:

C W Minkel

Vice Provost
and Dean of The Graduate School

STATEMENT OF PERMISSION TO USE

In presenting this thesis in partial fulfillment of the requirements for a Master's degree at The University of Tennessee, Knoxville, I agree that the Library shall make it available to borrowers under rules of the Library. Brief quotations from this thesis are allowable without special permission, provided that accurate acknowledgment of source is made.

Permission for extensive quotation from or reproduction of this thesis may be granted by my major professor, or in his absence, by the Head of Interlibrary Services when, in the opinion of either, the proposed use of the material is for scholarly purposes. Any copying or use of the material in this thesis for financial gain shall not be allowed without my written permission.

Signature James Edward Voss

Date 11/1/85

DIRECT LOCATION OF CLOSED-LOOP SINGULAR VALUES IN THE LINEAR QUADRATIC SERVO

A Thesis

Presented for the

Master of Science

Degree

The University of Tennessee, Knoxville

James Edward Doss

December 1985

ACKNOWLEDGEMENTS

The author would like to acknowledge the contributions of several people toward the completion of this work. Among them are:

- Dr. Walter L. Green, for allowing me the freedom to develop these ideas in an unrestrained environment, and for serving as my major professor.
- Drs. James C. Hung and Charles F. Moore, who were influential during both my on-campus days and later during the course of this work. Their guidance and knowledge have proven to be a source of continuous inspiration throughout my professional career.
- My children, Katy and Thomas, from whom I stole precious and irretrievable hours during the course of this work.
- Joyce, my wife, best friend, and lifelong partner, who means more to me than words can express.

ABSTRACT

In the last decade, a number of advances have been made in the application of modern control theory to process control problems. However, there are still a number of unresolved issues which hinder further applications of this theory.

One of these issues involves the modification of the conventional linear quadratic (LQ) regulator into a form suitable for command following and disturbance rejection. This modified form, called the LQ servo, has structure and properties which do not allow the singular values of its closed-loop transfer function to be located directly.

In this thesis, an attempt was first made to extend the theoretical tools which allow us to set the LQ regulator singular values into the domain of the LQ servo. However, the available theoretical tools specify only external properties of the LQ regulator, and cannot be extended to modify those internal properties which differentiate the LQ servo from the LQ regulator.

Next, several low-order state space models were developed in which the LQ servo was derived in pure algebraic form. The principal result of this effort was that the LQ servo and LQ regulator share similar s-domain transfer functions, but with different pole and zero locations, depending on the optimal control gain matrix $\underline{G}$ and, ultimately, on the state and control weighting matrices $\underline{Q}$ and $\underline{R}$, respectively.

Finally, a six-state, two-input, two-output LQ servo was investigated for a wide range of control/state weightings. The results of

this numerical study supported the principal result of the aforementioned algebraic study. In addition, the LQ servo demonstrated the following properties:

- For the particular case studied, the closed-loop transfer function singular value break points for both the LQ servo and the LQ regulator occurred at approximately the same frequencies.
- In contrast, singular value rolloff rates for the LQ servo and the LQ regulator were not consistent - a phenomenon which was particularly noticeable in the minimum singular value trends.
- Over the full range of control/state weightings examined in this study, the LQ servo proved remarkably effective in preserving a constant distance (condition number) between the maximum and minimum singular values as a function of frequency.

TABLE OF CONTENTS

LIST OF FIGURES

FIGURE PAGE

CHAPTER I

HISTORICAL PERSPECTIVE AND PREVIOUS RESULTS

A. CHAPTER INTRODUCTION

Over the last decade, some truly remarkable advances have been made in the reintegration of time-domain and frequency-domain concepts in the field of multivariable control system design. A number of researchers who heretofore had interests in only one domain or the other began to realize the importance of the dual-domain approach, since there are a number of extremely useful and attractive design procedures available in each domain (Bryson, 1979).

Since the early sixties, there has been a tremendous amount of research into time-domain state space approaches, particularly those that are used in conjunction with performance optimization based on quadratic performance indices (Athans, 1971; Athans, 1972). However, these techniques were not generally applied (nor were they applicable) in certain areas, such as the process control industry (Tomizuka and Auslander, 1979). Practitioners in the process control field (among them, Seborg and Fisher, 1979; Edgar and Schwanke, 1977; Edgar, 1980; Pearson, 1984; Ray, 1983) pointed out a number of problems with the state-space approach, such as:

1. The need for a reliable full-state model and full-state feedback control for LQ regulators.

2. Lack of stability or performance guarantees upon failure of sensors or actuators, although this problem applies to traditional techniques as well.
3. A lack of knowledge of future values for all reference inputs and disturbances in the open-loop case. (The closed-loop case explicitly handles these situations.)
4. Insufficiency in addressing the issue of state, control, and output constraint handling.
5. An inability to handle process dead time.
6. An inability to associate the state and control weighting matrices in the quadratic performance index with the location of closed-loop poles for the system.
7. Unclear applicability to the true process control regulator problem (rejection of unknown and unmeasurable disturbances) and the true process control servomechanism problem (command following).

These issues, together with research results which address each of them, form the subject of the next two sections of this chapter.

B. OPTIMAL CONTROL - THEORY AND PRACTICE

Appropriate Background Resources

One of the primary goals of this research was to chart a profitable path through the literature for the interested reader. Accordingly, several particularly useful references are noted, due more to their value as research milestones, summaries of past work, or overall readability, as opposed to their utility in resolving some fine theoretical point.

With this goal in mind, one should first establish a solid base of textbook reference material. Some of the earliest and most useful references are now classics in the field, and most are still in print in either revised or updated form. Included in this list are Athans and Falb (1966), Sage (1968), Bryson and Ho (1969, 1975), Meditch (1969), Anderson and Moore (1971), and Kwakernaak and Sivan (1972). Useful references in the broader field of linear systems theory include Horowitz (1963), Chen (1970), Saucedo and Schiring (1968), Brogan (1974), and Kailath (1980). Within the domain of applied optimal estimation techniques, some particularly noteworthy texts are Gelb (1974), Jazwinski (1970), Bierman (1977), Sinha and Kuszta (1983), Brown (1983), and Maybeck (1979). The above lists are in now way inclusive, but they do contain a sufficiently diverse mixture of applied and theoretical concepts such that the practitioner will generally have two or more references available on any given topic.

Optimal Control - The Valuable Results

Note that the majority of these texts were written in the mid to late sixties, or early seventies. The fifteen years from 1960 to 1975 represent the period during which state-space modern control theory underwent its most intensive theoretical development. There were two major driving forces behind this development:

- the discovery of certain mathematical techniques, such as the Discrete Maximum Principle (Pontryagin et al., 1962), Dynamic

Programming (Bellman, 1957), and Kalman and Bucy's original work (Kalman, 1960; Kalman and Bucy, 1961)

- the "space race" of the sixties and the resulting government funding for research and applications in areas of navigation guidance, and control

Interest was also stirred in the chemical process control community, but some early applications (and misapplications) produced disillusionment and disenchantment with the techniques. Some of this disillusionment was based on factors such as those outlined in Section A of this chapter. A great deal of it was also based on fundamental lack of knowledge and expertise on the part of practitioners - a factor still present today, and one which is felt to represent the largest single limitation to application of the techniques.

Despite all of the problems, there seems to be a number of valuable results from modern control theory which have survived:

- most current advanced control strategies are in some way model-based
- in addition to plant outputs, internal states within the process and its model are valuable for estimation and control purposes
- for the case of infinite time horizon, the linear deterministic optimal control is a matrix of constant gains which multiplies the state vector to produce the optimal control policy
- for certain very special cases (e.g., the linear time invariant plant), the state estimation problem and the optimal control

problem are separately solvable via the separation principle (Kalman and Koepcke, 1958; Joseph and Tou, 1961; Gunckel and Franklin, 1963); i.e., the optimal control is a product of the optimal gain matrix and the optimal state estimate, each calculated independently. (Note that this principle is not generally applicable.)

- the optimal state estimator contains an internal model of the process which is driven by the same variables which drive the plant, plus an error term relating differences between the measured output and the estimated output of the system; i.e., the optimal estimator contains within itself a feedback correction and control mechanism
- the optimal linear estimator and optimal linear regulator problems are mathematical duals; results for one problem translate immediately into results for the other problem
- both estimation and control problems necessitate the solution of a matrix Riccati problem, and, as a result, rugged and reliable software for solving matrix Riccati equations has been developed and is widely available (e.g., Alphatech's 1984 LQGALPHA package and Laub's 1984 RICPACK)
- these optimal estimation and control results are generally satisfactory for nonpersistent types of disturbances (e.g., white noise) and must be modified if they are to be satisfactory for nonzero-mean commands or disturbances, such as steps or ramps. (The case of nonwhite disturbances can be handled by incorporating them into a restatement of the overall model.)

- under fairly mild restrictions (linear, time-invariant models), both the optimal state estimator and the optimal control have guarantees of stability

One of the more valuable results of modern control theory is the notion of a Model-Based Compensator (MBC). The MBC has the appealing structure of the combined optimal estimator and controller, i.e., a state estimator containing an internal plant model, followed by an optimal constant-gain state feedback controller. Additional states may be readily appended to the optimal controller so that a form of integral control can be implemented as assurance that persistent disturbances (steps, ramps, etc.) may be suitably rejected. (One such approach is taken by Slader in his 1984 paper making use of the integral of the output states, as described in Kwakernaak and Sivan in the 1972 text.)

Optimal Control - The Caveats

Full-State Models

Truly optimal control demands complete knowledge of a system's internal dynamics - knowledge that we usually obtain in a state-space model of the plant. This requirement for state knowledge poses an impossible situation - no model is a completely accurate representation of the plant. By their very nature, models represent, at best, mathematical abstractions of physical reality - abstractions which are chosen for their tractability and manageable size, as much as for their accuracy at state replication. There are always unmodeled high frequency dynamics, nonlinearities, and distributed parameter processes within a physical system which constrain the accuracy of a linear, lumped-parameter model. At best, a model should be a reasonably accurate representation of the physical system only in certain frequency ranges of interest, and only for certain inputs belonging to the set of inputs felt by the designer to be those most likely to occur. Most of the work of Safanov, Lehtomaki, and others (to be covered in the next section of this chapter) has been directed toward researching the issues raised by incomplete and inaccurate modeling information. The central question here is: "If I can never obtain complete models, then what techniques will allow me the greatest degree of robustness and protection against this modeling ignorance?"

Stability/Performance Guarantees Upon Sensor or Actuator Failure

Much concern in this area has been raised by process control practitioners who are more comfortable with the single-input, single-output connectedness imposed by the pneumatic and electronic single-loop controllers so prevalent in the process industries. Operating strategies for these processes often demand that, due to start-ups or other upset conditions, the control system assume any number of alternate configurations in which one or more single-loop controllers would be placed in manual; i.e., that particular disabled single-loop "box" is not longer actively seeking to resolve the difference between setpoint and process variable. Conversely, the aircraft/aerospace control designers generally offer the pilot only two choices with his controller "box" - either the autopilot is actively engaged, examining all sensor inputs and manipulating aircraft control surfaces, or it is completely disengaged, and all control is in the hands of the pilot.

From the theoretical and practical point of view, there are several issues worthy of study in this arena. Important results on detection of sensor failure from jumplike discontinuities have been achieved by Willsky and are summarized in a survey paper on the entire field of failure detection (Willsky, 1976). Issues related to Linear Quadratic (LQ) controller design via solution of an associated Lyapunov equation have been examined by Harvey (1979), by Lehtomaki (1981), and by Wong and Athans (1977). Indeed, the standard LQ design, while having good robustness properties for a wide range of model mismatches, has been criticized (Rosenbrock and McMorran, 1971) for not having stability guarantees for the zero gain case, i.e., the saturated actuator (such as the hydrodynamic actuator surface in Wong's study (1975) of the Trident depth-keeping controller).

Lack of Knowledge of Future Values of Reference
Inputs and Disturbances in the Open-Loop Case

This problem is one which is of little interest or concern to the process control practitioner. The closed-loop LQG problem contains explicit presumptions about the future course of disturbance inputs (i.e., a set of mathematical assumptions which describe the process noise and sensor noise). The infinite horizon closed-loop problem actually yields one of the few results which are practical from the chemical process control point of view - the optimal feedback control is a matrix of gains which become constant as the time horizon goes to infinity.

State, Control, and Output Constraint Handling

Much of this work related to items in the previous heading covering sensor/actuator failure. Additional work has been performed by Makila, Westerlund, and Toivonen (1984), who illustrate a technique for appending constraints on variances in control signals and system states to the standard LQG problem. Their formulation is more rigorous than the standard ad hoc fixes, such as reevaluation of the LQG formulation with successively heavier weights on variables, until the LQG solver produces a satisfactory solution (Athans, 1971; Athans and Falb, 1966; MacGregor, 1973). Unfortunately, their formulation requires the solution of a nonlinear programming problem. In addition, parts of the separation theorem do not apply - the estimator is computed separately, but the feedback gain matrix is dependent on the process noise and measurement noise covariance matrices.

The subject of hard constraints on the control input (as opposed to variance constraints) was researched by Toivonen. He found an analytical solution for a first order plus delay system and a symmetric constraint (Toivonen, 1981). There are some suboptimal solutions to the more general case, which, while somewhat complex, can be achieved (Toivonen, 1983). It should be noted that the only analytical work in constraint handling is in the time domain. This author knows of no significant frequency domain work in this area.

An Inability to Handle Dead Time

Control designers in the process industries commonly face dead time. The standard LQ and LQG formulations, when modified for the inclusion of dead time, result in bulky sets of differential-difference equations. However, there are some research results available, including a bibliography (Ross and Flugge-Lotz, 1967). One of the earliest applications papers (Larson and Wells, 1969) uses a shift operator to eliminate the delay terms, and then uses the standard Kalman filter and linear quadratic regulator formulations to achieve the optimal control policy. The Kalman filter can be extended to include delays (Kwakernaak, 1967). More recently, Ogunnaike and Ray (1984) have developed an observer for time delay systems which estimates the states necessary for a multivariable Smith predictor. The end result of much of this work demonstrates that some of the modern control theory results, such as the Kalman filter, can be extended to include dead time, but at the expense of additional mathematical complexity and computational burden.

Association of Weighting Matrices with Pole Location

Of all of the complaints once registered against modern control theory, this is the one in which the most progress has been made. Based upon some early work by Kwakernaak which is summarized in his 1972 text and a 1976 paper, there are now a large number of techniques and results which relate values in the quadratic state and control weighting matrices to closed-loop pole locations. The interested reader is referred to Harvey and Stein (1978) and to Stein (1979) for fundamental results based on asymptotic properties of the regulator solution as weights on control tend to zero. Briefly, these two papers describe an extension of Kwakernaak's earlier work on asymptotic behavior of eigenvalues to include the asymptotic behavior of the associated eigenvectors. Moore (1976) is credited with the idea of eigenvector adjustment along with arbitrary pole placement in linear state feedback control systems.

Based on Francis (1979) and Harvey and Stein's work, Kawasaki and Shimemura (1983) have devised a decision method to locate closed-loop poles within a specified region. Their technique requires that the designer recursively compute solutions to the control algebraic Riccati equation which are then subjected to certain matrix algebraic constraints. Successive iteration through their procedure guarantees that all of the closed-loop poles will be moved into the prespecified region in the s-plane in, at most, a number of iterations equal to the dimensionality of the $\underline{A}$ matrix of the system's state description.

Gopal and Pratapachandran (1985) have proposed a technique for combining pole placement and optimal control in discrete systems. To the standard quadratic performance index, they add a term incorporating sensitivity to system parameter variations. A gradient algorithm is then used to compute the optimal controller, based on minimizing a calculated expression for the gradient of the performance index with respect to the control parameter vectors.

Lack of Applicability to the Regulator Problem
and the Servomechanism Problem

This issue is easily handled by suitable modifications of the LQ formulation. Briefly, one need only "trick" the LQ regulator by substituting an error term, equal to the difference between reference and actual states, into the state feedback loop. The LQ regulator sees this fictitious "state" error as a nonzero state and attempts to drive it to the origin, i.e., to reduce the "state" to zero. Athans and Falb (1966) refer to such a reformulation as the "tracking solution." A more complete mathematical description of this procedure will be deferred to Chapter III, where we modify the LQ regulator formulation to include command following and disturbance rejection.

C. SOME RECENT DEVELOPMENTS

As researchers in the seventies wrestled with some of the problems and limitations outlined in the previous section, some new theoretical results were achieved. Among the more valuable of these results were those which allowed modern control techniques to deal with the issue of robustness. The robustness issue deals with the performance and stability questions which invariably arise when one uses a simplified but erroneous model for state estimation and control. In this next section, we shall briefly outline some of the recent research milestones. A more detailed mathematical description of these results is contained in Chapter II.

Frequency domain SISO design techniques handle the robustness questions easily. The classical concepts of gain margin and phase margin are well understood and accepted. Unfortunately, there is no simple MIMO counterpart to the SISO Nyquist locus. Techniques such as Rosenbrock's Inverse Nyquist Array (1969) and MacFarlane's Characteristic Loci (1977) attempt to reduce the MIMO problem to a set of SISO problems by the addition of a precompensator matrix and a postcompensator matrix to achieve "diagonal dominance." Unfortunately, there are no robustness guarantees with these techniques, and one may even be lulled into a false sense of security by examining gain and phase margins within the compensator and not at the true inputs to the plant.

Zames (1966a, 1966b) is credited with some fundamental developments in the use of conic sectors and functional analysis in the study of input-output system stability. Safonov (1980) and Safonov et al. (1981), used these concepts to develop a powerful, but abstract, stability theorem involving topological separation of function spaces. He also obtained a more practical, special case (the sector stability theorem), which, along with some frequency-domain tests, allows one to specify realistic multivariable stability margins. Doyle's work (1978), plus Safonov's, resulted in the oft-quoted $[\frac{1}{2}, \infty]$ gain margin and $[+60°, -60°]$ phase margin guarantees for linear quadratic state feedback control systems.

Using some procedures outlined by Kwakernaak in his 1972 text, Doyle and Stein (1979, 1981) have developed a technique for achieving robust control designs, even in stochastic systems with state reconstructors (Kalman-Bucy filters). They show that it is possible to design the Kalman-Bucy filter within the Model Based Compensator to achieve the desired control performance specifications. The second step of their procedure involves the loop transfer recovery (LTR) of these properties within the LQ regulator.

Lehtomaki (1981) extended these results by deriving robustness theorems which use some prespecified forms of model error. He also shows that those tests which use model error structure can guarantee stability in the face of larger model uncertainty than those which use only the model error magnitude. The most important practical implications of his work are summarized in a set of robustness inequality theorems, which state conditions on the minimum singular values of certain loop transfer matrices relative to the maximum singular values of certain additive or multiplicative error factors. These test are easily mechanized, and the display of these two sets of singular values versus frequency allows the designer to readily assess the robustness of a particular design.

More recently, these procedures have been used on certain real-world control problems:

1. The F100 turbofan engine (Kappos, 1983; Athans et al., 1984)
2. The GE-21 turbofan engine (Kapasouris, 1984)
3. The GE T700 turboshaft engine (Pfeil, 1984)

It is recognized that there are many other LQG analysis and design references which could be cited. However, these three were chosen because they bear some resemblance to problems of interest to the process control practitioner. Berge and MacGregor (1984) have compared the robustness properties of a SISO unconstrained minimum variance controller, a constrained minimum variance controller (an LQG controller), and the internal model controller of Garcia and Morari (1982). Their simulations indicated that the addition of even a small constraint on control action (which produces an LQG controller) will greatly improve the robustness of the minimum variance controller, and will not result in any significant performance deterioration. When compared to the IMC controller designed to equivalent robustness specifications, the LQG controller demonstrated better performance in all of the cases studied.

D. THE GOAL OF THE PRESENT WORK

A number of the aforementioned research results have produced a nearly complete design methodology for linear time invariant (LTI) systems. The LQG/LTR procedure and the associated and analogous MBC/LTR procedure have led several theoretical researchers to turn their attentions to nonlinear techniques, on the premise that there are no "unturned stones" left in the linear field. From a purely theoretical point of view, their argument has some merit.

However, there remain a number of questions from a practical and algorithmic point of view. Many of the clean and elegant "textbook" techniques are poorly conditioned (Moore, 1981). These textbook techniques can be shown to have problems for those real-world situations which possess structural instabilities; i.e., systems in which small model perturbations produce dramatic changes in system properties, such as rank - a notion critical to the ideas of observability and controllability. Singular value decomposition (see, for example, Klema and Laub, 1980; Golub and Reinsch, 1970; Stewart, 1973; Forsythe and Moler, 1967; Forsythe, Malcolm, and Moler, 1977; Lawson and Hanson, 1974) provides a numerically robust and computationally efficient tool with which one can analyze these problems.

There are also some unresolved issues with certain aspects of the theory itself. In particular, the principal concern of this work relates to how the Linear Quadratic (LQ) regulator can be modified for command following and disturbance rejection. When the LQ regulator is adapted for command following and disturbance rejection (the so-called "LQ servo"), one does not have a good design methodology for directly achieving desired singular values and loop shapes in the frequency domain. One can only design the LQ regulator, and then accept the corresponding LQ servo singular values.

The intent of this work is to investigate the LQ regulator when adapted for servo purposes, in an attempt to derive theoretical relationships which directly associate LQ servo singular values with the system's (A,B,C) triple, and other design parameters, such as the state and control weighting matrices in the quadratic performance index.

E. CHAPTER SUMMARY

In this introductory chapter, we have discussed some of the historical research results one finds in the modern control literature, as well as some of the limitations and constraints on its practical use. This discussion is in no way exhaustive, nor should it be. However, it should serve as a key to some of the more commonly quoted textbook results of the sixties, as well as an introductory exposition on the more recent results in the areas of theoretical stability and robustness guarantees, as well as other frequency-domain properties, such as asymptotic pole location. Some of these results require a more fundamental mathematical presentation for their complete understanding. This mathematical presentation, along with a more detailed linkage of the appropriate mathematics to its location in the research literature, is the subject of Chapter II.

In addition, we have briefly described the research problem at hand - that of directly specifying the singular values and loop shapes of the LQ servo. This topic will be the subject of Chapter III, and numerical confirmation of the theoretical results and guidelines will be the major topic of Chapter IV. Results of this research work and its relevance to advancement of the state of the control art will be summarized in Chapter V.

CHAPTER II

MATHEMATICAL PRELIMINARIES

A. CHAPTER INTRODUCTION

In this chapter, we expose the reader to some of the significant and relevant results from optimal control theory in Section B, covering the Linear Quadratic Regulator (LQR) Problem. This material is offered to acquaint the reader with the relevant mathematical preliminaries and to familiarize him with the notation to be used throughout the remainder of this work. These results are useful in that they define the ultimate limits on achievable control quality for linear, time-invariant (LTI) systems, based upon the designer's choice of weighting factors in the quadratic performance objective. Most of this mathematics has been available since the mid-1960's.

In contrast to the above section, most of the mathematical results in Section C are relatively recent. These concepts define the bridge between time domain, state space models, and their frequency domain equivalents. Having this mathematics in hand allows us to work in the most convenient arena to solve the particular problem at hand.

Section D summarizes the more significant results presented in this chapter.

B. THE LINEAR QUADRATIC REGULATOR (LQR) PROBLEM

We are given the continuous-time state-space description of the plant:

$\underline{\dot{x}}(t) = \underline{A}\ \underline{x}(t) + \underline{B}\ \underline{u}(t)$

$\underline{y}(t) = \underline{C}\ \underline{x}(t)$

$\underline{x} \in R^n$

$\underline{u} \in R^m$

$\underline{y} \in R^m$

and the following assumptions:

$[\underline{A},\underline{B}]$ stabilizable

$[\underline{A},\underline{C}]$ detectable

We choose the following quadratic cost functional:

$$J = \int_0^\infty (q\ \underline{y}'(t)\underline{y}(t) + \underline{u}'(t)\underline{R}\ \underline{u}(t))dt$$

with $q > 0$ and

$\underline{R} = \underline{R}' > \underline{0}$ and is chosen to be diagonal

(The ' symbol denotes matrix transposition)

From the definition of $\underline{y}(t)$ and the fact that q is a scalar, the cost functional can also be rewritten as:

$$J = \int_0^{\infty} (\underline{x}'(t)\ \underline{Q}\ \underline{x}(t) + \underline{u}'(t)\ \underline{R}\ \underline{u}(t))\ dt$$

where

$$\underline{Q} = q\ \underline{C}'\underline{C}$$

Under the above assumptions, it is shown in any number of standard texts (Athans and Falb, Kwakernaak, Sage) that the following statements are applicable:

1. The optimal control exists
2. It is unique
3. It is realized in a full-state feedback form as follows:

$\underline{u}(t) = -\underline{G}\ \underline{x}(t)$ where $\underline{G}$ is the LQ control gain matrix

$$\underline{G} = \underline{R}^{-1}\ \underline{B}'\ \underline{K}$$

where $\underline{K}$ is the nxn unique positive-definite, symmetric matrix which solves the steady-state Control Algebraic Riccati Equation (CARE):

$$\underline{0} = -\underline{KA} - \underline{A}'\underline{K} - q\underline{C}'\underline{C} + \underline{KBR}^{-1}\underline{B}'\underline{K}$$

There are m+1 degrees of freedom available to the designer in the above formulation: the m elements along the diagonal of $\underline{R}$, and the value of the scalar q.

The closed-loop system looks like

$$\dot{\underline{x}}(t) = (\underline{A}-\underline{B}\underline{G})\ \underline{x}(t)$$

$$\underline{y}(t) = \underline{C}\ \underline{x}(t)$$

The nominal design can be shown to be stable (Athans and Falb, p. 773); i.e., given the stabilizability and detectability assumptions, we are guaranteed that all of the closed-loop eigenvalues are in the left half of the s-plane:

$$\mathrm{Re}\ \lambda_i[\underline{A}-\underline{B}\underline{G}] < 0$$

We can summarize the LQ regulator equations in either the time domain or the frequency domain, as illustrated in Figure 2.1.

C. SINGULAR VALUES, ROBUSTNESS MEASURES, AND THE ROLE OF THE RETURN DIFFERENCE MATRIX

The Single-Input, Single-Output Case

Let us begin this discussion with a simple single-input, single-output example. Consider the closed-loop unity feedback control system with conventional notation (Athans, 1984) as illustrated in Figure 2.2, where:

$r(s)$ = command reference input

$y(s)$ = system output

$e(s)$ = error signal = $r(s) - y(s)$

$d_i(s)$ = additive disturbance input signal introduced at the input to the plant

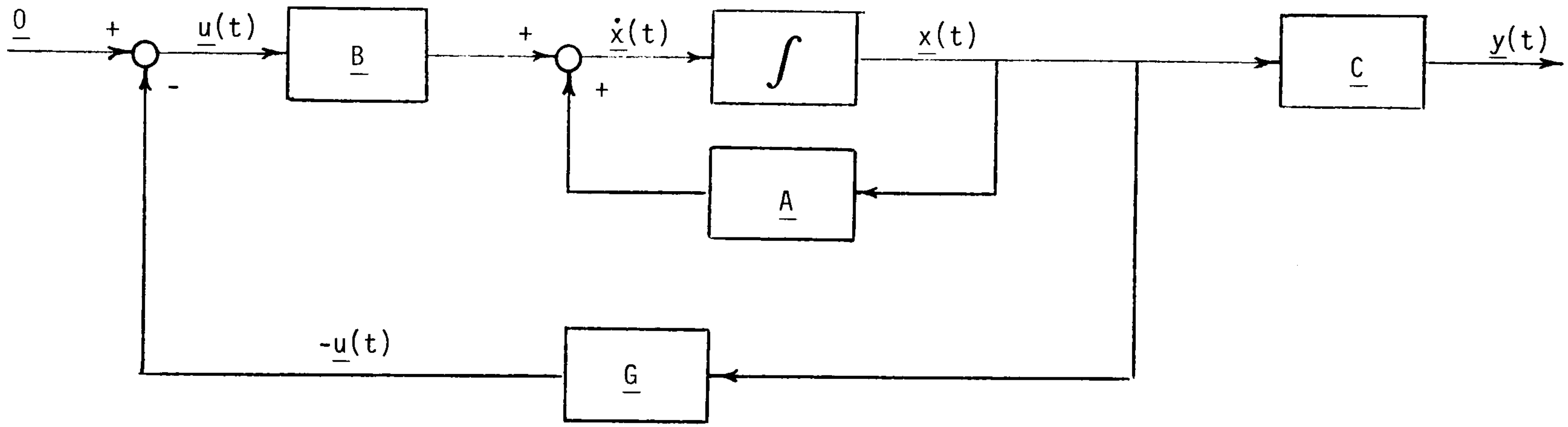

Time Domain

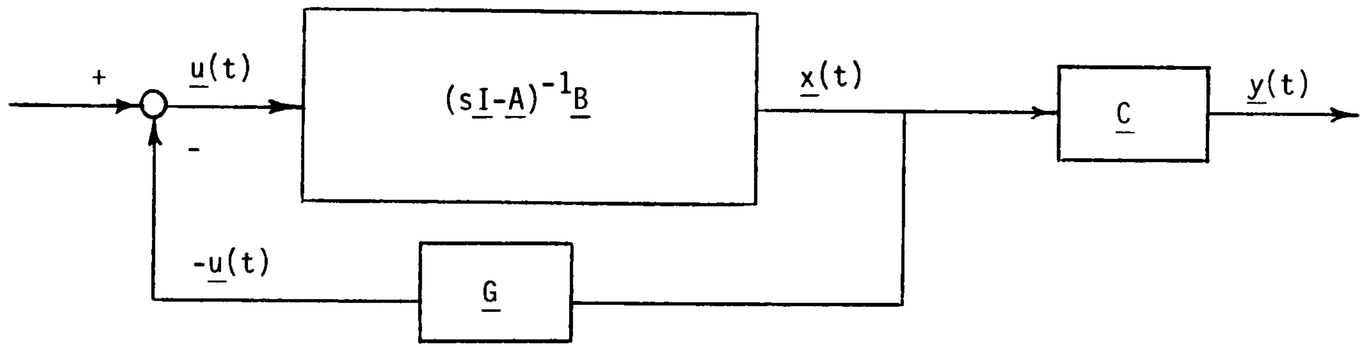

Frequency Domain

Figure 2.1. The linear quadratic (LQ) regulator.

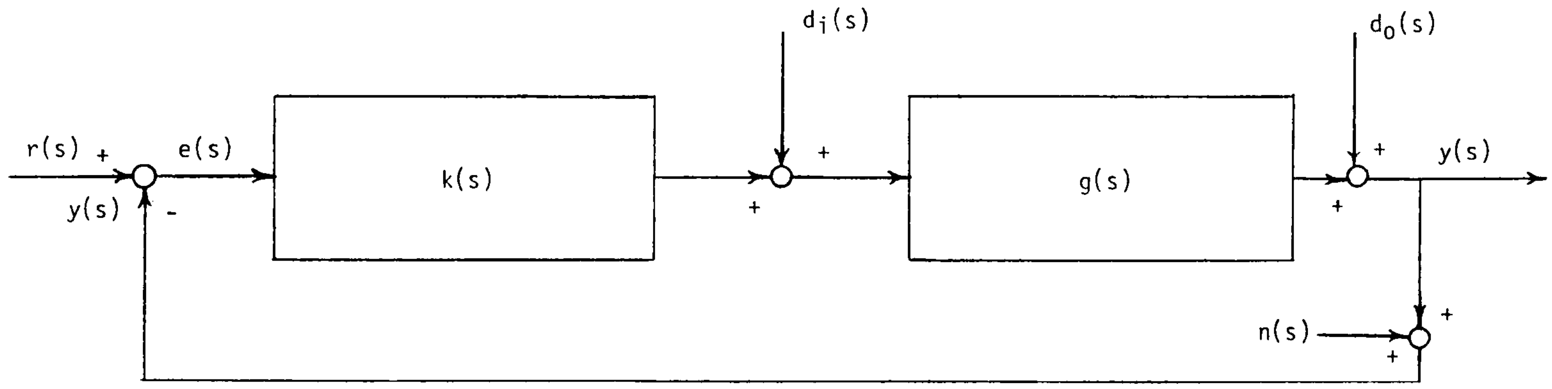

Figure 2.2. Single input-single output (SISO) unity feedback control system.

$d_o(s)$ = additive disturbance input signal introduced at the output of the plant

$n(s)$ = additive sensor noise

$k(s)$ = controller transfer function

$g(s)$ = plant transfer function

Via standard block diagram algebra reduction techniques, we can arrive at transfer functions which relate any of the four inputs $r(s)$, $d_i(s)$, $d_o(s)$, and $n(s)$, to the output $y(s)$.

In form, they all look like:

$$\frac{\Pi\ [\text{forward path elements between given input and output } y(s)]}{1 + \Pi(\text{all elements in the loop})}$$

In particular, $g(s)\ k(s)$ is referred to as the forward loop transfer function

$1 + g(s)\ k(s)$ is the return difference transfer function

$\dfrac{g(s)k(s)}{1 + g(s)k(s)}$ is the closed loop transfer function

$[1 + g(s)k(s)]^{-1}$ is the sensitivity transfer function

This terminology is standardized and relates back as far as Nyquist's (1932) and Bode's (1945) original work on electrical networks and feedback amplifiers.

There are a number of sensitivity functions which can be derived around the above model which relate incremental changes in various system parameters to incremental changes in the plant output. Conceptually, it is recognized that one of the major contributions of feedback is in reduction of output sensitivity to incremental changes in system blocks which are located in the forward path of the loop (such as the plant itself) (Kuo, 1967, pp. 193-194).

Feedback also has an effect on other system properties, such as overall gain, distortion, impedance, transient response, and bandwidth. These latter two effects are most important to the control system designer. However, as summarized in the Bode-Horowitz (1945, 1963) integral relationships, there are overall limits on the amount of effect that feedback may have. This relationship can be stated as:

$$\int_{-\infty}^{\infty} \ln[1 + g(j\omega)k(j\omega)]d\omega = 0$$

In words, this relationship states that large return difference transfer functions at some frequencies are always bought at the expense of smaller return difference transfer functions at other frequencies.

At this point, one may ask why large or small return difference transfer functions are important. Let us examine each of the two basic roles of a control system: command following and disturbance rejection. For command following, we would like to have $y(s) \cong r(s)$ over a wide range of possible command inputs $r(s)$.

Recall that: $$y(s) = \frac{g(s)k(s)}{1 + g(s)k(s)} r(s)$$

To satisfy the command-following requirement, we need for the closed-loop transfer function to be as close as possible to unity, which, in turn, requires a large value of g(s)k(s), relative to one.

Most typical command inputs (such as steps or ramps) have a large energy content at lower frequencies. Then our command-following requirement is that $g(j\omega)k(j\omega)$ be large for $\omega \varepsilon [0, \omega_{1c}]$ where ω_{1c} is an arbitrary low frequency cutoff value for energy content of the command signal r(s). Note that $g(j\omega)$ need not, itself, be large; only the value of $g(j\omega)k(j\omega)$ need be large; i.e., $k(j\omega)$ may be made large if $g(j\omega)$ is small in some particular frequency range.

We can follow a similar line of reasoning for disturbance rejection. The transfers from either $d_i(s)$, $d_o(s)$, or n(s) to the output y(s) all look like:

$$\frac{\Pi \text{ (forward path elements between given input and output } y(s))}{1 + \Pi \text{ (all elements in the loop)}}$$

Common to all of these disturbance transfer functions is the sensitivity transfer function

$$\frac{1}{1 + g(s)\, k(s)}$$

In order that y(s) approach zero for a given value of a noise or disturbance input, it is necessary that the sensitivity transfer function be small; or, equivalently, that $1 + g(s)k(s)$ be large in the range of frequencies prevalent in the particular disturbance.

However, we cannot have an absolutely free hand in locating these regions of large or small loop transfer, as we saw from the Bode-Horowitz integral criteria. Fortunately, a great number of command inputs have low-frequency content, and a great deal of the frequency content of typical noise signals is at the high end of the spectrum. Thus, our role as control designers is to make the loop transfer sufficiently large at low frequencies, and to make it sufficiently small at higher frequencies, as illustrated in Figure 2.3.

The Multiple-Input, Multiple-Output Case

These notions regarding command following and disturbance rejection carry over directly to the multiple-input, multiple-output (MIMO) situation. However, we must now generalize our concepts of "large" or "small" when discussing the value of a matrix transfer function.

Let us again use the closed-loop unity feedback structure illustrated above, but now consider all of the variables to be vectors rather than scalars. Similar block diagram algebra (Athans, 1984) yields:

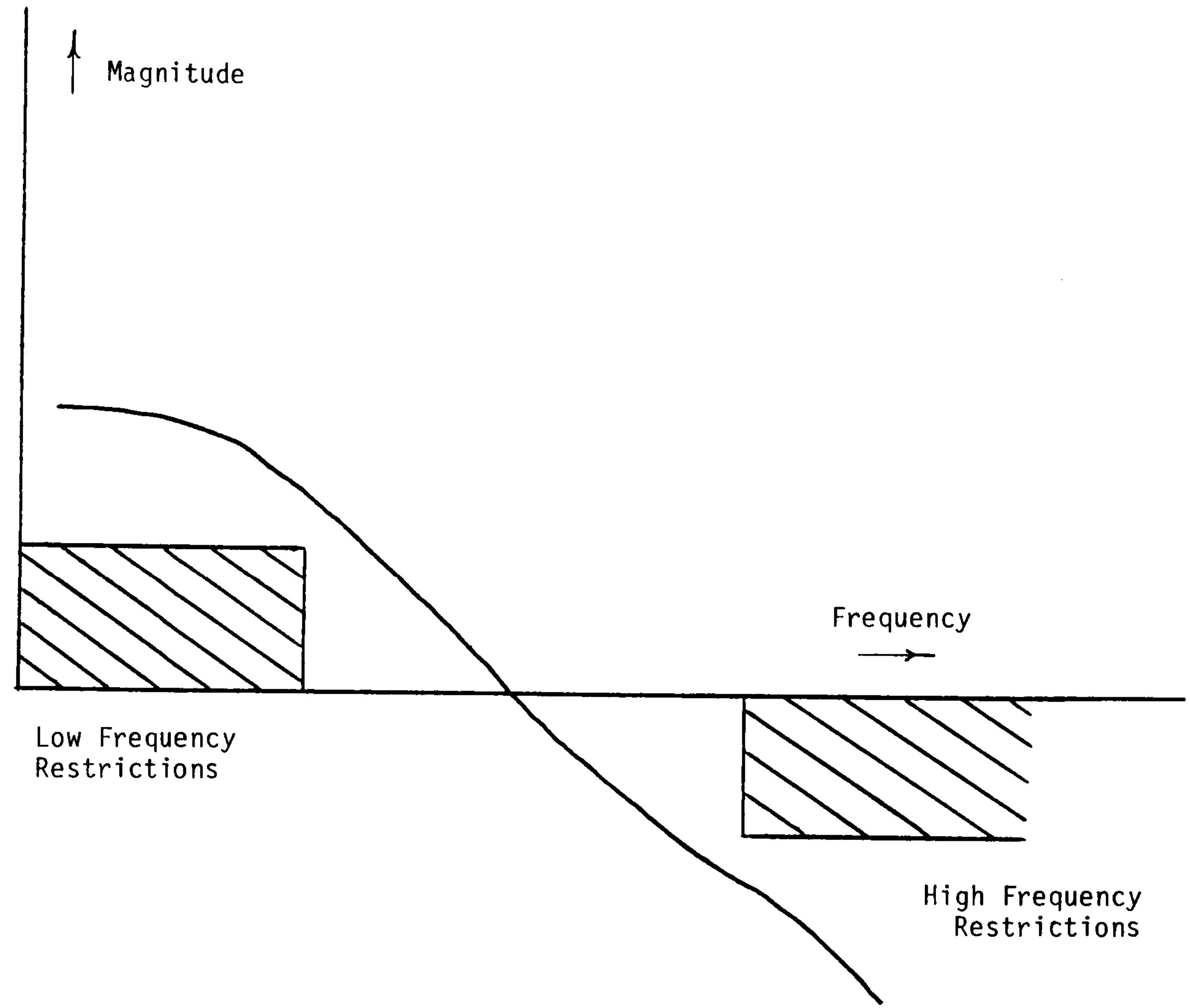

Figure 2.3. Ideal loop transfer behavior versus frequency.

$$\underline{y}(s) = [\underline{I} + \underline{G}(s)\ \underline{K}(s)]^{-1}\ \underline{G}(s)\ \underline{K}(s)\ \underline{r}(s)$$

For good command following, we want $\underline{y}(s) \simeq \underline{r}(s)$. Therefore, $[\underline{I} + \underline{G}(s)\ \underline{K}(s)]^{-1}\ \underline{G}(s)\ \underline{K}(s)$ must be nearly equal to $\underline{I}$ for the range of frequencies contained in $\underline{r}(s)$. Equivalently, $\underline{G}(s)\ \underline{K}(s)$ must be large, relative to $\underline{I}$, for this to hold true in the frequency range of interest.

The disturbance transfer from, say, $\underline{d}_o(s)$ looks like:

$$\underline{y}(s) = [\underline{I} + \underline{G}(s)\ \underline{K}(s)]^{-1}\ \underline{d}_o(s)$$

If, for a given $\underline{d}_o(s)$, we want $\underline{y}(s) \simeq \underline{0}$, then $[\underline{I} + \underline{G}(s)\ \underline{K}(s)]^{-1}$ must be nearly equal to $\underline{0}$. Equivalently, $\underline{G}(s)\ \underline{K}(s)$ must again be large for the above to hold true in the range of frequencies prevalent in $\underline{d}_o(s)$.

Conventional notation labels some of the above terms as follows:

$\underline{G}(s)\ \underline{K}(s)$ - open loop transfer matrix

$\underline{I} + \underline{G}(s)\ \underline{K}(s)$ - return difference transfer matrix

$\underline{I} + [\underline{G}(s)\ \underline{K}(s)]^{-1}$ - inverse return difference transfer matrix

$[\underline{I} + \underline{G}(s)\ \underline{K}(s)]^{-1}\ \underline{G}(s)\ \underline{K}(s)$ - closed-loop transfer matrix

Matrix Size and Singular Values

In the previous two sections, we have examined the role of the return difference $[1 + g(s)k(s)]$ for SISO systems, and the equivalent role played by $[\underline{I} + \underline{G}(s)\underline{K}(s)]$, the s-domain return difference matrix, for MIMO systems. This section is dedicated to defining more clearly what we mean by "size" of a general complex matrix, and in particular, how that "size" parameter affects certain closed-loop performance and robustness qualities of a control system design.

There are a number of different "size" parameters that can be defined for a given nxn complex matrix. To define these matrix size parameters, known as norms, we must first define vector norms and then extend these concepts to include operator norms induced by these vector norms on linear transformations.

A vector norm of $\underline{x}$ is a quantity, denoted by $\|x\|$, which has the following properties (Noble and Daniel, 1977):

1. $\|x\| > 0$ for all $\underline{x}$, except that $\|\underline{x}\| = 0$ iff $\underline{x} = \underline{0}$
2. $\|k\underline{x}\| = |k|\ \|\underline{x}\|$ for scalar k
3. $\|\underline{x} + \underline{y}\| \leq \|\underline{x}\| + \|\underline{y}\|$ (the triangle inequality)

The one-, two-, and infinity vector norms are defined as follows:

$\|\underline{x}\|_1 = |x_1| + |x_2| + \ldots + |x_n|$

$\|\underline{x}\|_2 = (|x_1|^2 + |x_2|^2 + \ldots + |x_n|^2)^{1/2}$ (the normal Euclidean length definition)

$\|\underline{x}\|_\infty = \max\limits_i |x_i|$

where $|x_i|$ represents the magnitude of the i^{th} component of $\underline{x}$

In a sense, all of these measures present equivalent information. It can be shown that constants c_1 and c_2 exist such that

$c_1 \|\underline{x}\| \leq |\|\underline{x}\|| \leq c_2 \|\underline{x}\|$ for any two norms $\|\cdot\|$ and $|\|\cdot\||$, and for any finite-dimensional $\underline{x}$

If we consider the complex matrix $\underline{A}$ to represent an mxn linear transformation of a vector $\underline{x}$ from C^n (the domain) to C^m (the range) (i.e., $\underline{y} = \underline{A}\ \underline{x}$), then there are induced norms corresponding to the appropriate vector norms in both the domain C^n and the range C^m:

$$\|\underline{A}\|_1 = \max_{\underline{x} \neq \underline{o}} \frac{\|\underline{A}\ \underline{x}\|_1}{\|\underline{x}\|_1}$$

$$\|\underline{A}\|_2 = \max_{\underline{x} \neq \underline{o}} \frac{\|\underline{A}\ \underline{x}\|_2}{\|\underline{x}\|_2}$$

$$\|\underline{A}\|_\infty = \max_{\underline{x} \neq \underline{o}} \frac{\|\underline{A}\ \underline{x}\|_\infty}{\|\underline{x}\|_\infty}$$

We can compute these norms from their elements as follows:

$\|\underline{A}\|_1 = \max_j \sum_{i=1}^{m} |a_{ij}|$ (the maximum absolute column sum; also referred to as the column norm)

$\|\underline{A}\|_2$ = the maximum eigenvalue of $(\underline{A}^H\underline{A})^{1/2}$ = the maximum singular value of $\underline{A}$

$\|\underline{A}\|_\infty = \max_i \sum_{j=1}^{n} |a_{ij}|$ (the maximum absolute row sum; also referred to as the row norm)

Note that we have introduced the notion of a matrix singular value above. In general, a complex mxn matrix $\underline{A}$ has k singular values, denoted by σ_i, defined as the k largest square roots of the eigenvalues of $\underline{A}^H\underline{A}$ where k = min (n,m) and $\underline{A}^H$ denotes the Hermetian, or conjugate transpose, of $\underline{A}$:

$$\sigma_i(\underline{A}) = (\lambda_i[\underline{A}^H\underline{A}])^{1/2} \qquad i = 1, 2, \ldots, k$$

We note the two equalities:

$$\sigma_{max}(\underline{A}) = \max_{\underline{x} \neq \underline{o}} \frac{\|\underline{A}\underline{x}\|_2}{\|\underline{x}\|_2} = \|\underline{A}\|_2$$

$$\sigma_{min}(\underline{A}) = \min_{\underline{x} \neq \underline{o}} \frac{\|\underline{A}\underline{x}\|_2}{\|\underline{x}\|_2} = \|\underline{A}^{-1}\|_2^{-1} \quad \text{if } \underline{A}^{-1} \text{ exists}$$

In words, the maximum and minimum singular values of $\underline{A}$ establish upper and lower bounds on the size relationship between the input $\underline{x}$ and the output $\underline{y}$ for the linear transformation $\underline{y} = \underline{A}\ \underline{x}$. More precisely, they indicate how the transformation itself scales the input Euclidean norm to the output Euclidean norm.

In particular, we will be interested in noting the singular values of the open-loop transfer matrix, $\sigma_i[\underline{G}(s)\underline{K}(s)]$, as a function of frequency ($s = j\omega$). One can easily see that, at the low frequency end of the spectrum where we expect most of the frequency content of command signals, we expect the <u>smallest</u> singular value $\sigma_{min}[\underline{G}(j\omega)\underline{K}(j\omega)]$ to be <u>greater</u> than some arbitrary value for good command-following properties (see Figure 2.4). Conversely, at the higher frequencies, we expect the <u>largest</u> singular value $\sigma_{max}[\underline{G}(j\omega)\underline{K}(j\omega)]$ to be <u>less</u> than some arbitrary value for good noise-rejection properties. (In addition,

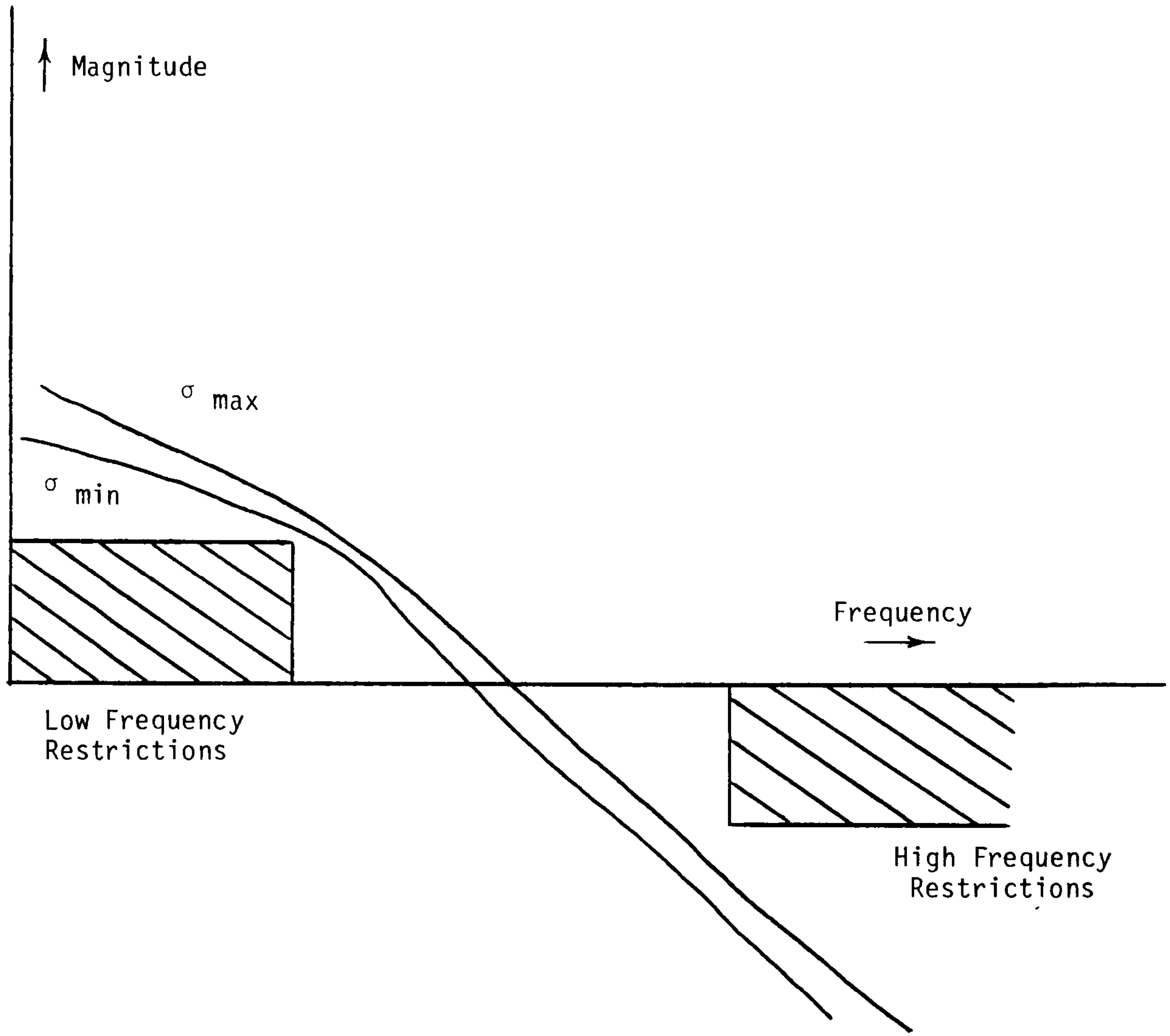

Figure 2.4. Ideal loop transfer singular value behavior versus frequency.

this last expectation is also true for situations where we have designed our control system with a reduced-order model: the maximum singular value should roll off quickly enough to become very small by the time we reach frequencies high enough to perturb the neglected high-frequency dynamics of the process.)

Singular Value Analysis Applied to Multivariable Control Design

Now that the reader is sufficiently armed with the proper mathematical tools, we can investigate two relevant multivariable control design areas: closed-loop performance specifications and stability/robustness considerations. We will see that there is a fundamental connectivity between these two areas and the notion of a matrix singular value introduced in the previous section.

The work of Safonov and co-workers, based on Zames' "conic sectors," is particularly notable when one considers issues relating to feedback properties of multivariable systems. Their work established relationships between the return difference and inverse return difference matrices, and fundamental properties of a feedback system, such as noise and disturbance response, stability margins, and sensitivity to plant and sensor variation. More precisely, they show that the singular values of the return difference matrix and the inverse return difference matrix are not independent. The practical effect of these relationships is to force the designer to trade off stability margins against insensitivity to plant disturbances and plant gain variations.

Safonov, Laub, and Hartmann (1981), then apply these considerations to the LQG design problem. Minimization of the quadratic performance index is shown to be equivalent to minimization of a weighted sum of terms involving singular values of the return difference and inverse return difference matrices. They use these relationships in an aircraft control design to show how proper choice of the $\underline{Q}$ and $\underline{R}$ weighting matrices, plus the two noise intensity matrices, can be used to control the magnitude vs. frequency characteristics of the singular values of the return difference and inverse return difference matrices. When presented in a Bode-like plot (singular value magnitudes expressed in db, frequencies on a semi-log axis), this information allows the control designer to iterate quickly on allowable LQG designs and to locate a design which satisfies the given frequency-domain specifications.

Lehtomaki et al. (1981) relate the robustness of a feedback system to the singular values of the return difference matrix. (In the context of this discussion, "robustness" relates to the controller's insensitivity to differences between the actual physical plant, and the nominal plant model used for controller design.) More precisely, the minimum singular value of the return difference matrix defines how close one is to instability: A small σ_{min} indicates near-singularity of $[\underline{I} + \underline{G}(j\omega)\underline{K}(j\omega)]$, and also implies that a small difference between the actual plant and the plant model would destabilize the system.

Lehtomaki defines model differences in the following manner:

Let $\underline{\tilde{G}}(s) = \underline{L}(s)\ \underline{G}(s)$

where $\underline{\tilde{G}}(s)$ represents the plant itself

and $\underline{G}(s)$ represents the plant model

Assume that $\underline{E}(s)$ represents the post-multiplicative error between the model $\underline{G}(s)$ and the plant $\underline{\tilde{G}}(s)$.

Then

$$\underline{L}(s) = \underline{E}(s) + \underline{I} \quad \text{or,}$$

$$\underline{E}(s) = (\underline{\tilde{G}}(s) - \underline{G}(s))\ \underline{G}^{-1}(s)$$

A compensator $\underline{K}(s)$ which stabilizes the plant model will also stabilize the actual plant if

$$\sigma_{max}[\underline{L}(jw) - \underline{I}] < \sigma_{min}[\underline{I} + (\underline{G}(jw)\underline{K}(jw))^{-1}]$$

and

$$\sigma_{max}[\underline{L}^{-1}(jw) - \underline{I}] < \sigma_{min}[\underline{I} + \underline{G}(jw)\underline{K}(jw)]$$

These robustness results are based on the multivariable Nyquist circle criterion, which relates the value of σ_{min} to the distance between the Nyquist locus and the -1 critical point. For small σ_{min}, a small change in $\underline{G}(j\omega)$ will result in a shift in the path of the Nyquist locus such that the number of clockwise encirclements of the -1 point would change and the system would be destabilized.

For SISO LQ regulators, Kalman (1964) derived fundamental inequalities for gain margin properties which state that a linear SISO system is optimal with respect to some quadratic performance index if, and only if, the Nyquist locus for such a system lies outside of a circle which is centered at the critical -1 point and which has a radius of 1. Anderson and Moore (1971, pp. 70-76) extend this result to show that the SISO LQ regulator has the following guaranteed gain margins (GM) and phase margins (PM)

$$1/2 \leq GM \leq \infty$$

$$-60° \leq PM \leq 60°$$

These results have been extended by Lehtomaki, Safonov, and others to the MIMO case, and equivalent results are obtained, but only for diagonal $\underline{R}$ weighting matrices. In fact, Lehtomaki (1981, p. 206) shows a counterexample with a nondiagonal $\underline{R}$ in which gain margins become arbitrarily small. Unfortunately, the results for diagonal $\underline{R}$ have entered the folklore of modern control theory, and one is very likely to encounter these results in misquoted form devoid of any accompanying set of assumptions with regard to choice of $\underline{R}$. Note also that these guarantees hold for any and all forms of simultaneous variations from any input channels to any output channels. Conversely, the price one pays for such guarantees is a great deal of conservatism (Lehtomaki et al., 1981, p. 88; Kawasaki and Shimemura, 1983) - the results yield absolute worst-case results in that $\sigma_{min}\,[\underline{I} + \underline{G}(j\omega)\underline{K}(j\omega)]$ defines the smallest possible destabilizing perturbation, with no thought given to the actual possibility of its occurrence.

A bit of ancillary research which has been somewhat overlooked relates to corresponding margins achieved when one solves a Lyapunov equation, rather than the Riccati equation, to find the gain matrix $\underline{K}$. Recall that the Control Algebraic Riccati Equation (CARE) is given by:

$$\underline{0} = -\underline{KA} - \underline{A}'\underline{K} - q\underline{C}'\underline{C} + \underline{KBR}^{-1}\underline{B}'\underline{K}$$

The corresponding Lyapunov equation is:

$$\underline{0} = -\underline{KA} - \underline{A}'\underline{K} - q\underline{C}'\underline{C}$$

and, if $\underline{K} \geq \underline{0}$ and $[\underline{A},\underline{Q}^{1/2}]$ is detectable, the closed-loop poles are guaranteed stable; i.e., the real parts of their eigenvalues are strictly in the left half of the s-plane.

Results by Harvey (1979) and Wong and Athans (1977) lead to Lyapunov-based gain and phase margins given by the following (but only for diagonal $\underline{R}$):

$$0 \leq GM \leq \infty$$

$$-90° \leq PM \leq + 90°$$

The importance to the practical industrial control designer of such a result is that multivariable solutions of this type are guaranteed stable, even under conditions of actuator failure, saturation, or disengagement (i.e., auto to manual transfer). However, the use of the Lyapunov formulation is limited to open-loop stable systems, while the LQ formulation will work with open-loop unstable systems.

Lehtomaki (1981) parameterizes the standard Riccati equation in an attempt to compromise the Riccati and Lyapunov results:

$$\underline{0} = -\underline{KA} - \underline{A}'\underline{K} - q\underline{C}'\underline{C} + \beta\underline{KBR}^{-1}\underline{B}'\underline{K}$$

for $\quad 0 < \beta < 2$

As $\beta \to 0$, one hopes to recover the wider Lyapunov margins. Note that the above equation is a mild variation of the standard Riccati form, and a similar analysis yields:

$$\beta/2 \leq \text{GM} \leq \infty$$

$$-\cos^{-1}(\beta/2) \leq \text{PM} \leq +\cos^{-1}(\beta/2)$$

for $\quad 0 < \beta < 2$, diagonal $\underline{R}$, and $\underline{Q}$ positive definite.

The value in this work is that, using the LQ methodology, the control designer has at hand a design procedure which guarantees some nominal closed-loop properties for LQ regulators, such as stability and robustness, under a set of relatively mild assumptions. Conceptually, the designer, sitting at his interactive computer terminal, is free to examine a wide range of state and control weightings, and noise intensity matrices, knowing all the while that his multivariable controller designs possess certain minimum guaranteed properties.

Stability Margins for LQG Regulators

The comfort sensed by our hypothetical control designer is illusory, and not at all well-grounded. In the real world, one rarely, if ever, has all of the states available directly for full-state feedback as required by the LQ regulator formulation. One must then resort to observers (Kalman filters) for (optimal) state reconstruction. Safonov and Athans (1978) have developed guaranteed robustness properties for the Kalman filter - a relatively straightforward procedure since the Kalman filter and the LQ regulator are mathematical duals. Provided that the Kalman filter is given the exact model of the true system (perturbed or otherwise), the guaranteed KF and LQ margins still apply when the two are coupled into an LQG configuration. However, in the real world case where the Kalman filter model remains constant while the plant is perturbed, there are no guaranteed LQG stability margins whatsoever, as was demonstrated by Doyle (1978) with a relatively simple, non-pathological example. Doyle's work precipitated some reexamination of certain LQG designs already in the literature, which, upon investigation, revealed frighteningly small margins - in one case (Bryson, 1972), phase margins less than 10°.

This setback for the LQG champions actually proved to be a blessing in disguise. Research by Doyle and Stein (1979, 1981) indicated that a procedure originally proposed by Kwakernaak (1969, 1972) for producing low-sensitivity feedback systems could be used to asymptotically recover the robustness properties of the LQ regulator. As this procedure was more fully investigated, it was acknowledged to have much wider implications than simply "robustness recovery," and was more descriptively dubbed as "loop transfer recovery." Further numerical investigations, principally on jet engine control applications (Kappos, 1983; Kapasouris, 1984; Pfeil, 1984), support the idea that we now have available a complete LQG regulator design methodology, and form the basis for Athans' comment to the effect that "all the good stuff for LQG design of linear systems is already here." The control designer can, indeed, sit at his interactive terminal and design good LQG systems which are guided by theoretically sound guarantees for stability and robustness. The next section of this chapter will briefly outline this procedure.

D. THE LINEAR QUADRATIC GAUSSIAN/LOOP TRANSFER RECOVERY (LQG/LTR) TECHNIQUE

The Linear Quadratic Gaussian/Loop Transfer Recovery (LQG/LTR) technique was discovered as researchers attempted to find an answer to the following question:

"How do we obtain the stability and robustness guarantees of the LQ technique, in the face of the real-world constraints of having to reconstruct unknown states with a Kalman filter whose state model parameters are virtually guaranteed not to be equivalent to those of the real-world plant?"

There are actually two subproblems associated with the above question, and these subproblems relate to the point at which the loop is broken. If the loop is broken at the plant output (see Figure 2.5), then the relevant loop transfer matrix is $\underline{T}^{o}(s) = \underline{G}(s)\underline{K}(s)$ where $\underline{G}$ refers to the plant transfer function and $\underline{K}$ refers to the compensator transfer function. For this case, one designs a proper Kalman-Bucy filter (KBF) which satisfies the given frequency-domain design requirements and constraints, and then "recovers" the full-state loop transfer properties by judicious choice of the design parameters available in the LQR. This technique (Kwakernaak, 1969) was originally referred to as a "sensitivity recovery" procedure.

Conversely, if the loop is broken at the plant input, then the relevant loop transfer matrix is $\underline{T}^{i}(s) = \underline{K}(s)\underline{G}(s)$. For this case, one designs a proper LQ regulator which satisfies the given frequency-domain design requirements and constraints, and then "recovers" the full-state loop transfer properties by judicious choice of the design parameters available in the KBF. This technique is a mathematical dual to the first procedure, and its discovery is credited to Doyle and Stein (1979).

The mathematical derivations of the above relationships are adequately elucidated in the references mentioned, and they will not be repeated here.

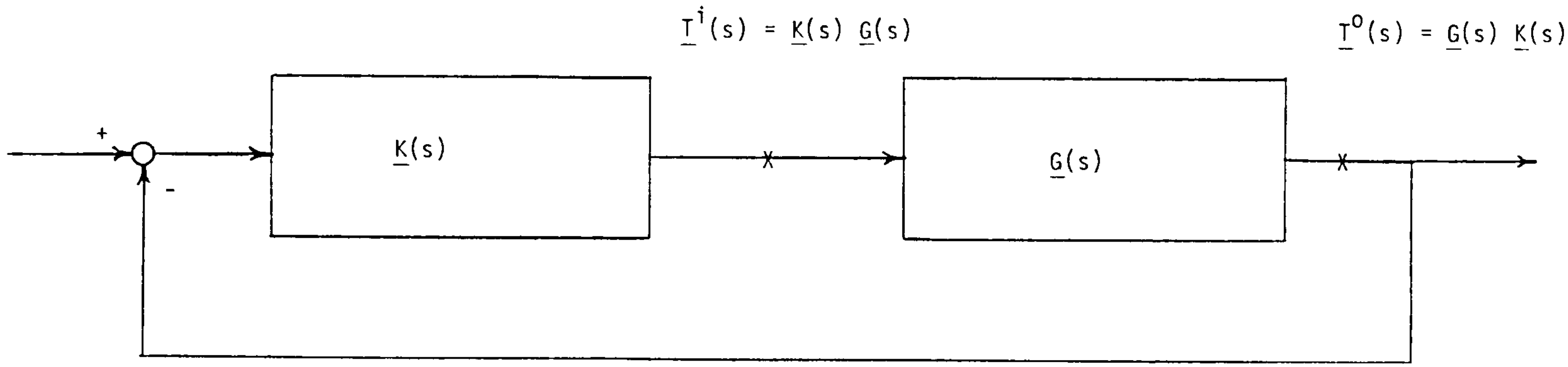

Figure 2.5. Loop transfer matrices $\underline{T}^i(s)$ and $\underline{T}^o(s)$.

However, there are some relevant points to be mentioned here that add perspective and broaden the scope of applicability of the loop transfer recovery technique:

- The current literature allows use to recover properties only at the plant input or the plant output. As of yet, there are no procedures which allow us to simultaneously guarantee properties at the plant input and and the plant output, but current H^{∞}-based work holds promise.
- These procedures are actually more encompassing than the pure LQG/LTR problem. Other more general techniques, such as observers (for state reconstruction) and pole placement (for feedback law generation) can also be utilized. The vital necessary condition is that one define a scalar functional parameterization of the filter or controller gains which assures stability at all points along the path of the scalar, and that one be guaranteed of appropriate asymptotic limiting behavior (Doyle and Stein, 1979, p. 608). The recognition of this fact has led Athans to expand the entire technique into the Model Based Compensator/Loop Transfer Recovery (MBC/LTR) procedure. The use of the KBF and LQR techniques within the MBC/LTR procedure is not demanded, but is motivated by the presence of readily-available computation software for solving the KBF and LQR Riccati equations, and by the theoretical guarantees related to stability and asymptotic behavior contained within the KBF and LQR techniques.

- Most of the real-world problems relate to performance guarantees for the plant's output variables. We can readily describe the desired performance of the real-world system in terms of command following and output disturbance rejection, and we frequently desire for robustness properties to be associated with the plant output. Consequently, most of the examples described in the literature (Kappos, 1983; Kapasouris, 1984) involve the design of a full-state KBF, and subsequent recovery of loop transfer properties with iterations on the Riccati equation describing the LQ regulator.

E. CHAPTER SUMMARY

In this chapter, we have outlined all of the basic mathematics necessary to describe continuous LQ regulators. We have also outlined briefly some ideas connecting basic SISO and MIMO properties. Singular values were introduced in the context of loop robustness, and some robustness results and limitations for LQ and LQG loops were discussed.

At this stage, the reader should have a reasonably clear picture of the current situation: we now have at hand techniques and software for producing high quality filter and regulator designs. It is still uncertain how these design techniques (in particular singular value analysis) can be extended to perform command following and disturbance rejection for the LQ regulator. These extensions form the basis for the next chapter and the remainder of this work.

CHAPTER III

ON EXPANDING THE ROLE OF "OPTIMAL" CONTROL THEORY

A. CHAPTER INTRODUCTION

Up until this point, we have dealt exclusively with LQ regulators - compensators designed to force internal nonzero states back to zero. Such devices have limited practical utility in the chemical process control world. The more appropriate device would be a modification of the standard LQ regulator formulation which would allow for command-following and output-disturbance rejection. The next section of this chapter illustrates one way that the standard LQ regulator can be modified to incorporate such needs.

This modified LQR - dubbed the LQ servo by Athans - has a loop transfer function which is considerably different from the standard LQ regulator. As of yet, there are no theoretical foundations for directly setting the singular values of the modified LQR. In the next section of the chapter, we briefly examine potential theoretical modifications of the LQ servo in an attempt to directly set these singular values, or at least to set them by some inferential means.

Also included is a complete examination of the LQ servo for the simplest possible case - two-state and three-state plants. The results of these rather tedious algebraic exercises illustrate that there are no clearly-seen general principles which relate the LQ regulator and the LQ servo. However, there is one broad familial relationship which is demonstrated - the overall transfer functions of both LQ forms exhibited similar dynamic structure - identical numbers of zeros and poles.

Given the lack of theoretical guidance, and connectivity between the LQ forms, and the lengthy expressions which characterize the closed forms, what is needed is good computer software which will allow the designer to closely interact with the computer during the design stage. This issue will be the principal topic of Chapter IV.

B. ADAPTING THE LINEAR QUADRATIC REGULATOR FOR COMMAND FOLLOWING AND DISTURBANCE REJECTION

The material up to this point has served to establish a proper mathematical perspective in the mind of the reader. This next section serves as an introduction to the major focus of the remainder of this work - the proper adaptation of the LQR for command following (the servomechanism problem) and for output disturbance rejection (the regulator problem).

This material follows closely the presentation of Athans and Stein (1984, 840418/6232 notes). It was their presentation that first attracted this author's attention to this particular area of research, and much of the remaining numerical study in this work relates directly to the mathematics of their modified LQ regulator.

In principle, one accepts the output of the system to be a subvector of the system's state vector. One can then partition the LQ regulator feedback gain matrix into two submatrices - one multiplied by the output vector and the other multiplied by the vector containing all of the states not included in the output vector.

This partitioning defines the LQ servo structure of Figure 3.1. This structure is really an ad hoc proposition arising out of the need to show proper system entry points for reference commands (setpoints), and for output disturbances. Note that, in Figure 3.1, the LQ servo collapses into the conventional LQ regulator if the command signals and disturbance signals are zero. Note also that the presence of these exogenous signals in the LQ servo structure is merely a device to make the conventional LQ regulator act on an apparent nonzero fictitious "state."

The LQ Servo

We next describe Athans' LQ servo in more detailed terms. The notation and terminology to be used in the remainder of this work will be defined in this section.

He begins with the standard LTI state space model:

$$\dot{\underline{x}}(t) = \underline{A}\ \underline{x}(t) + \underline{B}\ \underline{u}(t)$$

where $\underline{x}(t)$ is n-dimensional and $\underline{u}(t)$ is m-dimensional.

A conventional, full-state LQ regulator has the following form:

$$\underline{u}(t) = -\ \underline{G}\ \underline{x}(t)$$

Athans' next presumption is that the output vector, $\underline{y}_p(t)$ is a subvector of the state vector itself:

$$\underline{x}(t) = \begin{bmatrix} \underline{y}_p(t) \\ \cdots\cdots \\ \underline{x}_r(t) \end{bmatrix} \begin{matrix} \} \ \text{dim(mx1)} \\ \\ \} \ \text{dim(n-m)x1} \end{matrix}$$

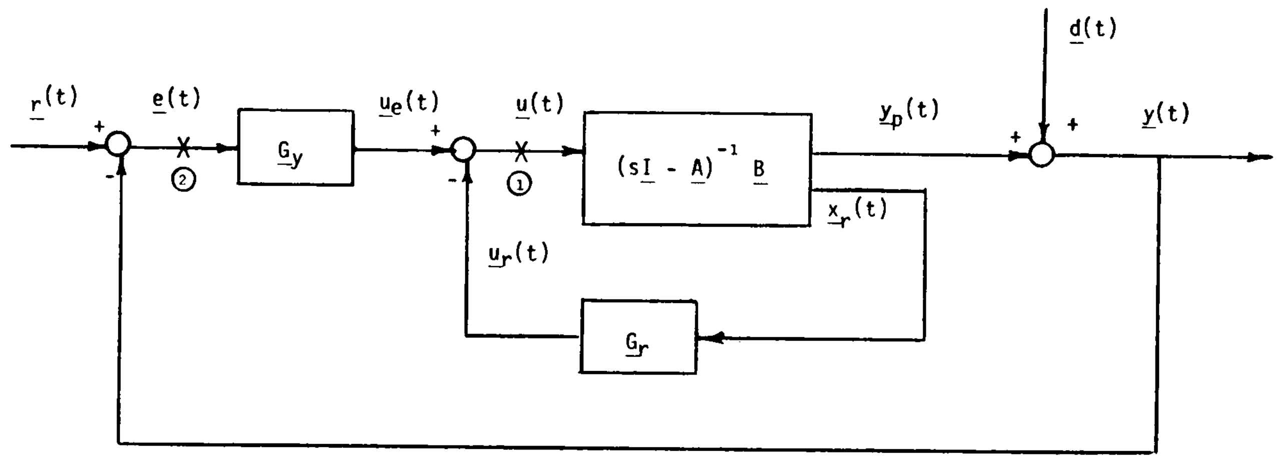

Figure 3.1. The LQ servo structure.

The dimension of $\underline{y}_p(t)$, m, is assumed to be equal to that of the input $\underline{u}(t)$, so that we have a square system. Note that we could derive a more general form, such as $\underline{y} = \underline{E}\ \underline{y}_p$, so that the output $\underline{y}$ would be a linear combination of the state subvector $\underline{y}_p$. However, such a general form is a fairly straightforward extension of the simpler form given here, and its inclusion obscures some important details.

The plant model is now:

$$\dot{\underline{x}}(t) = \underline{A}\ \underline{x}(t) + \underline{B}\ \underline{u}(t)$$

$$\underline{y}_p(t) = \underline{C}_p\ \underline{x}(t) \text{ where}$$

$$\underline{C}_p = \left[\underline{I}_{mxm} \ \vdots\ \underline{0}_{mx(n-m)}\right]$$

The partitioning of $\underline{x}(t)$ into $\underline{y}_p(t)$ and $\underline{x}_r(t)$ allows us to partition $\underline{G}$ as follows:

$$\underline{G} = [\underline{G}_y \ \vdots\ \underline{G}_r] \text{ where } \underline{G}_y \text{ is mxm and } \underline{G}_r \text{ is mx(n-m)}$$

The control vector $\underline{u}(t)$ is now given by:

$$\underline{u}(t) = -\ \underline{G}_y\ \underline{y}_p(t) - \underline{G}_r\ \underline{x}_r(t)$$

Athans next transforms the partitioned LQ regulator into the LQ servo by adding in summing junctions to incorporate the command inputs and disturbance signals. Refer again to Figure 3.1 for notation and LQ servo structure.

We are now faced with a problem: different loop transfer function matrices for the LQ regulator and for the LQ servo. The LQ regulator's loop transfer function is, as always,

$$\underline{T}_1(s) = \underline{G}_{LQ}(s) = \underline{G}(s\underline{I} - \underline{A})^{-1}\underline{B}$$

However, this matrix is different from the transfer matrix from $\underline{e}(s)$ to $\underline{y}_p(s)$:

$$\underline{T}_2(s) = \underline{Q}(s)\ \underline{G}_y \text{ where}$$

$$\underline{Q}(s) = \underline{C}_p(s\underline{I} - \underline{A} + \underline{B}\ \underline{G}_r\ \underline{D}_p)^{-1}\underline{B}$$

and

$$\underline{D}_p = [\underline{O}_{(n-m)xm} \vdots \underline{I}_{(n-m)x(n-m)}]$$

to allow for $\underline{x}_r(t)$ to be written as a function of $\underline{x}(t)$

$$\underline{x}_r(t) = \underline{D}_p\ \underline{x}(t)$$

We have at hand a number of tools for working with the LQ regulator to achieve desirable loop shapes in the frequency domain (i.e., plots of $\underline{T}_1(s)$ loop transfer singular values as a function of frequency). However, such tools do not exist for directly establishing the singular values of $\underline{T}_2(s)$. Through the defining relationships for $\underline{T}_1(s)$ and $\underline{T}_2(s)$, we know that, once we establish the singular values for $\underline{T}_1(s)$, then the singular values of $\underline{T}_2(s)$ are fixed - "what you see is what you get." The next section of this chapter examines the mathematics at hand to see if there are any tools or relationships available to us for directly setting the singular values of $\underline{T}_2(s)$.

C. CAN WE SHAPE THE SINGULAR VALUES OF $T_2(s)$ DIRECTLY?

In this section, we look at two potential routes for directly setting the singular values of $\underline{T}_2(s)$, the transfer function relating the output vector $\underline{y}_p(s)$ to the error vector $\underline{e}(s)$.

A Modified Kalman Frequency Domain Equality (KFDE)

The full KFDE for the LQ regulator looks like:

$$[\underline{I} + \underline{G}_{LQ}]^H \underline{R} [\underline{I} + \underline{G}_{LQ}] = \underline{R} + \underline{G}_{OL}{}^H \underline{G}_{OL}$$

where $\underline{G}_{LQ} = \underline{G}(s\underline{I} - \underline{A})^{-1}\underline{B}$

$$\underline{G}_{OL} = \underline{C}(s\underline{I} - \underline{A})^{-1}\underline{B}$$

and $\underline{R}$ is the control weighting matrix in the quadratic performance index.

For the special case where $\underline{R} = \rho\ \underline{I}$, we have:

$$[\underline{I} + \underline{G}_{LQ}]^H [\underline{I} + \underline{G}_{LQ}] = \underline{I} + 1/\rho\ \underline{G}_{OL}^H \underline{G}_{OL}$$

One can then substitute the partitioned LQ servo $\underline{G}$ matrix ($\underline{G}$ = $[\underline{G}_y \vdots \underline{G}_r]$) into the above relationship and work backward. Such an approach yielded a great deal of algebra and no new insights for this author.

As an alternative approach, one can begin with the LQ regulator feedback gain matrix definition, $\underline{G} = \underline{R}^{-1}\underline{B}'\underline{K}$, or its equivalent, $(\underline{B}')^{-1}\underline{R}\ \underline{G} = \underline{K}$, substitute the partitioned matrix definition, and work forward in the Control Algebraic Riccati Equation in a fashion similar to the KFDE proof. This approach also proved fruitless.

The fundamental reason for lack of success with this approach is that the act of merely partitioning the gain matrix into the $\underline{G}_y$ and $\underline{G}_r$ submatrices for the LQ servo introduces no new information. We are still viewing only a single relationship, the CARE, and the only relationship which can be derived (the KFDE) is one involving properties of the overall gain matrix only. Viewed externally, the LQ servo and the LQ regulator are identical.

Use of Matrix Algebra Identities

This approach would suggest that we examine the component parts of $\underline{T}_2(s)$ with an eye toward reducing some of the terms to their counterparts in the $\underline{T}_1(s)$ LQ regulator loop transfer function. One might then transform, through these identities, information easily obtainable in the $\underline{T}_1(s)$ formulation to the $\underline{T}_2(s)$ formulation.

More specifically, the interior term in $\underline{T}_2(s)$ looks like:

$$[s\underline{I} - \underline{A} + \underline{B}\ \underline{G}_r\ \underline{D}_p]^{-1}$$

One might be able to group the $(s\underline{I} - \underline{A})$ terms and then apply the Matrix Inversion Lemma (MIL):

$$[\underline{A} + \underline{B}\ \underline{C}\ \underline{D}]^{-1} = \underline{A}^{-1} - \underline{A}^{-1}\underline{B}(\underline{C}^{-1} + \underline{D}\ \underline{A}^{-1}\underline{B})^{-1}\ \underline{D}\ \underline{A}^{-1}$$

A moment's reflection suggests a problem with this approach: incompatible dimensionality. The matrices which we would substitute for $\underline{B}$, $\underline{C}$, and $\underline{D}$ in the above MIL are $\underline{B}$, $\underline{G}_r$, and $\underline{D}_p$, respectively, and are non-square. There may be some other matrix identity which sill circumvent this problem involving, e.g., the Moore-Penrose pseudoinverse, but its existence is unknown to this author.

From the above two approaches, there appear to be no theoretical relationships which would allow us to directly set the singular values of $\underline{T}_2(s)$, given complete knowledge of the elements of the $\underline{T}_1(s)$ loop transfer matrix. The alternative are to either derive an overall relationship, matrix element by matrix element, or to use a purely numerical approach at each point in frequency space. Obviously, the latter approach would demand good software and an interactive session with a computer.

D. A SET OF LOW-ORDER ALGEBRAIC EXAMPLES

In this section, we begin an attempt to make up for the lack of serious theoretical guidance when dealing with the LQ servo. We look at the simplest possible system structure in which an output vector is a subvector of the state vector, and we carry through the calculations on an element-by-element algebraic basis. We next compare these algebraic results with their LQ regulator counterparts in an attempt to move from the specific to the general.

We examine the following form:

Example 1:

$\underline{\dot{x}}(t) = \underline{A}\ \underline{x}(t) + \underline{B}\ \underline{u}(t)$ where n = 2 and m = 1 (i.e., scalar input and output)

$$\begin{bmatrix} \dot{x}_1 \\ \dot{x}_2 \end{bmatrix} = \begin{bmatrix} a_{11} & a_{12} \\ a_{21} & a_{22} \end{bmatrix} \begin{bmatrix} x_1 \\ x_2 \end{bmatrix} + \begin{bmatrix} b_{11} \\ b_{12} \end{bmatrix} m_1$$

$$\text{where} \quad \underline{x}(t) \left\langle \begin{bmatrix} x_1 \\ x_2 \end{bmatrix} \right. = \begin{bmatrix} x_1 \\ \cdots \\ x_2 \end{bmatrix} \begin{matrix} \rangle\ \underline{y}_p(t) \\ \rangle\ \underline{x}_r(t) \end{matrix}$$

$$\underline{u}(t) = -\ \underline{G}\ \underline{x}(t) = -\ \underline{G}_y\ \underline{y}_p(t) - \underline{G}_r\ \underline{x}_r(t)$$

$$u_1 = [g_{11} \ \vdots \ g_{12}] \begin{bmatrix} x_1 \\ x_2 \end{bmatrix} \qquad \begin{matrix} \underline{G}_y = g_{11} \\ \underline{G}_r = g_{12} \end{matrix}$$

For this case, $\underline{y}_p(t) = \underline{C}_p\ \underline{x}(t)$ looks like:

$$\underline{y}_p(t) = x_1 = [1 \quad 0] \begin{bmatrix} x_1 \\ x_2 \end{bmatrix}$$

and $\underline{x}_r(t) = \underline{D}_p\ \underline{x}(t)$ looks like:

$$\underline{x}_r(t) = x_2 = [0 \quad 1] \begin{bmatrix} x_1 \\ x_2 \end{bmatrix}$$

We can now form $\underline{B}\ \underline{G}_r\ \underline{D}_p$:

$$\begin{bmatrix} b_{11} \\ b_{21} \end{bmatrix} [g_{12}] \quad [0 \quad 1] \quad = \begin{bmatrix} 0 & b_{11}g_{12} \\ 0 & b_{21}g_{12} \end{bmatrix}$$

We can also form $\underline{T}_2(s) = \underline{C}_p(s\underline{I} - \underline{A} + \underline{B}\ \underline{G}_r\underline{D}_p)^{-1}\underline{B}\ \underline{G}_y$

$$\underline{T}_2(s) = [1 \quad 0] \begin{bmatrix} s - a_{11} & -a_{12} + b_{11}g_{12} \\ -a_{21} & s - a_{22} + b_{21}g_{12} \end{bmatrix}^{-1} \begin{bmatrix} b_{11} \\ b_{12} \end{bmatrix} \quad g_{11}$$

Recall the form for 2 x 2 inversion:

$$\begin{bmatrix} a & b \\ c & d \end{bmatrix}^{-1} = \frac{\begin{bmatrix} d & -b \\ -c & a \end{bmatrix}}{ad - bc}$$

Now $\underline{T}_2(s)$ looks like:

$$\frac{[1 \quad 0]}{D_2} \begin{bmatrix} s - a_{22} + b_{21}g_{12} & a_{12} - b_{11}g_{12} \\ a_{21} & s - a_{11} \end{bmatrix} \begin{bmatrix} b_{11} \\ b_{12} \end{bmatrix} \quad g_{11}$$

where $D_2 = (s - a_{11})(s - a_{22} + b_{21}g_{12})$

which simplifies to:

$$\frac{b_{11}g_{11}}{D_2}(s - a_{22} + b_{21}g_{12}) + \frac{b_{21}g_{11}}{D_2}(a_{12} - b_{11}g_{12})$$

and finally:

$$\underline{T}_2(s) = \frac{(b_{11}g_{11})s + (a_{12}b_{21}g_{11} - a_{22}b_{11}g_{11})}{s^2 - (a_{11}+a_{22}-b_{21}g_{12})s+(a_{11}a_{22}-a_{12}a_{21}-a_{11}b_{21}g_{12}-a_{21}b_{11}g_{12})}$$

For the corresponding LQ regulator, the loop transfer function $\underline{T}_1(s)$ is

$$\underline{T}_1(s) = \underline{G}\,(s\underline{I} - \underline{A})^{-1}\,\underline{B} =$$

$$\frac{[g_{11} \quad g_{12}]}{D_1}\begin{bmatrix} s - a_{22} & a_{12} \\ a_{21} & s - a_{11} \end{bmatrix}\begin{bmatrix} b_{11} \\ b_{21} \end{bmatrix}$$

where $D_1 = (s - a_{11})(s - a_{22}) - a_{12}a_{21}$

and finally:

$\underline{T}_1(s) =$

$$\frac{(b_{11}g_{11} + b_{21}g_{12})s + (-a_{11}b_{21}g_{12} + a_{12}b_{21}g_{11} + a_{21}b_{11}g_{12} - a_{22}b_{11}g_{11})}{s^2 - (a_{11} + a_{22})s + (a_{11}a_{22} - a_{12}a_{21})}$$

A term-by-term comparison indicates the following:

1. Both $\underline{T}_1(s)$ and $\underline{T}_2(s)$ have similar structures:

$$\frac{K_1 s + K_2}{s^2 + K_3 s + K_4}$$

   but with different K_i coefficients. Almost all that can be said is that the two transfer functions will exhibit similar overall dynamic characteristics, but with differing pole and zero locations in the s-plane.

2. $\underline{T}_1(s)$ can be made equivalent to $\underline{T}_2(s)$ for the following case:

$$g_{11} = 1$$

$$g_{21} = 0$$

   This result suggests a possible extrapolation into a more general case:

$$\underline{G} = \underline{I}$$

i.e., diagonal elements equal to one; nondiagonal elements equal to zero.

We can attempt to extend our speculation by looking at our 2-state, 1-input/output example for the situation where $\underline{G} = k\underline{I}$, i.e., a very strongly diagonally dominant LQ gain matrix. For this situation, we have

$$\underline{T}_1(s) = \frac{(b_{11}k)s + (a_{12}b_{21}k - a_{22}b_{11}k)}{s^2 - (a_{11} + a_{22})s + (a_{11}a_{22} - a_{12}a_{21})}$$

$$= \frac{k[(b_{11})s + (a_{12}b_{21} - a_{22}b_{11})]}{s^2 - (a_{11} + a_{22})s + (a_{11}a_{22} - a_{12}a_{21})}$$

and

$$\underline{T}_2(s) = \frac{(b_{11}k)s + (a_{12}b_{21}k - a_{22}b_{11}k)}{s^2 - (a_{11} + a_{22})s + (a_{11}a_{22} - a_{12}a_{21})}$$

Note that, like our previous case, $\underline{T}_1(s)$ and $\underline{T}_2(s)$ are again equivalent forms. This situation suggests an invariance under gain scaling: when plotted against frequency, the singular values of $\underline{T}_1(jw)$ and $\underline{T}_2(jw)$ are identical for the case of $\underline{G} = k\underline{I}$. Further, the $\underline{T}_1(jw)$ and $\underline{T}_2(jw)$ plots exhibit identical shifts upwards or downwards on the amplitude axis as the gain parameter k increases or decreases.

<u>Example 2</u>: Assume a 3-state, 1-input/output case

$$\begin{bmatrix} \dot{x}_1 \\ \dot{x}_2 \\ \dot{x}_3 \end{bmatrix} = \begin{bmatrix} a_{11} & a_{12} & a_{13} \\ a_{21} & a_{22} & a_{23} \\ a_{31} & a_{32} & a_{33} \end{bmatrix} \begin{bmatrix} x_1 \\ x_2 \\ x_3 \end{bmatrix} + \begin{bmatrix} b_{11} \\ b_{21} \\ b_{31} \end{bmatrix} u_1$$

where $x(t) \left\langle \begin{bmatrix} x_1 \\ x_2 \\ x_3 \end{bmatrix} \right. = \begin{bmatrix} x_1 \\ \cdots \\ x_2 \\ x_3 \end{bmatrix} \begin{matrix} \rangle \underline{y}_p(t) \\ \rangle \underline{x}_r(t) \end{matrix}$

and

$$u_1 = \underline{u}(t) = - \underline{G}\ \underline{x}(t) = - \underline{G}_y\ \underline{y}_p(t) - \underline{G}_r\ \underline{x}_r(t)$$

$$u_1 = [g_{11} \ \vdots \ g_{12} \quad g_{13}] \begin{bmatrix} x_1 \\ x_2 \\ x_3 \end{bmatrix} \qquad \begin{matrix} \underline{G}_y = g_{11} \\ \underline{G}_r = [g_{12} \quad g_{13}] \end{matrix}$$

$\underline{y}_p(t) = \underline{C}_p\ \underline{x}(t)$ looks like:

$$\underline{y}_p(t) = x_1 = [1 \quad 0 \quad 0] \begin{bmatrix} x_1 \\ x_2 \\ x_3 \end{bmatrix}$$

and $\underline{x}_r(t) = \underline{D}_p\ \underline{x}(t)$ looks like:

$$\underline{x}_r(t) = \begin{bmatrix} x_2 \\ x_3 \end{bmatrix} = \begin{bmatrix} 0 & 1 & 0 \\ 0 & 0 & 1 \end{bmatrix} \begin{bmatrix} x_1 \\ x_2 \\ x_3 \end{bmatrix}$$

We now form $\underline{B}\ \underline{G}_r\ \underline{D}_p$:

$$\begin{bmatrix} b_{11} \\ b_{21} \\ b_{31} \end{bmatrix} [g_{12} \quad g_{13}] \begin{bmatrix} 0 & 1 & 0 \\ 0 & 0 & 1 \end{bmatrix}$$

But, by assumption, $g_{12} = g_{13} = 0$, and $\underline{B}\ \underline{G}_r\ \underline{D}_p = \underline{0}$ for this case.

Then $\underline{T}_2(s) =$

$$[1 \quad 0 \quad 0] \ (s\underline{I} - \underline{A})^{-1}\ \underline{B}\ g_{11}$$

which is identical to the transfer function $\underline{T}_1(s)$ for the case of diagonally dominant $\underline{G}$ (i.e., cases for which $\underline{G}_{ij} \neq 0$, $i = j$, $\underline{G}_{ii} = k$).

<u>Example 3</u>: Assume a 3-state, 2-input/output case

$$\begin{bmatrix} \dot{x}_1 \\ \dot{x}_2 \\ \dot{x}_3 \end{bmatrix} = \begin{bmatrix} a_{11} & a_{12} & a_{13} \\ a_{21} & a_{22} & a_{23} \\ a_{31} & a_{32} & a_{33} \end{bmatrix} \begin{bmatrix} x_1 \\ x_2 \\ x_3 \end{bmatrix} + \begin{bmatrix} b_{11} & b_{12} \\ b_{21} & b_{22} \\ b_{31} & b_{32} \end{bmatrix} \begin{bmatrix} u_1 \\ u_2 \end{bmatrix}$$

where

$$\underline{x}(t) \left\langle \begin{bmatrix} x_1 \\ x_2 \\ x_3 \end{bmatrix} \right. = \begin{bmatrix} x_1 \\ x_2 \\ \cdots \\ x_3 \end{bmatrix} \begin{matrix} \left.\vphantom{\begin{matrix} x_1 \\ x_2 \end{matrix}}\right\rangle \underline{y}_p(t) \\ \left.\vphantom{x_3}\right\rangle \underline{x}_r(t) \end{matrix}$$

and $\underline{u}(t) = - \underline{Gx}(t) = - \underline{G}_y \, \underline{y}_p(t) - \underline{G}_r \, \underline{x}_r(t)$

$$\begin{bmatrix} u_1 \\ u_2 \end{bmatrix} = \left[\begin{array}{cc:c} g_{11} & g_{12} & g_{13} \\ g_{21} & g_{22} & g_{23} \end{array}\right] \begin{bmatrix} x_1 \\ x_2 \\ x_3 \end{bmatrix}$$

$$\underline{G}_y = \begin{bmatrix} g_{11} & g_{12} \\ g_{21} & g_{22} \end{bmatrix} \qquad \underline{G}_r = \begin{bmatrix} g_{13} \\ g_{23} \end{bmatrix}$$

$\underline{y}_p(t) = \underline{C}_p \, \underline{x}(t)$ looks like:

$$\begin{bmatrix} x_1 \\ \\ x_2 \end{bmatrix} = \begin{bmatrix} 1 & 0 & . & 0 \\ & & . & \\ 0 & 1 & . & 0 \end{bmatrix} \begin{bmatrix} x_1 \\ x_2 \\ x_3 \end{bmatrix}$$

and $\underline{x}_r(t) = \underline{D}_p\ \underline{x}(t)$ looks like:

$$\underline{x}_r(t) = x_3 = [0 \quad 0 \quad 1] \begin{bmatrix} x_1 \\ x_2 \\ x_3 \end{bmatrix}$$

We now form $\underline{B}\ \underline{G}_r\ \underline{D}_p$:

$$\begin{bmatrix} b_{11} & b_{12} \\ b_{21} & b_{22} \\ b_{31} & b_{32} \end{bmatrix} \begin{bmatrix} g_{13} \\ g_{23} \end{bmatrix} [0 \quad 0 \quad 1]$$

Performing the indicated multiplication, we have $\underline{B}\ \underline{G}_r\ \underline{D}_p$ =

$$\begin{bmatrix} 0 & 0 & b_{11}g_{13} + b_{12}g_{23} \\ 0 & 0 & b_{21}g_{13} + b_{22}g_{23} \\ 0 & 0 & b_{31}g_{13} + b_{32}g_{23} \end{bmatrix}$$

Given that the g_{ij} elements equal zero ($i \neq j$), $\underline{T}_2(s)$ then looks like:

$$\begin{bmatrix} 1 & 0 & 0 \\ 0 & 1 & 0 \end{bmatrix} (s\underline{I} - \underline{A})^{-1} \underline{B} \begin{bmatrix} g_{11} & 0 \\ 0 & g_{22} \end{bmatrix}$$

Note that the net effect of zero off-diagonal elements is to eliminate the $\underline{B}\ \underline{G}_r\ \underline{D}_p$ matrix.

Let the elements of the nxm matrix $(s\underline{I} - \underline{A})^{-1}\ \underline{B}$ be denoted by z_{ij}.

$\underline{T}_2(s)$ now looks like:

$$\begin{bmatrix} g_{11}z_{11} & g_{22}z_{12} \\ g_{11}z_{21} & g_{22}z_{22} \end{bmatrix}$$

By way of comparison, we form $\underline{T}_1(s) = \underline{G}(s\underline{I} - \underline{A})\underline{B}$:

$$\begin{bmatrix} g_{11}z_{11} & g_{22}z_{12} \\ g_{11}z_{21} & g_{22}z_{22} \end{bmatrix}$$

which is identical to the expression for $\underline{T}_2(s)$.

Note that in this case, we do not require $g_{11} = g_{22}$; all that is necessary is that the $g_{ij} \neq 0$ for $i = j$. One can easily extend this methodology to higher order models in an inductive fashion, and achieve similar results.

E. CHAPTER SUMMARY

In this chapter, we have illustrated the approach taken by Athans in defining the LQ servo - an ad hoc modification to the LQ regulator to allow inclusion of the real world necessities of command following and output disturbance rejection.

In the next section, we made an attempt to derive theoretically sound techniques which would allow us to directly set the loop singular values of the LQ servo. We note that such attempts are not successful principally due to the fact that the LQ servo is a simple internal modification to the LQ regulator, and all of the good theoretical properties and potential avenues of exploration involve external properties of the LQ regulator.

We are now ready to summarize the results achievable through term-by-term algebraic analysis:

- the pole-zero structures of $\underline{T}_1(s)$ and $\underline{T}_2(s)$ will be similar, but the actual locations of the poles and zeros will be influenced by the size of the off-diagonal elements in the LQ gain matrix.
- For situations in which the designer's choices of weighting parameters in the CARE have resulted in a diagonally-dominant

LQ gain matrix, the loop singular value plots for $\underline{T}_1(s)$ and $\underline{T}_2(s)$ will be identical. By diagonally-dominant, we mean a matrix with $E_{ij} = 0$ for all $i \neq j$.

- The effect of increasing off-diagonal LQ gain elements is to add in more contribution of the $\underline{B}$ matrix and the $\underline{G}_r$ matrix, through the effect of the $\underline{B}\ \underline{G}_r\ \underline{D}_p$ term in the $\underline{T}_2(s)$ expression:

$$\underline{T}_2(s) = \underline{C}_p(s\underline{I} - \underline{A} + \underline{B}\ \underline{G}_r\ \underline{D}_p)^{-1}\ \underline{B}\ \underline{G}_y$$

The subsequent section outlined an alternate approach in which simple algebraic examples were explored in a term-by-term manner, to see if there was any insight to be gained on the similarity of the LQ regulator and LQ servo structures in terms of their loop transfer functions. The principal results were that the two loop transfers can be made to be nearly or exactly identical, but only in very specific, isolated (and trivial) situations in which the LQ gain matrix is very strongly diagonally dominant. As the off-diagonal elements of $\underline{G}$ become larger, the poles and zeros of $\underline{T}_1(s)$ and $\underline{T}_2(s)$ will begin to separate.

At this stage we have exhausted the two principal routes for theoretical insight into the question of directly setting LQ servo loop singular values. It appears that any additional insights will have to be obtained on a case-by-case basis using numerical analysis of a specific problem. Such an analysis is the subject of Chapter IV.

CHAPTER IV

A NUMERICAL EXAMPLE

A. CHAPTER INTRODUCTION

In this chapter, we examine a specific LQ servo numerical example to see if we can build further on the algebraic base established at the end of the previous chapter. The reader will recall that the LQ servo formulation given by Athans appeared to be resistant to additional theoretical development, mainly due to the fact that the LQ servo is simply an internal modification to the conventional LQ regulator. (The work of the LQ servo is accomplished by "tricking" the LQ regulator into seeing and acting upon a difference between set point and measurement as if that difference were a non-zero state. The LQ regulator, in turn, tries to drive this non-zero state toward zero.)

The specific example detailed in this chapter was selected to illustrate principles, and to reinforce notions and ideas suggested by simple algebraic analyses. The state variable representation and parameters are not selected to represent any particular physical system, but are chosen so as to illustrate our LQ servo concepts, while still having some appeal to intuition, at least for expected long-term behavior of certain states and controls.

After introducing the base-case model, we illustrate its performance in the open loop. Note that this particular model is chosen to be stable, so all non-zero initial states should ultimately relax and approach zero in the limit as time increases.

This model was chosen to have a sufficiently small number of states so as not to be overwhelming, but at the same time the model's states are sufficiently interconnected so as to defy a quick, simple analysis of what the best control ought to look like based on intuition.

The loop is next closed around our simple model with a variety of full state LQ regulators. Calculation results include the open-loop and closed-loop eigenvalues, the Riccati solution $\underline{K}$, the optimal closed-loop matrix ($\underline{A}$ - $\underline{B}$ $\underline{G}$), and the optimal gain matrix $\underline{G}$. We then illustrate the closed-loop behavior of the LQ regulator for various sets of control weighting matrices $\underline{R}$.

We next compare the LQ regulator singular value plots obtained from breaking the loop at the input, $T_1(s)$, to the singular value plots for the LQ servo, $T_2(s)$. We also compare eigenvalue locations for various feedback gain matrices, and conclude that the results of the previous chapter are correct - the LQ regulator and LQ servo have very similar pole-zero structures. The value of the specific numerical example here is in quantifying these effects, so that the control designer can acquire a "feel" for just how much pole displacement he can expect for a given set of $\underline{Q}$ and $\underline{R}$ state and control weighting matrices, and for the resulting feedback gain matrix $\underline{G}$.

The chapter concludes with some general guidelines and rules of thumb regarding the linkage of LQ regulator singular values and LQ servo singular values.

B. THE STATE SPACE PLANT MODEL

In this section, we detail the structure and parameters in our illustrative state variable model. This model was chosen more from the pedagogical perspective than from the viewpoint of representing any particular physical system.

The particular model used has six states, two control inputs, and two outputs. In its simplest form, the model (see Figure 4.1) consists of two parallel sections, each with three first-order lags in series. The corresponding state variable representation for this structure is illustrated in Figure 4.2. Note the particular numbering convention in both of these diagrams. The states chosen as outputs are x_1 and x_2, the first two of the six states in the model. This nomenclature is in keeping with that chosen for the LQ servo, where the output subvector $\underline{y}_p$ is chosen to be the first m states in the state vector. Odd numbered states are in the upper three-state section and even numbered states are in the lower three-state section. This choice allows for a more transparent structure in the system's $\underline{A}$ matrix.

We then add in the interconnections among the various system states to produce the final plant model, as illustrated in Figure 4.3. Note that in the state variable representations, we have located $1/\tau_i$ gain blocks in the proper locations so as to

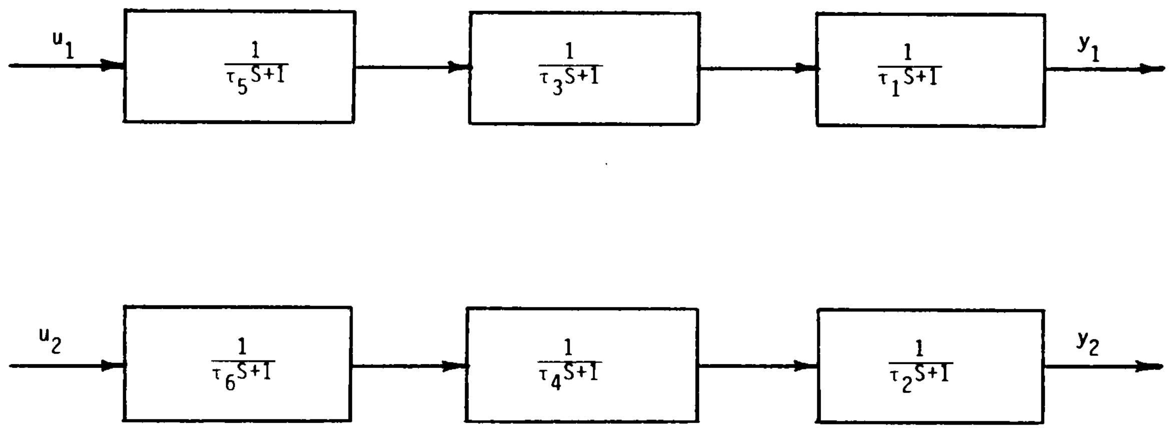

Figure 4.1. Simplified six-state plant model.

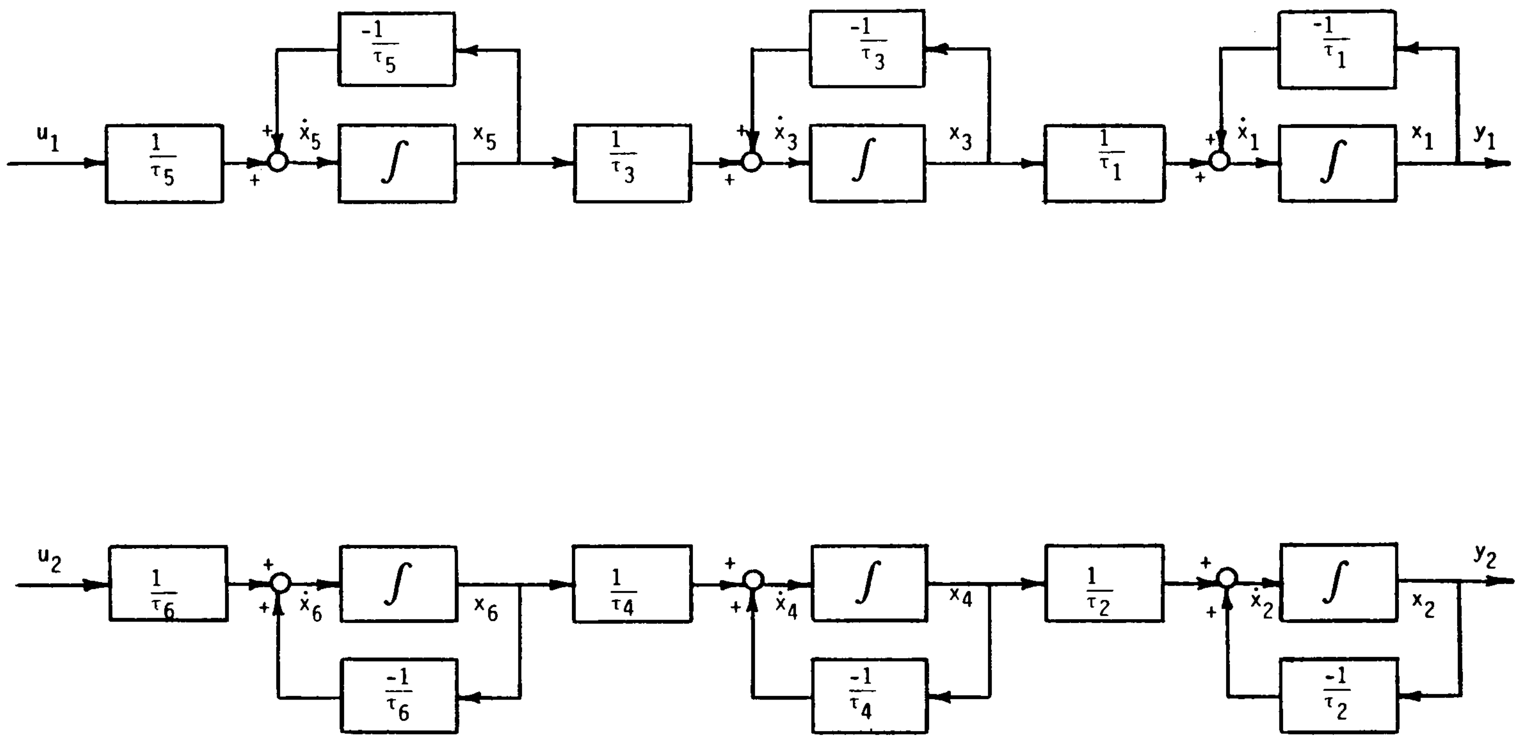

Figure 4.2. State space plant model - no interconnections.

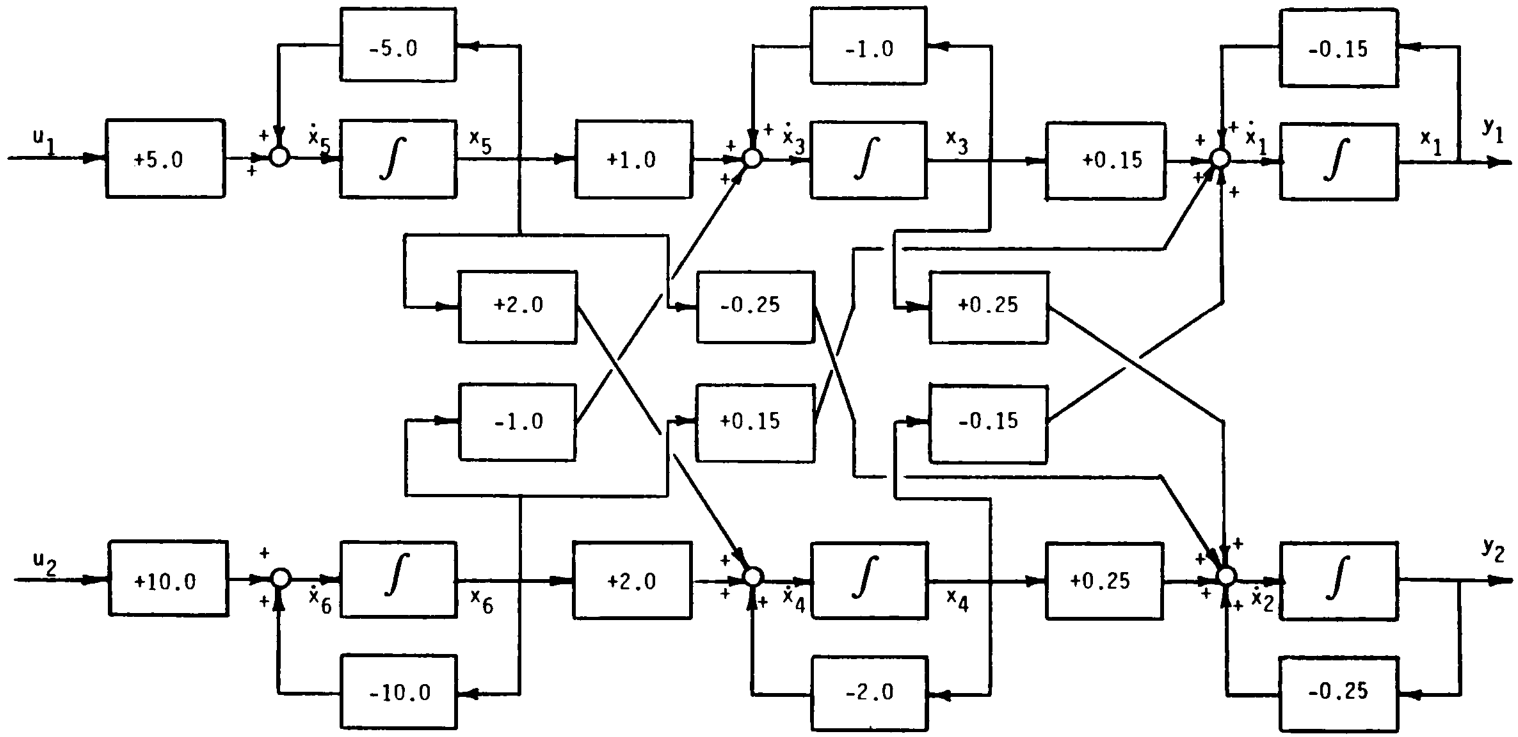

Figure 4.3. Complete state-space plant model.

provide an overall unity gain system. The degree of interconnection, plus the alternation in signs for various state additions, precludes the development of any sort of intuitively obvious multivariable control strategy.

With this particular structure, we can then write out the system ($\underline{A}$, $\underline{B}$, $\underline{C}$) triple by inspection. Due to the choice of state variable representation, the system exhibits its eigenvalues along the diagonal of the $\underline{A}$ matrix. All interconnections are displayed in the upper triangular portion of $\underline{A}$, and the lower triangular portion is null.

The parameters for the six time constants were chosen such that x_1 and x_2 would have nearly equivalent poles, as would x_3 and x_4, and x_5 and x_6. The actual values of these poles were selected to provide almost a full order of magnitude difference between successive pole locations for a given set of either three upper or three lower states. Additionally, this set of values yields singular value plots which demonstrate significant changes in the range of 0.01 to 1000 radians/sec. - the range used for all plots.

The system triple ($\underline{A}$, $\underline{B}$, $\underline{C}$) is as follows:

$$\underline{A} = \begin{bmatrix} -0.15 & 0.0 & 0.15 & -0.15 & 0.0 & 0.15 \\ 0.0 & -0.25 & 0.25 & 0.25 & -0.25 & 0.0 \\ 0.0 & 0.0 & -1.0 & 0.0 & 1.0 & -1.0 \\ 0.0 & 0.0 & 0.0 & -2.0 & 2.0 & 2.0 \\ 0.0 & 0.0 & 0.0 & 0.0 & -5.0 & 0.0 \\ 0.0 & 0.0 & 0.0 & 0.0 & 0.0 & -10.0 \end{bmatrix}$$

$$\underline{B} = \begin{bmatrix} 0.0 & 0.0 \\ 0.0 & 0.0 \\ 0.0 & 0.0 \\ 0.0 & 0.0 \\ 5.0 & 0.0 \\ 0.0 & 10.0 \end{bmatrix}$$

$$\underline{C} = \begin{bmatrix} 1.0 & 0.0 & 0.0 & 0.0 & 0.0 & 0.0 \\ 0.0 & 1.0 & 0.0 & 0.0 & 0.0 & 0.0 \end{bmatrix}$$

For all of the LQ controller design cases, we have chosen the state penalty matrix $\underline{Q}$ equal to $\underline{I}_{6x6}$. Note that no attempt was made to compress the maximum and minimum singular values through the use of a "balancing" matrix. For all of the simulation runs shown, the initial state matrix XZERO was chosen to be:

$$\underline{\mathrm{XZERO}} = \begin{bmatrix} 1 \\ -1 \\ 0 \\ 0 \\ 0 \\ 0 \end{bmatrix}$$

C. RESULTS OF SIMULATION RUNS

The LQ regulators and LQ servos were designed for a total of six cases:

$$\underline{R} = 10^{6}\ \underline{I}$$

$$\underline{R} = 10^{8}\ \underline{I}$$

$$\underline{R} = 10^{10}\ \underline{I}$$

$$\underline{R} = 10^{12}\ \underline{I}$$

$$\underline{R} = 10^{14}\ \underline{I}$$

$$\underline{R} = 10^{16}\ \underline{I}$$

The LQ regulator gain matrices, open-loop and closed-loop simulations, and singular value plots were obtained from standard software contained in the LQGALPHA package licensed from Alphatech, Inc. (Burlington, Mass.).

The LQ servo singular value calculations are currently not available in any commercial package. These singular values were calculated with an extensively-modified version of SVPLOT, the LQGALPHA singular value calculation and plotting subroutine. Since this modified version of SVPLOT contains a great deal of proprietary code, the full set of FORTRAN statements which constitute the LQ servo calculation subroutine is not included in this work. However, the LQ servo singular value calculation is straightforward linear algebra, and the specific portion of code written by this author can be quickly regenerated. The interested reader can easily mesh this code with any generalized singular value calculation routine (such as LINPACK's ZSVDC subroutine), a routine to calculate the magnitude of the system transfer function "$\underline{C}$"$(jw\underline{I}$ - "$\underline{A}$"$)^{-1}$"$\underline{B}$" as a function of frequency w, and a print-plot graphic output routine to duplicate these simulation runs. (One simply substitutes $\underline{C}_p$ for "$\underline{C}$", $\underline{A} - \underline{BG}_r\underline{D}_p$ for "$\underline{A}$", and $\underline{BG}_y$ for "$\underline{B}$" in the above program structure.)

We begin by examining the results of open-loop simulation. As shown in Figure 4.4, the system relaxes from its initial state given by XZERO towards zero. Recall that y_1, the first output, equals x_1, the first state, and y_2, the second output, equals x_2, the second state.

The next series of figures (Figures 4.5 through 4.10) details the open-loop and closed-loop eigenvalues, the Riccati solution $\underline{K}$, the optimal closed-loop matrix ($\underline{A}$ - $\underline{B}$ $\underline{G}$) and the optimal gain matrix $\underline{G}$ for each of the six sets of $\underline{R}$ matrices. Note that these six sets cover a range of 10^{10} $\underline{I}$ - enough to span the extremes from very little control weighting (relative to state weighting $\underline{Q}$) at the $\underline{R} = 10^6$ $\underline{I}$ end of the scale to an excessive amount of control weighting, at the $\underline{R} = 10^{16}$ $\underline{I}$ end of the scale. Values of $\underline{R}$ <

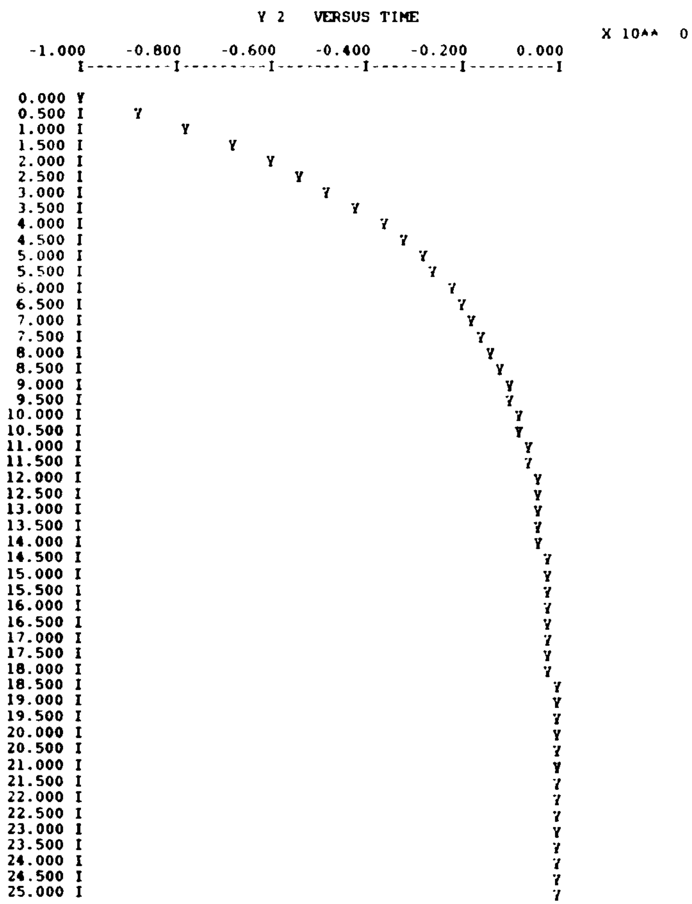

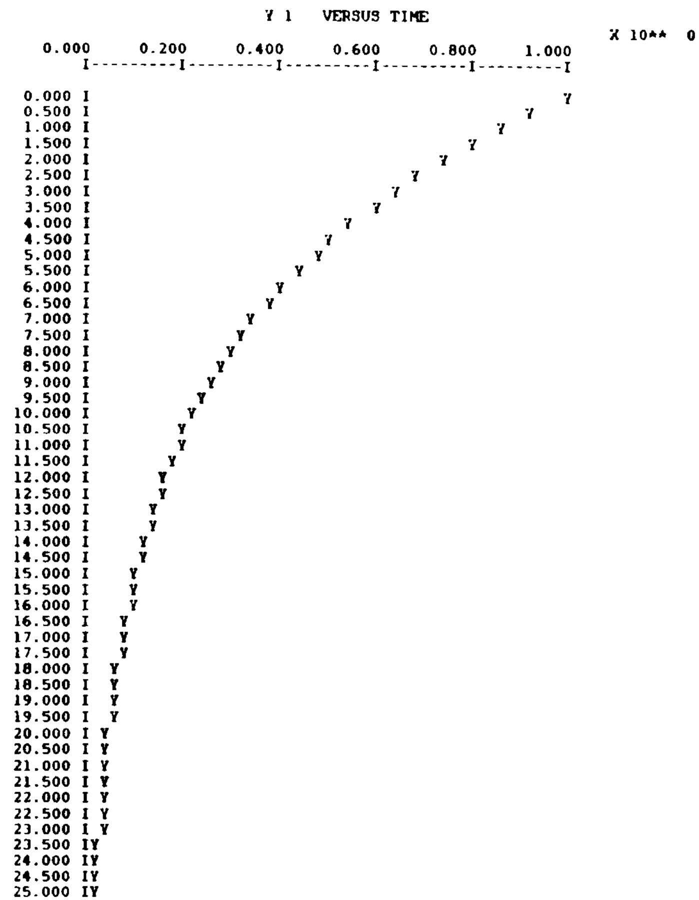

Figure 4.4. Results of open-loop simulation.

OUTPUT FROM REG

OPEN LOOP EIGENVALUES

	---EIGENVALUES---			
	REAL PART	IMAG PART	NAT FREQ(HZ)	ZETA
1	-1.500D-01	0.000D+00	1.500D-01	1.000000
2	-2.500D-01	0.000D+00	2.500D-01	1.000000
3	-1.000D+00	0.000D+00	1.000D+00	1.000000
4	-2.000D+00	0.000D+00	2.000D+00	1.000000
5	-5.000D+00	0.000D+00	5.000D+00	1.000000
6	-1.000D+01	0.000D+00	1.000D+01	1.000000

CLOSED LOOP EIGENVALUES

REAL PART	IMAGINARY PART
-0.659798543966529D-01	0.202330424183189D+01
0.295417377163920D+00	0.126932646588834D+01
0.357964501649361D-02	0.000000000000000D+00
0.262916675377791D-01	0.000000000000000D+00
-0.326536826762617D+00	0.000000000000000D+00
-0.141747465434362D+00	0.000000000000000D+00

RICCATI SOLUTION K

ROW 1	2.264D+02	-2.474D+02	1.805D+04	-3.094D+03	-2.014D+01	1.948D+03
ROW 2	1.019D+00	-1.471D+00	7.182D+01	-1.937D+01	-9.740D-02	6.915D+00
ROW 3	2.237D+01	-5.377D+01	3.994D+03	-7.966D+02	-4.475D+00	1.734D+02
ROW 4	-6.195D+01	1.022D+02	-6.106D+03	1.509D+03	7.973D+00	-3.407D+02
ROW 5	3.284D+02	-5.656D+02	6.273D+04	-8.536D+03	-2.985D+01	1.246D+03
ROW 6	-3.538D+02	6.351D+02	-2.669D+04	6.809D+03	3.932D+01	-3.579D+03

OPTIMAL CLOSED LOOP MATRIX ACL

ROW 1	-1.500D-01	0.000D+00	1.500D-01	-1.500D-01	0.000D+00	1.500D-01
ROW 2	0.000D+00	-2.500D-01	2.500D-01	2.500D-01	-2.500D-01	0.000D+00
ROW 3	0.000D+00	0.000D+00	-1.000D+00	0.000D+00	1.000D+00	-1.000D+00
ROW 4	0.000D+00	0.000D+00	0.000D+00	-2.000D+00	2.000D+00	2.000D+00
ROW 5	-8.210D-03	1.414D-02	-1.568D+00	2.134D-01	-4.999D+00	-3.116D-02
ROW 6	3.538D-02	-6.351D-02	2.669D+00	-6.809D-01	-3.932D-03	-9.642D+00

OPTIMAL GAIN MATRIX G

ROW 1	1.642D-03	-2.828D-03	3.136D-01	-4.268D-02	-1.492D-04	6.232D-03
ROW 2	-3.538D-03	6.351D-03	-2.669D-01	6.809D-02	3.932D-04	-3.579D-02

Figure 4.5. Results of LQ calculations - $\underline{R} = 10^6 \underline{I}$.

OUTPUT FROM REG

OPEN LOOP EIGENVALUES

	---EIGENVALUES---			
	REAL PART	IMAG PART	NAT FREQ(HZ)	ZETA
1	-1.500D-01	0.000D+00	1.500D-01	1.000000
2	-2.500D-01	0.000D+00	2.500D-01	1.000000
3	-1.000D+00	0.000D+00	1.000D+00	1.000000
4	-2.000D+00	0.000D+00	2.000D+00	1.000000
5	-5.000D+00	0.000D+00	5.000D+00	1.000000
6	-1.000D+01	0.000D+00	1.000D+01	1.000000

CLOSED LOOP EIGENVALUES

REAL PART	IMAGINARY PART
0.163655905165254D+01	0.188802155900189D+01
-0.188556673082882D+02	0.120107865361525D+01
0.524556611935464D-03	0.000000000000000D+00
0.257432071335525D-03	0.000000000000000D+00
-0.491274129176184D-01	0.000000000000000D+00
-0.224924700358613D-01	0.000000000000000D+00

RICCATI SOLUTION K

ROW 1	-8.604D+00	-2.620D+01	3.917D+04	-1.175D+02	1.139D+02	-9.964D+02
ROW 2	-3.534D-03	-8.604D-03	-1.963D+02	-3.072D-01	1.071D-01	4.217D-01
ROW 3	2.417D+02	4.765D+02	-1.660D+06	4.143D+03	-9.907D+02	1.379D+04
ROW 4	-1.321D+01	-4.113D+01	2.756D+05	-6.491D+02	-3.793D+02	-1.311D+03
ROW 5	1.960D+02	-3.446D+03	7.054D+07	-1.631D+05	-1.598D+05	-1.334D+05
ROW 6	1.553D+03	1.128D+03	-1.650D+07	3.868D+04	3.009D+04	-1.667D+04

OPTIMAL CLOSED LOOP MATRIX ACL

ROW 1	-1.500D-01	0.000D+00	1.500D-01	-1.500D-01	0.000D+00	1.500D-01
ROW 2	0.000D+00	-2.500D-01	2.500D-01	2.500D-01	-2.500D-01	0.000D+00
ROW 3	0.000D+00	0.000D+00	-1.000D+00	0.000D+00	1.000D+00	-1.000D+00
ROW 4	0.000D+00	0.000D+00	0.000D+00	-2.000D+00	2.000D+00	2.000D+00
ROW 5	-4.900D-05	8.616D-04	-1.764D+01	4.078D-02	-4.960D+00	3.336D-02
ROW 6	-1.553D-03	-1.128D-03	1.650D+01	-3.868D-02	-3.009D-02	-9.983D+00

OPTIMAL GAIN MATRIX G

ROW 1	9.801D-06	-1.723D-04	3.527D+00	-8.156D-03	-7.989D-03	-6.672D-03
ROW 2	1.553D-04	1.128D-04	-1.650D+00	3.868D-03	3.009D-03	-1.667D-03

Figure 4.6. Results of LQ calculations - $\underline{R} = 10^8 \underline{I}$.

OUTPUT FROM REG

OPEN LOOP EIGENVALUES

	---EIGENVALUES---			
	REAL PART	IMAG PART	NAT FREQ(HZ)	ZETA
1	-1.500D-01	0.000D+00	1.500D-01	1.000000
2	-2.500D-01	0.000D+00	2.500D-01	1.000000
3	-1.000D+00	0.000D+00	1.000D+00	1.000000
4	-2.000D+00	0.000D+00	2.000D+00	1.000000
5	-5.000D+00	0.000D+00	5.000D+00	1.000000
6	-1.000D+01	0.000D+00	1.000D+01	1.000000

CLOSED LOOP EIGENVALUES

REAL PART	IMAGINARY PART
0.189034525063397D+00	0.206194588311895D+01
-0.912325461736267D+00	0.131203209972072D+01
-0.609216637101171D-04	0.000000000000000D+00
0.234643862523172D-03	0.000000000000000D+00
-0.800272482051995D-02	0.000000000000000D+00
-0.577334306542972D-01	0.000000000000000D+00

RICCATI SOLUTION K

ROW 1	-8.309D+00	9.807D+00	-2.148D+03	-5.739D+00	8.008D-01	-1.113D+03
ROW 2	1.634D-04	9.262D-05	7.873D-01	-5.088D-05	-4.153D-04	-6.060D-01
ROW 3	3.709D+00	1.316D+01	2.453D+04	-2.835D+00	-2.034D+01	-2.195D+04
ROW 4	5.102D+01	-1.183D+01	3.381D+04	-3.459D+00	-2.272D+01	1.959D+03
ROW 5	2.720D+04	-9.466D+02	4.297D+06	-2.612D+02	-7.807D+02	1.595D+07
ROW 6	4.019D+03	-1.250D+03	-1.439D+06	-7.824D+01	-1.919D+03	2.243D+06

OPTIMAL CLOSED LOOP MATRIX ACL

ROW 1	-1.500D-01	0.000D+00	1.500D-01	-1.500D-01	0.000D+00	1.500D-01
ROW 2	0.000D+00	-2.500D-01	2.500D-01	2.500D-01	-2.500D-01	0.000D+00
ROW 3	0.000D+00	0.000D+00	-1.000D+00	0.000D+00	1.000D+00	-1.000D+00
ROW 4	0.000D+00	0.000D+00	0.000D+00	-2.000D+00	2.000D+00	2.000D+00
ROW 5	-6.800D-05	2.366D-06	-1.074D-02	6.529D-07	-5.000D+00	-3.988D-02
ROW 6	-4.019D-05	1.250D-05	1.439D-02	7.824D-07	1.919D-05	-1.002D+01

OPTIMAL GAIN MATRIX G

ROW 1	1.360D-05	-4.733D-07	2.148D-03	-1.306D-07	-3.904D-07	7.975D-03
ROW 2	4.019D-06	-1.250D-06	-1.439D-03	-7.824D-08	-1.919D-06	2.243D-03

Figure 4.7. Results of LQ calculations - $\underline{R} = 10^{10}\underline{I}$.

OUTPUT FROM REG

OPEN LOOP EIGENVALUES

	---EIGENVALUES---			
	REAL PART	IMAG PART	NAT FREQ(HZ)	ZETA
1	-1.500D-01	0.000D+00	1.500D-01	1.000000
2	-2.500D-01	0.000D+00	2.500D-01	1.000000
3	-1.000D+00	0.000D+00	1.000D+00	1.000000
4	-2.000D+00	0.000D+00	2.000D+00	1.000000
5	-5.000D+00	0.000D+00	5.000D+00	1.000000
6	-1.000D+01	0.000D+00	1.000D+01	1.000000

CLOSED LOOP EIGENVALUES

REAL PART	IMAGINARY PART
0.780463832833368D+01	0.207408718363416D+01
-0.124305262322416D+01	0.131986565864320D+01
0.826644925637999D-06	0.000000000000000D+00
0.656846313894064D-05	0.000000000000000D+00
-0.199129918465223D-01	0.000000000000000D+00
-0.574964056280919D-03	0.000000000000000D+00

RICCATI SOLUTION K

ROW 1	1.099D+01	2.226D+01	7.283D+05	-5.733D+02	6.992D-01	-8.061D+02
ROW 2	-1.715D-03	2.445D-03	3.836D+01	-5.471D-02	-2.284D-04	5.941D-01
ROW 3	1.754D+01	-7.298D+01	1.703D+06	2.567D+02	-2.237D+00	1.516D+04
ROW 4	3.366D+01	-1.641D+02	9.861D+04	1.105D+03	-4.875D-01	-3.044D+03
ROW 5	-2.969D+05	-2.082D+06	-1.309D+10	6.444D+06	4.579D+04	-4.233D+08
ROW 6	2.020D+03	3.559D+04	-4.000D+09	1.146D+06	-7.444D+03	2.003D+07

OPTIMAL CLOSED LOOP MATRIX ACL

ROW 1	-1.500D-01	0.000D+00	1.500D-01	-1.500D-01	0.000D+00	1.500D-01
ROW 2	0.000D+00	-2.500D-01	2.500D-01	2.500D-01	-2.500D-01	0.000D+00
ROW 3	0.000D+00	0.000D+00	-1.000D+00	0.000D+00	1.000D+00	-1.000D+00
ROW 4	0.000D+00	0.000D+00	0.000D+00	-2.000D+00	2.000D+00	2.000D+00
ROW 5	7.422D-06	5.204D-05	3.274D-01	-1.611D-04	-5.000D+00	1.058D-02
ROW 6	-2.020D-07	-3.559D-06	4.000D-01	-1.146D-04	7.444D-07	-1.000D+01

OPTIMAL GAIN MATRIX G

ROW 1	-1.484D-06	-1.041D-05	-6.547D-02	3.222D-05	2.290D-07	-2.117D-03
ROW 2	2.020D-08	3.559D-07	-4.000D-02	1.146D-05	-7.444D-08	2.003D-04

Figure 4.8. Results of LQ calculations - $\underline{R} = 10^{12}\underline{I}$.

OUTPUT FROM REG

OPEN LOOP EIGENVALUES

---EIGENVALUES---

	REAL PART	IMAG PART	NAT FREQ(HZ)	ZETA
1	-1.500D-01	0.000D+00	1.500D-01	1.000000
2	-2.500D-01	0.000D+00	2.500D-01	1.000000
3	-1.000D+00	0.000D+00	1.000D+00	1.000000
4	-2.000D+00	0.000D+00	2.000D+00	1.000000
5	-5.000D+00	0.000D+00	5.000D+00	1.000000
6	-1.000D+01	0.000D+00	1.000D+01	1.000000

CLOSED LOOP EIGENVALUES

REAL PART	IMAGINARY PART
-0.202072214443100D+00	0.207347531125256D+01
-0.369742995020908D+00	0.131994129770944D+01
-0.157130494035174D-05	0.000000000000000D+00
0.603248669745285D-05	0.000000000000000D+00
-0.318615145284600D-02	0.000000000000000D+00
-0.147192095718667D-02	0.000000000000000D+00

RICCATI SOLUTION K

ROW 1	-8.707D+02	2.946D+00	5.981D+05	-1.646D+05	-4.731D+01	-2.048D+05
ROW 2	2.971D-04	3.553D-05	-6.041D+00	2.794D-01	1.088D-04	-6.578D-01
ROW 3	-3.527D+03	-1.673D+02	1.227D+07	-3.314D+06	-1.164D+03	-4.420D+06
ROW 4	-3.332D+03	-1.321D+02	9.935D+06	-3.022D+06	-9.612D+02	-3.623D+06
ROW 5	1.207D+07	-2.693D+05	-1.267D+10	1.079D+10	1.640D+06	6.728D+09
ROW 6	-1.793D+07	3.485D+04	3.136D+10	-1.676D+10	-3.471D+06	-1.541D+10

OPTIMAL CLOSED LOOP MATRIX ACL

ROW 1	-1.500D-01	0.000D+00	1.500D-01	-1.500D-01	0.000D+00	1.500D-01
ROW 2	0.000D+00	-2.500D-01	2.500D-01	2.500D-01	-2.500D-01	0.000D+00
ROW 3	0.000D+00	0.000D+00	-1.000D+00	0.000D+00	1.000D+00	-1.000D+00
ROW 4	0.000D+00	0.000D+00	0.000D+00	-2.000D+00	2.000D+00	2.000D+00
ROW 5	-3.018D-06	6.733D-08	3.169D-03	-2.699D-03	-5.000D+00	-1.682D-03
ROW 6	1.793D-05	-3.485D-08	-3.136D-02	1.676D-02	3.471D-06	-9.985D+00

OPTIMAL GAIN MATRIX G

ROW 1	6.035D-07	-1.347D-08	-6.337D-04	5.397D-04	8.199D-08	3.364D-04
ROW 2	-1.793D-06	3.485D-09	3.136D-03	-1.676D-03	-3.471D-07	-1.541D-03

Figure 4.9. Results of LQ calculations - $\underline{R} = 10^{14}\underline{I}$.

OUTPUT FROM REG

OPEN LOOP EIGENVALUES

	---EIGENVALUES---			
	REAL PART	IMAG PART	NAT FREQ(HZ)	ZETA
1	-1.500D-01	0.000D+00	1.500D-01	1.000000
2	-2.500D-01	0.000D+00	2.500D-01	1.000000
3	-1.000D+00	0.000D+00	1.000D+00	1.000000
4	-2.000D+00	0.000D+00	2.000D+00	1.000000
5	-5.000D+00	0.000D+00	5.000D+00	1.000000
6	-1.000D+01	0.000D+00	1.000D+01	1.000000

CLOSED LOOP EIGENVALUES

REAL PART	IMAGINARY PART
-0.332900370782231D+03	0.207975934440088D+01
0.300718384983949D+03	0.132364856007425D+01
-0.461256074296240D-05	0.000000000000000D+00
0.137178984375769D-04	0.000000000000000D+00
-0.509781598389528D-03	0.000000000000000D+00
-0.376811570190189D-02	0.000000000000000D+00

RICCATI SOLUTION K

ROW 1	1.018D+02	-5.798D+01	2.802D+08	2.948D+03	-2.136D+01	-5.005D+06
ROW 2	-1.982D-05	6.737D-06	-2.534D+02	-3.295D-04	-2.189D-08	-3.397D+00
ROW 3	7.128D+03	-4.331D+03	-3.849D+10	1.890D+05	-1.527D+03	-9.617D+08
ROW 4	4.150D+03	-1.710D+03	-2.947D+10	8.284D+04	-6.482D+02	-6.389D+08
ROW 5	1.757D+07	6.941D+06	3.205D+13	-1.843D+08	-2.748D+06	-1.401D+12
ROW 6	-1.525D+07	2.023D+06	1.196D+14	-1.587D+08	1.529D+06	2.518D+12

OPTIMAL CLOSED LOOP MATRIX ACL

ROW 1	-1.500D-01	0.000D+00	1.500D-01	-1.500D-01	0.000D+00	1.500D-01
ROW 2	0.000D+00	-2.500D-01	2.500D-01	2.500D-01	-2.500D-01	0.000D+00
ROW 3	0.000D+00	0.000D+00	-1.000D+00	0.000D+00	1.000D+00	-1.000D+00
ROW 4	0.000D+00	0.000D+00	0.000D+00	-2.000D+00	2.000D+00	2.000D+00
ROW 5	-4.394D-08	-1.735D-08	-8.012D-02	4.608D-07	-5.000D+00	3.502D-03
ROW 6	1.525D-07	-2.023D-08	-1.196D+00	1.587D-06	-1.529D-08	-1.003D+01

OPTIMAL GAIN MATRIX G

ROW 1	8.787D-09	3.471D-09	1.602D-02	-9.216D-08	-1.374D-09	-7.004D-04
ROW 2	-1.525D-08	2.023D-09	1.196D-01	-1.587D-07	1.529D-09	2.518D-03

Figure 4.10. Results of LQ calculations - $\underline{R} = 10^{16}\underline{I}$.

10^6 $\underline{I}$ produced numerical problems (in the form of near-singular matrices) with the LQGALPHA software package. Values of $\underline{R} > 10^{16}$ $\underline{I}$ penalized control movements to the point that numerical values of controller gains in $\underline{G}$ and values of the control inputs u_1 and u_2 were nearly zero, and there was no discernible difference between the open-loop state relaxation and the closed-loop optimal control.

The next series of figures (Figures 4.11 through 4.16) illustrates the closed-loop behavior of the outputs y_1 and y_2, together with the control inputs u_1 and u_2. Note that to get maximum print-plot resolution, there is an adjustment in the range of the abscissa on each of these plots, so that one must compare actual numerical values, rather than superimposed print-plots, to obtain a valid comparison from one set of $\underline{R}$ matrices to the next. (On all of the simulation runs, the finish time was set equal to 25 seconds.)

For a given set of $\underline{Q}$ and $\underline{R}$ matrices, there are five different types of singular value plots which can be developed:

1. The singular values for the LQ regulator loop broken at the input.
2. The singular values for the LQ servo loop.
3. The singular values for the LQ regulator loop broken at the output.
4. The singular values of the return difference at the input.

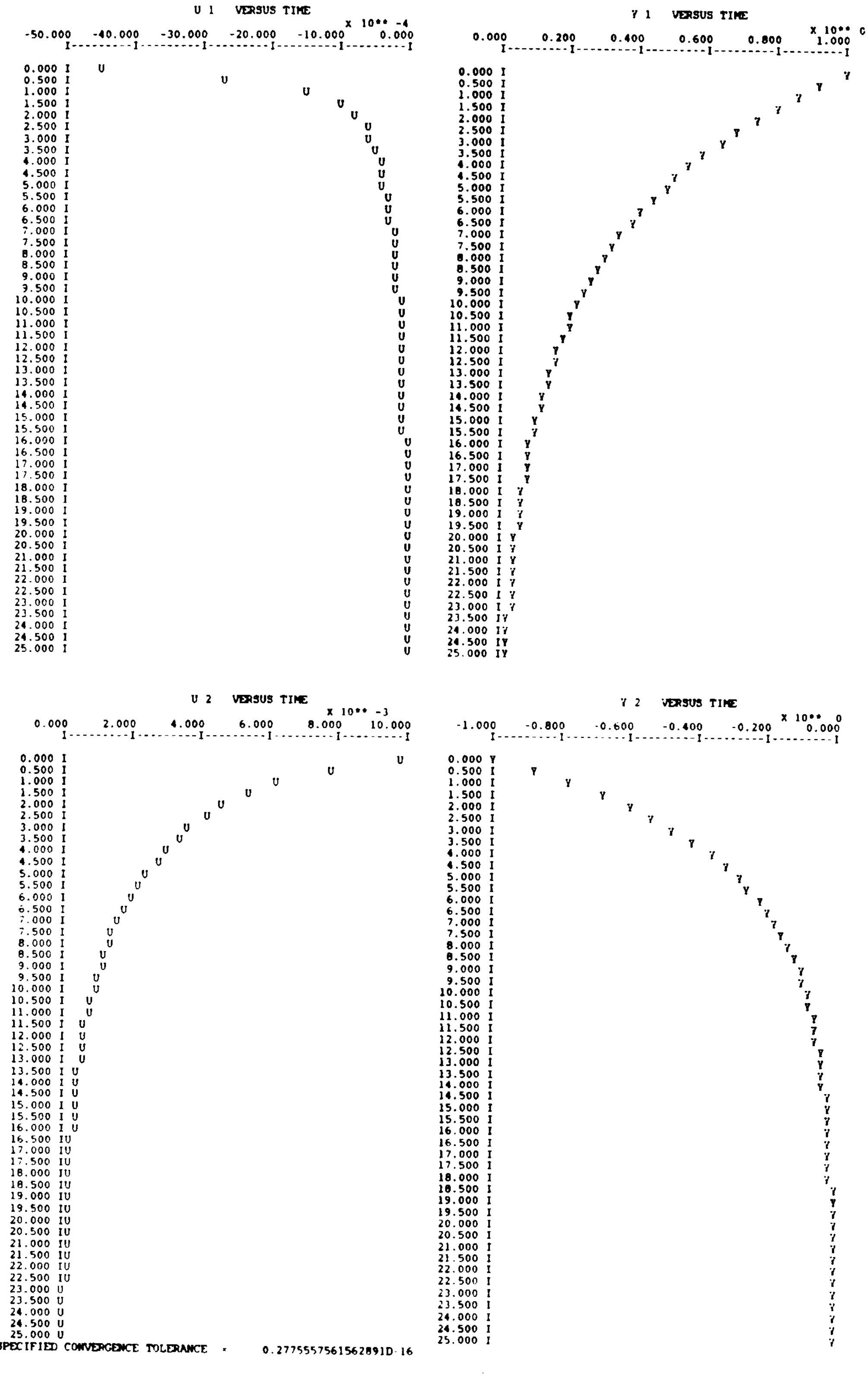

Figure 4.11. Closed-loop LQ regulator behavior - $\underline{R} = 10^6\underline{I}$.

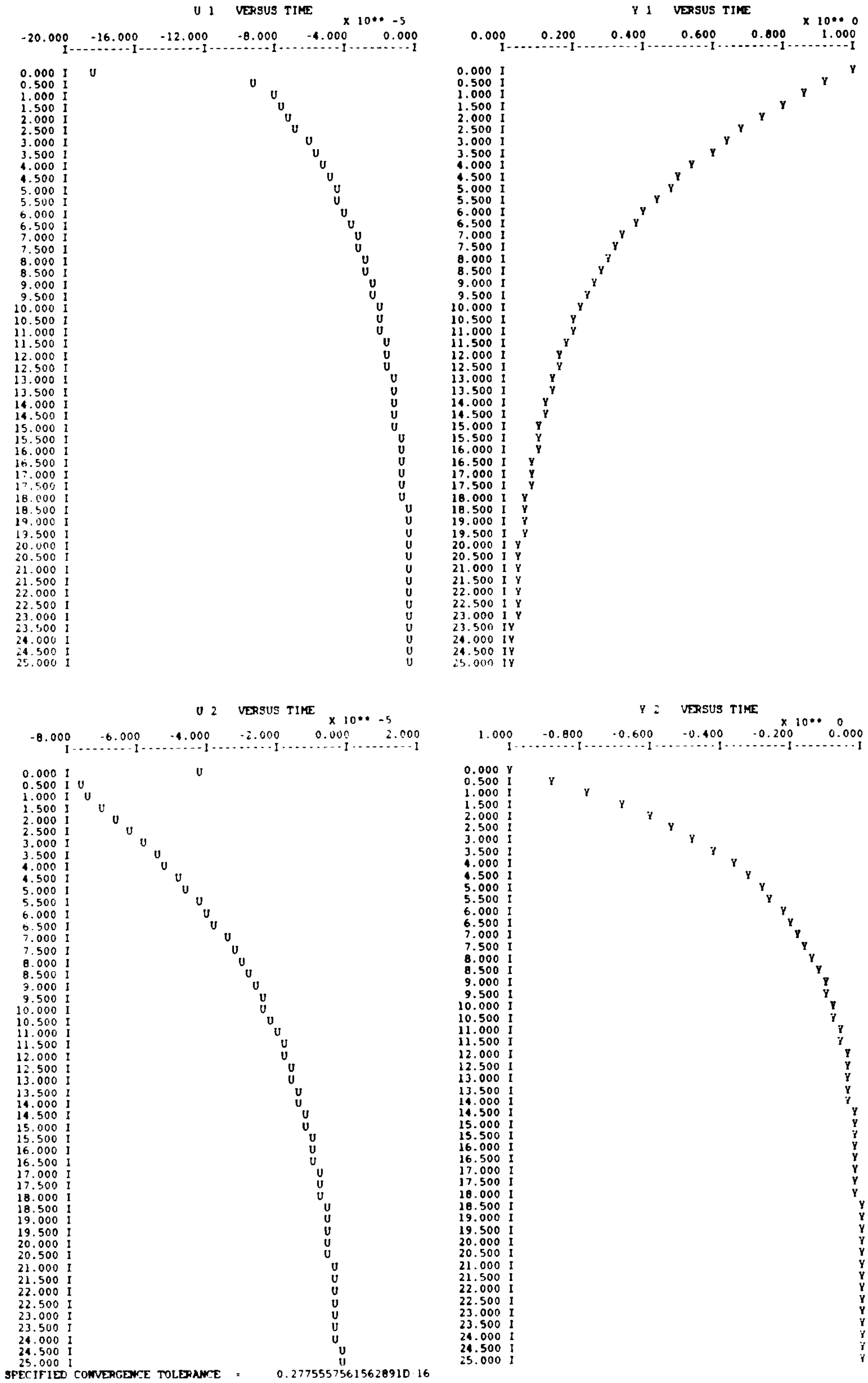

Figure 4.12. Closed-loop LQ regulator behavior - $\underline{R} = 10^8\underline{I}$.

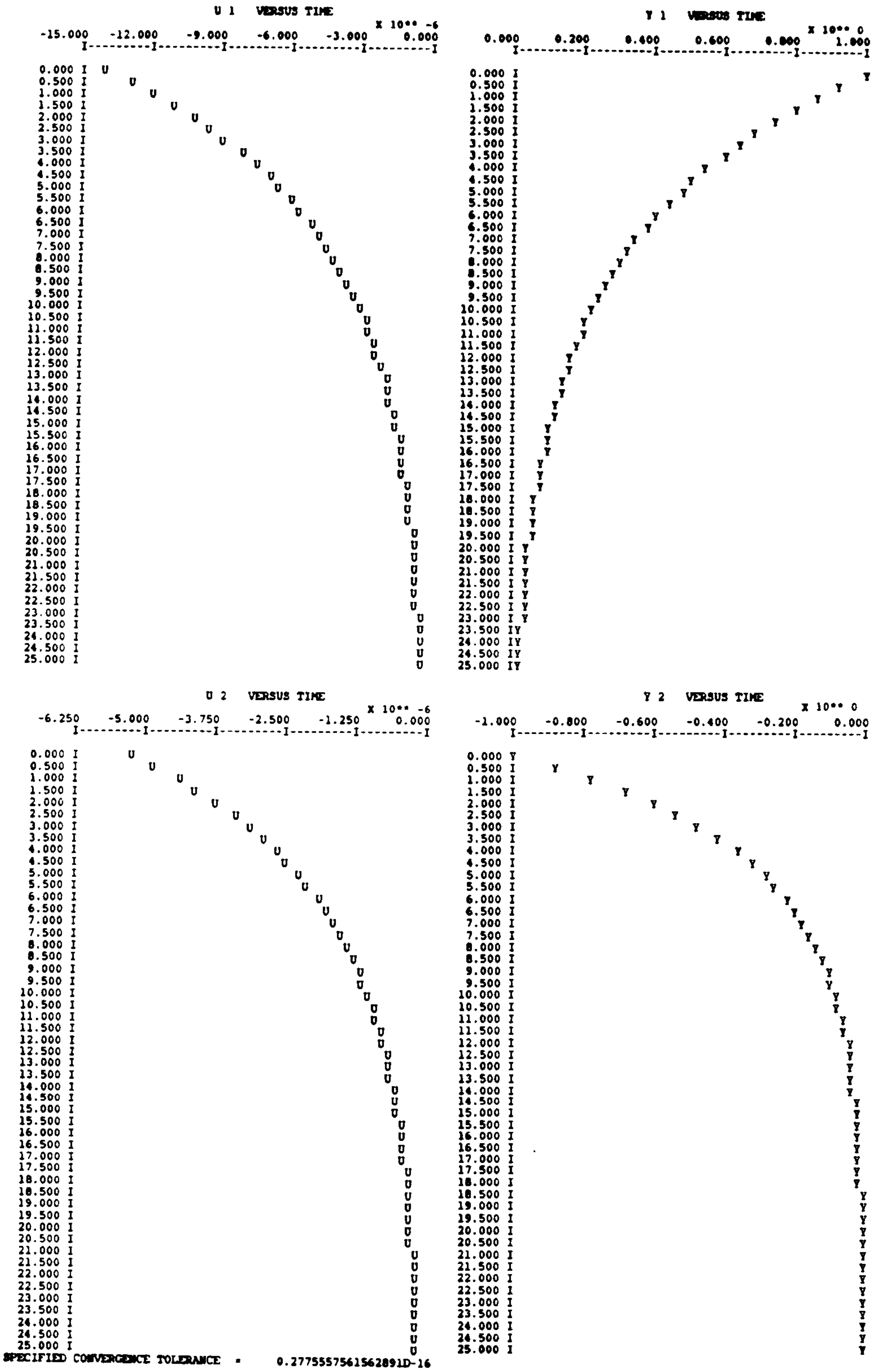

Figure 4.13. Closed-loop LQ regulator behavior - $\underline{R} = 10^{10}\underline{I}$.

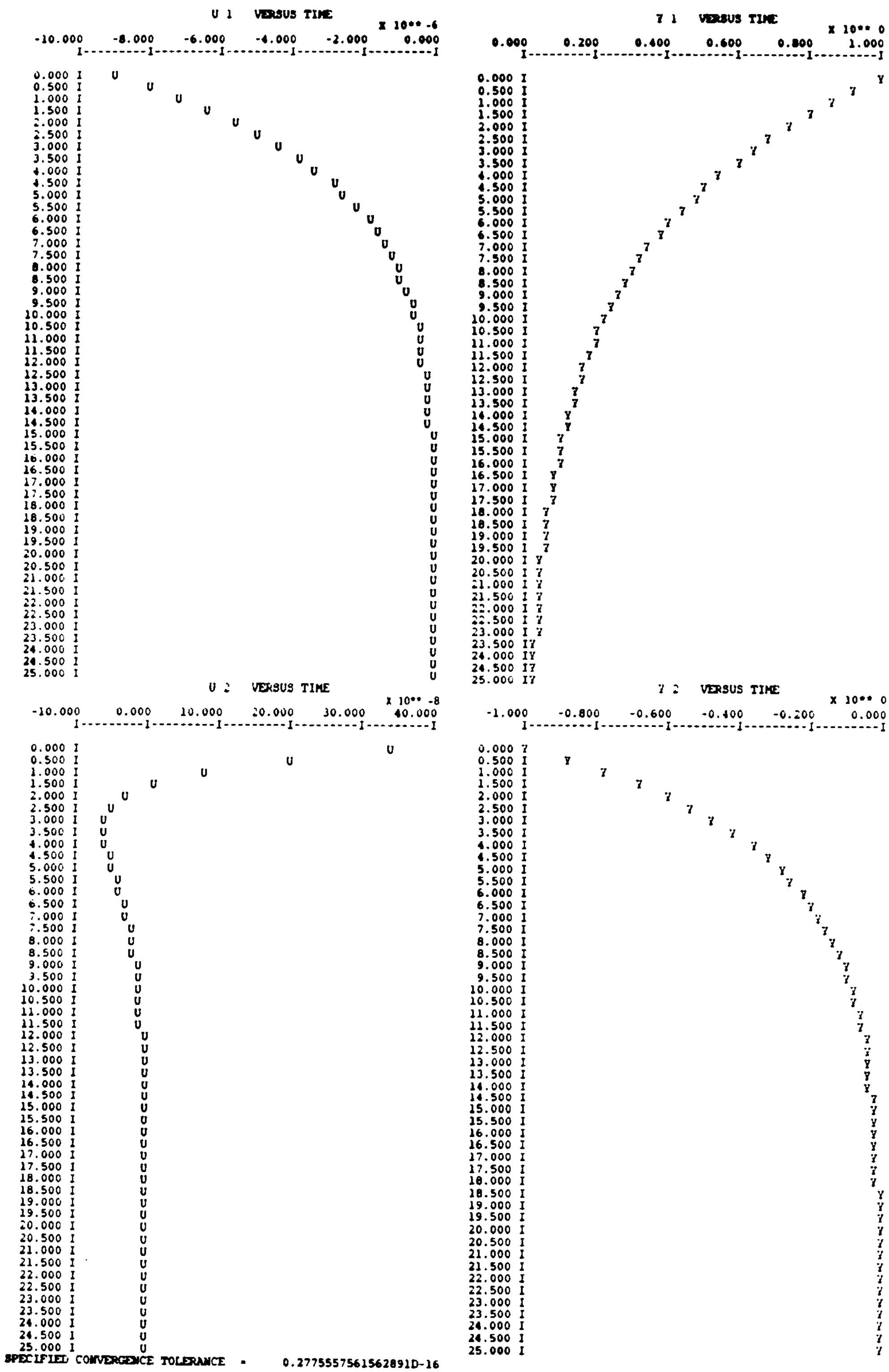

Figure 4.14. Closed-loop LQ regulator behavior - $\underline{R} = 10^{12}\underline{I}$.

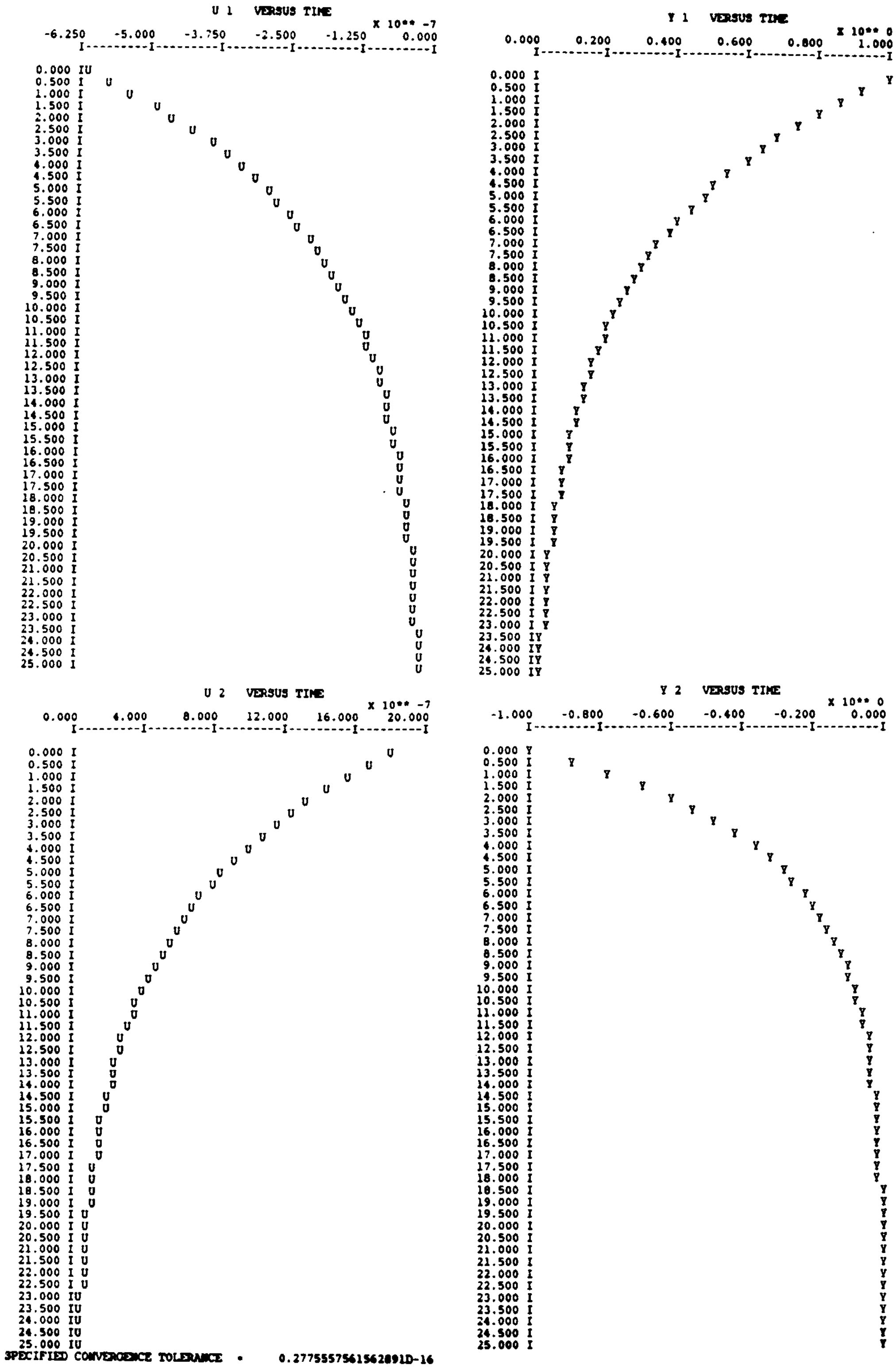

Figure 4.15. Closed-loop LQ regulator behavior - $\underline{R} = 10^{14}\underline{I}$.

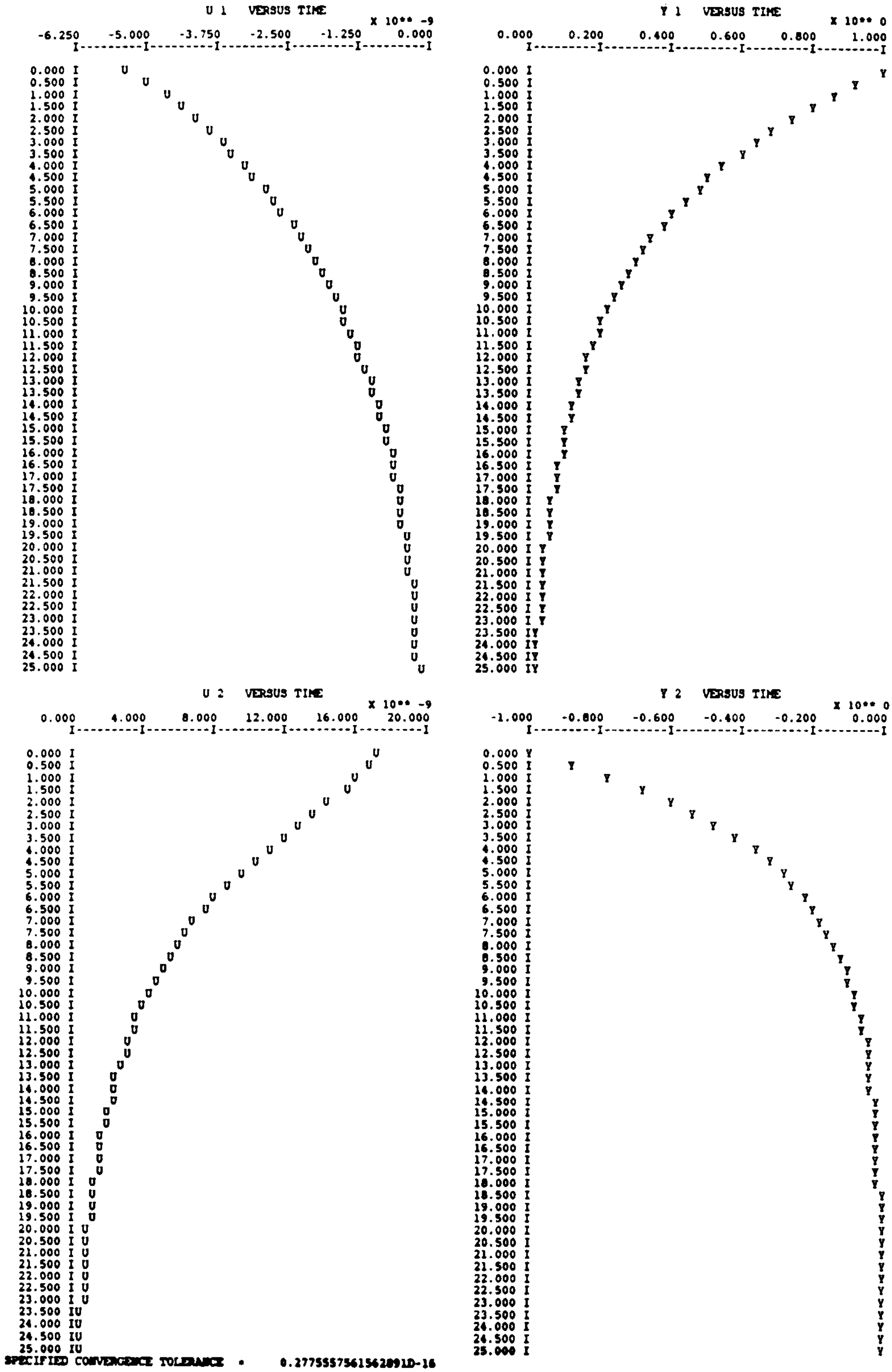

Figure 4.16. Closed-loop LQ regulator behavior - $\underline{R} = 10^{16}\underline{I}$.

5. The singular values of the return difference at the output.

The first two of these represent the $\underline{T}_1(jw)$ and $\underline{T}_2(jw)$ transfer functions discussed in the previous chapter, and are closely related (i.e., setting $\underline{T}_1(jw)$ automatically fixes $\underline{T}_2(jw)$). Since we can only shape the singular values of $\underline{T}_1(jw)$ directly, it is important that we examine the singular value plots for a given $\underline{T}_1(jw)$ and the corresponding LQ servo singular value plots $\underline{T}_2(jw)$ to seek out any generalizations or rules of thumb.

In our particular computer code, we have substituted the LQ regulator gain matrix $\underline{G}$ for the output matrix $\underline{C}$ in the call to the SVPLOT subroutine. We have also used an identity matrix for the feedback compensator "$\underline{FL}$." These two actions produce a net plant transfer function "$\underline{PL}$" equal to $\underline{G}(s\underline{I} - \underline{A})^{-1}\underline{B}$ - identical to $\underline{T}_1(s)$ in the LQ regulator formulation. As another consequence of this procedure, the singular value plots for the LQ regulator loop broken at the "input" are identical to the singular value plots for the LQ regulator loop broken at the "output." Likewise, the singular value plots for the two types of return differences (defined by 4. and 5. above) are also identical.

The next series of figures (Figures 4.17 through 4.22) outlines the $\underline{A}$ and the $(\underline{A} - \underline{BG}_r \underline{D}_p)$ matrices and their corresponding open-loop eigenvalues. As predicted, there is a similar pole-zero structure in the LQ regulator and the LQ servo. However, what is important to note here is the LQ servo's relatively minor

A

ROW 1	-1.500D-01	0.000D+00	1.500D-01	-1.500D-01	0.000D+00	1.500D-01
ROW 2	0.000D+00	-2.500D-01	2.500D-01	2.500D-01	-2.500D-01	0.000D+00
ROW 3	0.000D+00	0.000D+00	-1.000D+00	0.000D+00	1.000D+00	-1.000D+00
ROW 4	0.000D+00	0.000D+00	0.000D+00	-2.000D+00	2.000D+00	2.000D+00
ROW 5	0.000D+00	0.000D+00	0.000D+00	0.000D+00	-5.000D+00	0.000D+00
ROW 6	0.000D+00	0.000D+00	0.000D+00	0.000D+00	0.000D+00	-1.000D+01

A

---EIGENVALUES---

	REAL PART	IMAG PART	NAT FREQ(HZ)	ZETA
1	-1.500D-01	0.000D+00	1.500D-01	1.000000
2	-2.500D-01	0.000D+00	2.500D-01	1.000000
3	-1.000D+00	0.000D+00	1.000D+00	1.000000
4	-2.000D+00	0.000D+00	2.000D+00	1.000000
5	-5.000D+00	0.000D+00	5.000D+00	1.000000
6	-1.000D+01	0.000D+00	1.000D+01	1.000000

AMBGD

ROW 1	-1.500D-01	0.000D+00	1.500D-01	-1.500D-01	0.000D+00	1.500D-01
ROW 2	0.000D+00	-2.500D-01	2.500D-01	2.500D-01	-2.500D-01	0.000D+00
ROW 3	0.000D+00	0.000D+00	-1.000D+00	0.000D+00	1.000D+00	-1.000D+00
ROW 4	0.000D+00	0.000D+00	0.000D+00	-2.000D+00	2.000D+00	2.000D+00
ROW 5	0.000D+00	0.000D+00	-1.568D+00	2.134D-01	-4.999D+00	-3.116D-02
ROW 6	0.000D+00	0.000D+00	2.669D+00	-6.809D-01	-3.932D-03	-9.642D+00

(A - B*GR*DP)

---EIGENVALUES---

	REAL PART	IMAG PART	NAT FREQ(HZ)	ZETA
1	-1.500D-01	0.000D+00	1.500D-01	1.000000
2	-2.500D-01	0.000D+00	2.500D-01	1.000000
3	-9.132D+00	0.000D+00	9.132D+00	1.000000
4	-4.697D+00	0.000D+00	4.697D+00	1.000000
5	-1.906D+00	2.326D-01	1.920D+00	0.992634
6	-1.906D+00	-2.326D-01	1.920D+00	0.992634

Figure 4.17. LQ servo open loop eigenvalues - $\underline{R} = 10^6\underline{I}$.

A

ROW 1	-1.500D-01	0.000D+00	1.500D-01	-1.500D-01	0.000D+00	1.500D-01
ROW 2	0.000D+00	-2.500D-01	2.500D-01	2.500D-01	-2.500D-01	0.000D+00
ROW 3	0.000D+00	0.000D+00	-1.000D+00	0.000D+00	1.000D+00	-1.000D+00
ROW 4	0.000D+00	0.000D+00	0.000D+00	-2.000D+00	2.000D+00	2.000D+00
ROW 5	0.000D+00	0.000D+00	0.000D+00	0.000D+00	-5.000D+00	0.000D+00
ROW 6	0.000D+00	0.000D+00	0.000D+00	0.000D+00	0.000D+00	-1.000D+01

A

---EIGENVALUES---

	REAL PART	IMAG PART	NAT FREQ(HZ)	ZETA
1	-1.500D-01	0.000D+00	1.500D-01	1.000000
2	-2.500D-01	0.000D+00	2.500D-01	1.000000
3	-1.000D+00	0.000D+00	1.000D+00	1.000000
4	-2.000D+00	0.000D+00	2.000D+00	1.000000
5	-5.000D+00	0.000D+00	5.000D+00	1.000000
6	-1.000D+01	0.000D+00	1.000D+01	1.000000

AMBGD

ROW 1	-1.500D-01	0.000D+00	1.500D-01	-1.500D-01	0.000D+00	1.500D-01
ROW 2	0.000D+00	-2.500D-01	2.500D-01	2.500D-01	-2.500D-01	0.000D+00
ROW 3	0.000D+00	0.000D+00	-1.000D+00	0.000D+00	1.000D+00	-1.000D+00
ROW 4	0.000D+00	0.000D+00	0.000D+00	-2.000D+00	2.000D+00	2.000D+00
ROW 5	0.000D+00	0.000D+00	-1.764D+01	4.078D-02	-4.960D+00	3.336D-02
ROW 6	0.000D+00	0.000D+00	1.650D+01	-3.868D-02	-3.009D-02	-9.983D+00

(A - B*GR*DP)

---EIGENVALUES---

	REAL PART	IMAG PART	NAT FREQ(HZ)	ZETA
1	-1.500D-01	0.000D+00	1.500D-01	1.000000
2	-2.500D-01	0.000D+00	2.500D-01	1.000000
3	-3.647D+00	4.709D+00	5.957D+00	0.612331
4	-3.647D+00	-4.709D+00	5.957D+00	0.612331
5	-8.646D+00	0.000D+00	8.646D+00	1.000000
6	-2.003D+00	0.000D+00	2.003D+00	1.000000

Figure 4.18. LQ servo open loop eigenvalues - $\underline{R} = 10^8\underline{I}$.

A

ROW 1	-1.500D-01	0.000D+00	1.500D-01	-1.500D-01	0.000D+00	1.500D-01
ROW 2	0.000D+00	-2.500D-01	2.500D-01	2.500D-01	-2.500D-01	0.000D+00
ROW 3	0.000D+00	0.000D+00	-1.000D+00	0.000D+00	1.000D+00	-1.000D+00
ROW 4	0.000D+00	0.000D+00	0.000D+00	-2.000D+00	2.000D+00	2.000D+00
ROW 5	0.000D+00	0.000D+00	0.000D+00	0.000D+00	-5.000D+00	0.000D+00
ROW 6	0.000D+00	0.000D+00	0.000D+00	0.000D+00	0.000D+00	-1.000D+01

A

---EIGENVALUES---

	REAL PART	IMAG PART	NAT FREQ(HZ)	ZETA
1	-1.500D-01	0.000D+00	1.500D-01	1.000000
2	-2.500D-01	0.000D+00	2.500D-01	1.000000
3	-1.000D+00	0.000D+00	1.000D+00	1.000000
4	-2.000D+00	0.000D+00	2.000D+00	1.000000
5	-5.000D+00	0.000D+00	5.000D+00	1.000000
6	-1.000D+01	0.000D+00	1.000D+01	1.000000

AMBGD

ROW 1	-1.500D-01	0.000D+00	1.500D-01	-1.500D-01	0.000D+00	1.500D-01
ROW 2	0.000D+00	-2.500D-01	2.500D-01	2.500D-01	-2.500D-01	0.000D+00
ROW 3	0.000D+00	0.000D+00	-1.000D+00	0.000D+00	1.000D+00	-1.000D+00
ROW 4	0.000D+00	0.000D+00	0.000D+00	-2.000D+00	2.000D+00	2.000D+00
ROW 5	0.000D+00	0.000D+00	-1.074D-02	6.529D-07	-5.000D+00	-3.988D-02
ROW 6	0.000D+00	0.000D+00	1.439D-02	7.824D-07	1.919D-05	-1.002D+01

(A - B*GR*DP)

---EIGENVALUES---

	REAL PART	IMAG PART	NAT FREQ(HZ)	ZETA
1	-1.500D-01	0.000D+00	1.500D-01	1.000000
2	-2.500D-01	0.000D+00	2.500D-01	1.000000
3	-1.002D+01	0.000D+00	1.002D+01	1.000000
4	-1.004D+00	0.000D+00	1.004D+00	1.000000
5	-4.997D+00	0.000D+00	4.997D+00	1.000000
6	-2.000D+00	0.000D+00	2.000D+00	1.000000

Figure 4.19. LQ servo open loop eigenvalues - $\underline{R} = 10^{10}\underline{I}$.

A

ROW 1	-1.500D-01	0.000D+00	1.500D-01	-1.500D-01	0.000D+00	1.500D-01
ROW 2	0.000D+00	-2.500D-01	2.500D-01	2.500D-01	-2.500D-01	0.000D+00
ROW 3	0.000D+00	0.000D+00	-1.000D+00	0.000D+00	1.000D+00	-1.000D+00
ROW 4	0.000D+00	0.000D+00	0.000D+00	-2.000D+00	2.000D+00	2.000D+00
ROW 5	0.000D+00	0.000D+00	0.000D+00	0.000D+00	-5.000D+00	0.000D+00
ROW 6	0.000D+00	0.000D+00	0.000D+00	0.000D+00	0.000D+00	-1.000D+01

A

---EIGENVALUES---

	REAL PART	IMAG PART	NAT FREQ(HZ)	ZETA
1	-1.500D-01	0.000D+00	1.500D-01	1.000000
2	-2.500D-01	0.000D+00	2.500D-01	1.000000
3	-1.000D+00	0.000D+00	1.000D+00	1.000000
4	-2.000D+00	0.000D+00	2.000D+00	1.000000
5	-5.000D+00	0.000D+00	5.000D+00	1.000000
6	-1.000D+01	0.000D+00	1.000D+01	1.000000

AMBGD

ROW 1	-1.500D-01	0.000D+00	1.500D-01	-1.500D-01	0.000D+00	1.500D-01
ROW 2	0.000D+00	-2.500D-01	2.500D-01	2.500D-01	-2.500D-01	0.000D+00
ROW 3	0.000D+00	0.000D+00	-1.000D+00	0.000D+00	1.000D+00	-1.000D+00
ROW 4	0.000D+00	0.000D+00	0.000D+00	-2.000D+00	2.000D+00	2.000D+00
ROW 5	0.000D+00	0.000D+00	3.274D-01	-1.611D-04	-5.000D+00	1.058D-02
ROW 6	0.000D+00	0.000D+00	4.000D-01	-1.146D-04	7.444D-07	-1.000D+01

(A - B*GR*DF)

---EIGENVALUES---

	REAL PART	IMAG PART	NAT FREQ(HZ)	ZETA
1	-1.500D-01	0.000D+00	1.500D-01	1.000000
2	-2.500D-01	0.000D+00	2.500D-01	1.000000
3	-9.957D+00	0.000D+00	9.957D+00	1.000000
4	-9.631D-01	0.000D+00	9.631D-01	1.000000
5	-5.082D+00	0.000D+00	5.082D+00	1.000000
6	-2.000D+00	0.000D+00	2.000D+00	1.000000

Figure 4.20. LQ servo open loop eigenvalues - $\underline{R} = 10^{12}\underline{I}$.

A

ROW 1	-1.500D-01	0.000D+00	1.500D-01	-1.500D-01	0.000D+00	1.500D-01
ROW 2	0.000D+00	-2.500D-01	2.500D-01	2.500D-01	-2.500D-01	0.000D+00
ROW 3	0.000D+00	0.000D+00	-1.000D+00	0.000D+00	1.000D+00	-1.000D+00
ROW 4	0.000D+00	0.000D+00	0.000D+00	-2.000D+00	2.000D+00	2.000D+00
ROW 5	0.000D+00	0.000D+00	0.000D+00	0.000D+00	-5.000D+00	0.000D+00
ROW 6	0.000D+00	0.000D+00	0.000D+00	0.000D+00	0.000D+00	-1.000D+01

A

---EIGENVALUES---

	REAL PART	IMAG PART	NAT FREQ(HZ)	ZETA
1	-1.500D-01	0.000D+00	1.500D-01	1.000000
2	-2.500D-01	0.000D+00	2.500D-01	1.000000
3	-1.000D+00	0.000D+00	1.000D+00	1.000000
4	-2.000D+00	0.000D+00	2.000D+00	1.000000
5	-5.000D+00	0.000D+00	5.000D+00	1.000000
6	-1.000D+01	0.000D+00	1.000D+01	1.000000

AMBGD

ROW 1	-1.500D-01	0.000D+00	1.500D-01	-1.500D-01	0.000D+00	1.500D-01
ROW 2	0.000D+00	-2.500D-01	2.500D-01	2.500D-01	-2.500D-01	0.000D+00
ROW 3	0.000D+00	0.000D+00	-1.000D+00	0.000D+00	1.000D+00	-1.000D+00
ROW 4	0.000D+00	0.000D+00	0.000D+00	-2.000D+00	2.000D+00	2.000D+00
ROW 5	0.000D+00	0.000D+00	3.169D-03	-2.699D-03	-5.000D+00	-1.682D-03
ROW 6	0.000D+00	0.000D+00	-3.136D-02	1.676D-02	3.471D-06	-9.985D+00

(A - B*GR*DF)

---EIGENVALUES---

	REAL PART	IMAG PART	NAT FREQ(HZ)	ZETA
1	-1.500D-01	0.000D+00	1.500D-01	1.000000
2	-2.500D-01	0.000D+00	2.500D-01	1.000000
3	-9.992D+00	0.000D+00	9.992D+00	1.000000
4	-9.957D-01	0.000D+00	9.957D-01	1.000000
5	-4.999D+00	0.000D+00	4.999D+00	1.000000
6	-1.998D+00	0.000D+00	1.998D+00	1.000000

Figure 4.21. LQ servo open loop eigenvalues - $\underline{R} = 10^{14}\underline{I}$.

A

ROW 1	-1.500D-01	0.000D+00	1.500D-01	-1.500D-01	0.000D+00	1.500D-01
ROW 2	0.000D+00	-2.500D-01	2.500D-01	2.500D-01	-2.500D-01	0.000D+00
ROW 3	0.000D+00	0.000D+00	-1.000D+00	0.000D+00	1.000D+00	-1.000D+00
ROW 4	0.000D+00	0.000D+00	0.000D+00	-2.000D+00	2.000D+00	2.000D+00
ROW 5	0.000D+00	0.000D+00	0.000D+00	0.000D+00	-5.000D+00	0.000D+00
ROW 6	0.000D+00	0.000D+00	0.000D+00	0.000D+00	0.000D+00	-1.000D+01

A

---EIGENVALUES---

	REAL PART	IMAG PART	NAT FREQ(HZ)	ZETA
1	-1.500D-01	0.000D+00	1.500D-01	1.000000
2	-2.500D-01	0.000D+00	2.500D-01	1.000000
3	-1.000D+00	0.000D+00	1.000D+00	1.000000
4	-2.000D+00	0.000D+00	2.000D+00	1.000000
5	-5.000D+00	0.000D+00	5.000D+00	1.000000
6	-1.000D+01	0.000D+00	1.000D+01	1.000000

AMBCD

ROW 1	-1.500D-01	0.000D+00	1.500D-01	-1.500D-01	0.000D+00	1.500D-01
ROW 2	0.000D+00	-2.500D-01	2.500D-01	2.500D-01	-2.500D-01	0.000D+00
ROW 3	0.000D+00	0.000D+00	-1.000D+00	0.000D+00	1.000D+00	-1.000D+00
ROW 4	0.000D+00	0.000D+00	0.000D+00	-2.000D+00	2.000D+00	2.000D+00
ROW 5	0.000D+00	0.000D+00	-8.012D-02	4.608D-07	-5.000D+00	3.502D-03
ROW 6	0.000D+00	0.000D+00	-1.196D+00	1.587D-06	-1.529D-08	-1.003D+01

(A - B*GR*DP)

---EIGENVALUES---

	REAL PART	IMAG PART	NAT FREQ(HZ)	ZETA
1	-1.500D-01	0.000D+00	1.500D-01	1.000000
2	-2.500D-01	0.000D+00	2.500D-01	1.000000
3	-1.016D+01	0.000D+00	1.016D+01	1.000000
4	-8.887D-01	0.000D+00	8.887D-01	1.000000
5	-4.981D+00	0.000D+00	4.981D+00	1.000000
6	-2.000D+00	0.000D+00	2.000D+00	1.000000

Figure 4.22. LQ servo open loop eigenvalues - $\underline{R} = 10^{16}\underline{I}$.

displacement of the open-loop poles from their LQ regulator position. Obviously, these results are a strong function of the particular ($\underline{A}$, $\underline{B}$, $\underline{C}$) system triple, as well as the calculated $\underline{G}$. However, over a fairly large range of control weighting, the pole displacements could be considered to be small in all cases.

This result is due, in part, to the fact that the slowest (dominant) poles are in the upper left-hand locations in the $\underline{A}$ matrix, and the fastest poles are in the lower right-hand locations in $\underline{A}$ for our particular state-space description. Since the $\underline{B}\ \underline{G}_r\ \underline{D}_p$ contributions add only to the rightmost m columns in the $\underline{A} - \underline{BG}_r\ \underline{D}_p$ matrix, their effect is minimal - tending only to speed up or slow down by relatively small increments the fastest (and least significant) poles in the system.

Obviously, this result is a strong function of the state space representation and nomenclature chosen for a particular problem. Other representations which had more dominant system dynamics in the rightmost m columns of $\underline{A}$ would be affected to a greater degree.

D. RELATIONSHIPS WITH THEORETICAL PREDICTIONS

An examination of the six plots (Figures 4.23 through 4.28) of LQ regulator and LQ servo singular values reveals several interesting characteristics of the LQ servo:

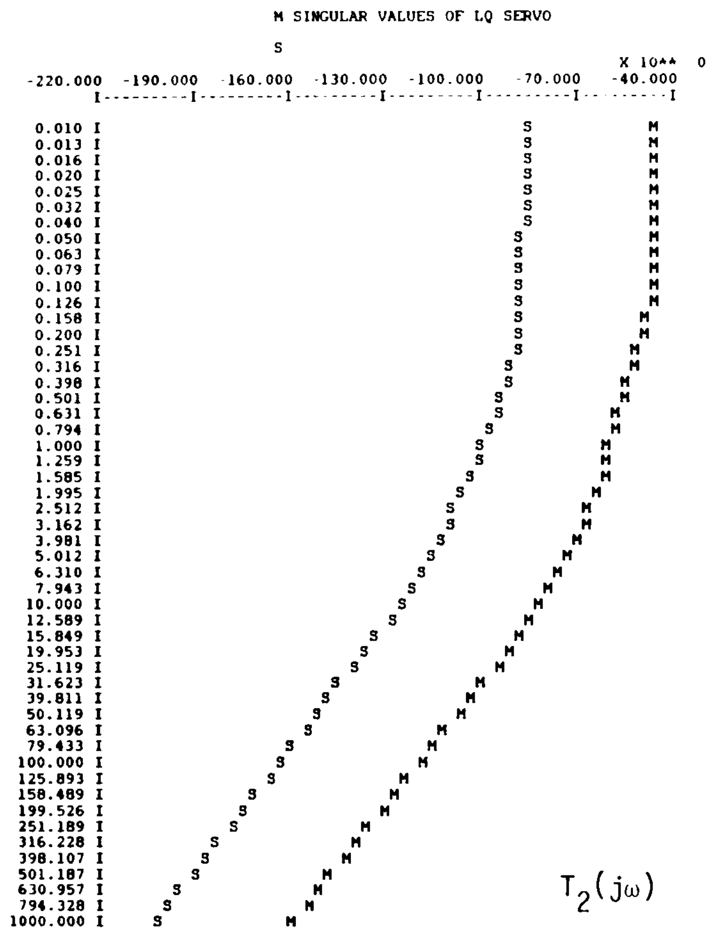

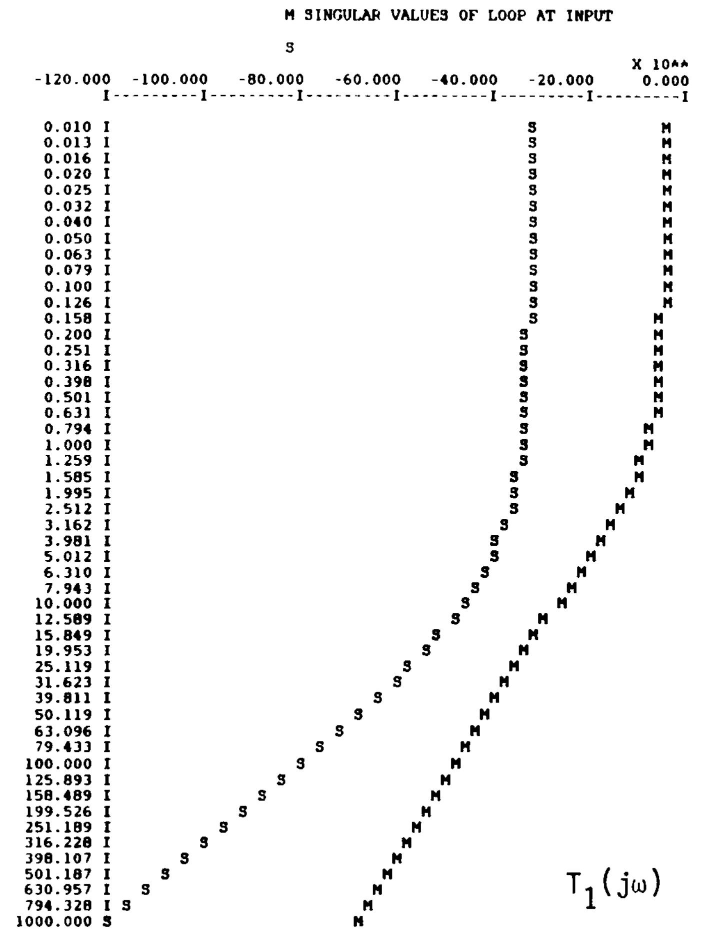

Figure 4.23. LQ regulator and LQ servo singular values - $\underline{R} = 10^6\underline{I}$.

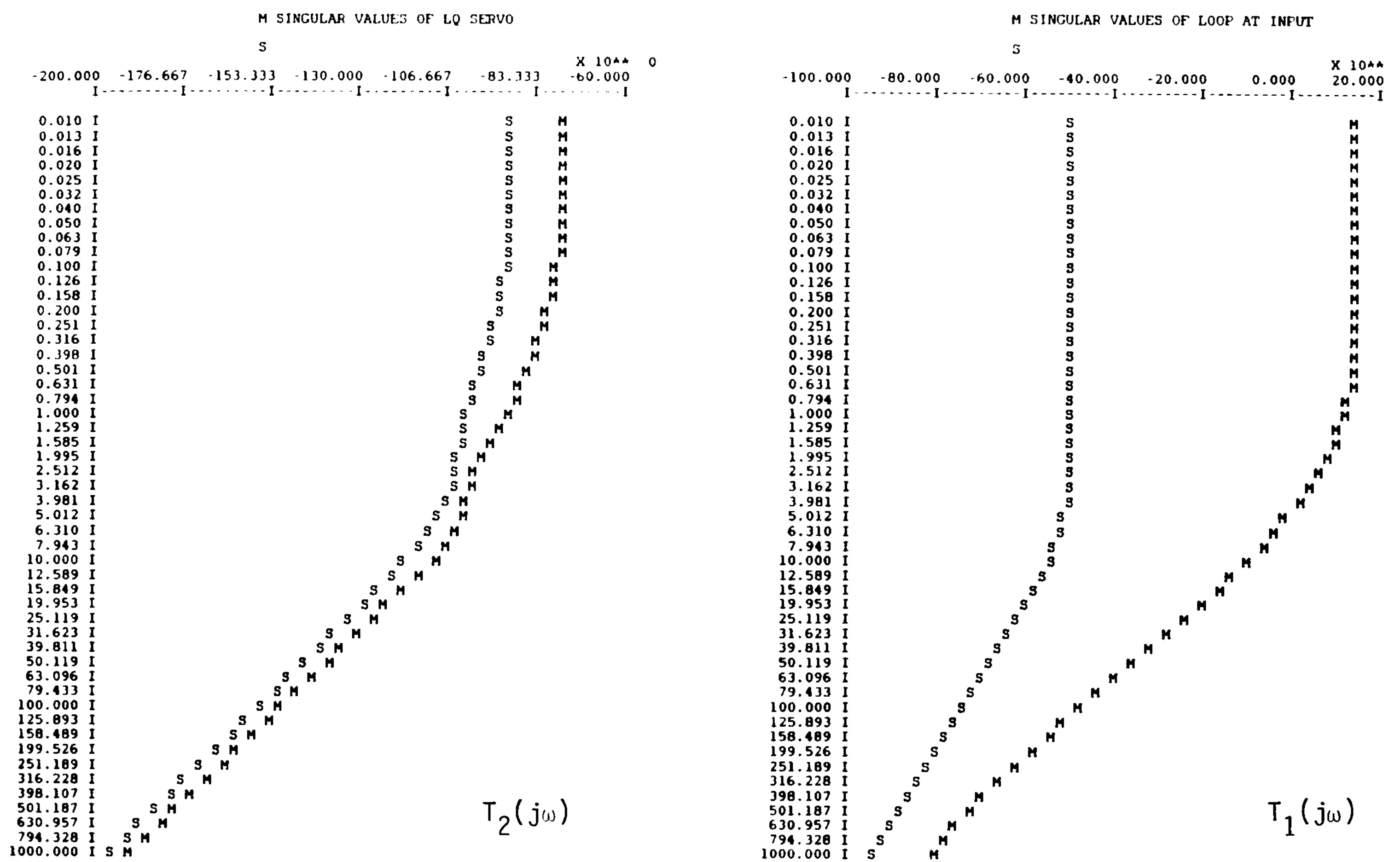

Figure 4.24. LQ regulator and LQ servo singular values - $\underline{R} = 10^8\underline{I}$.

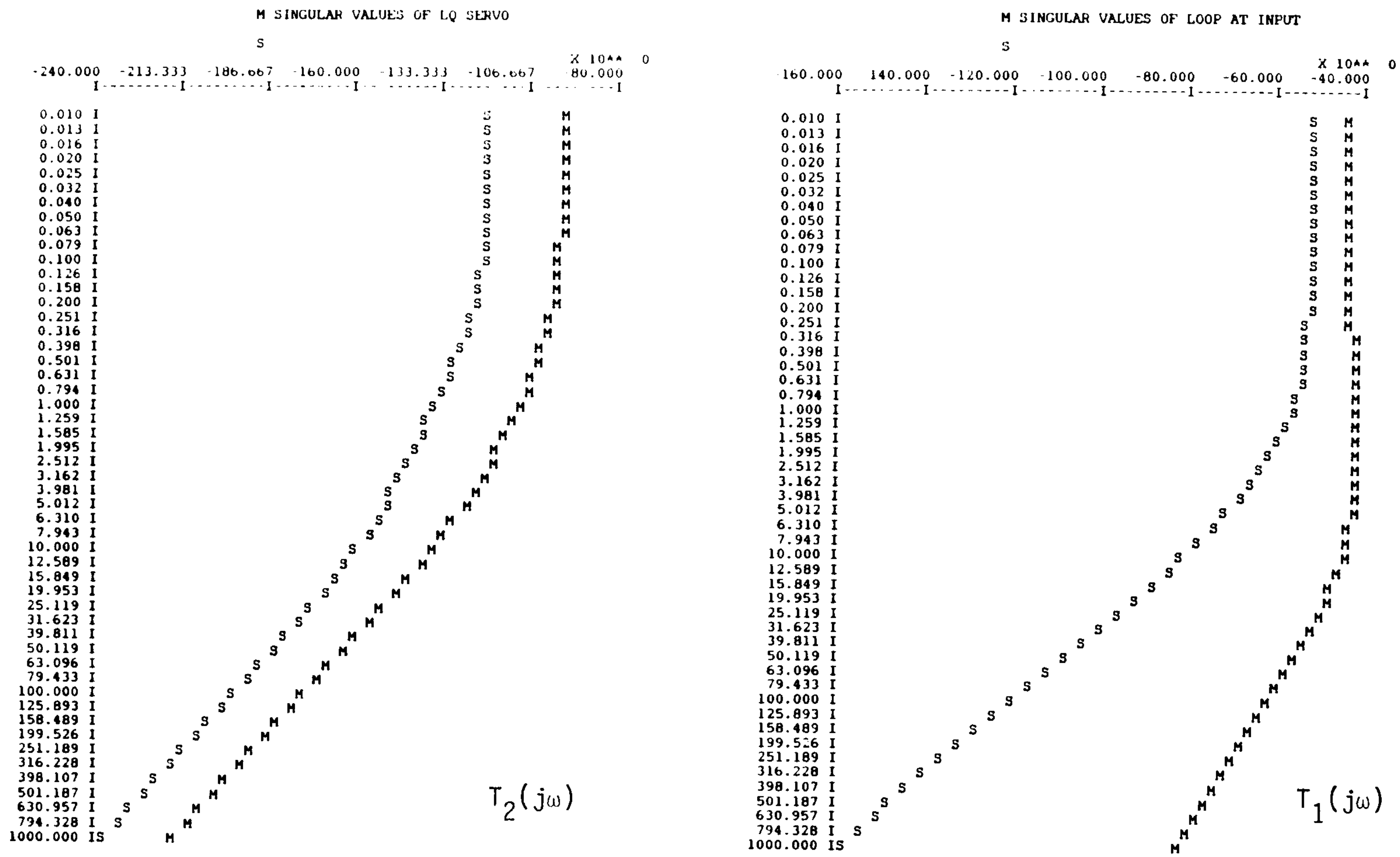

Figure 4.25. LQ regulator and LQ servo singular values - $\underline{R} = 10^{10}\underline{I}$.

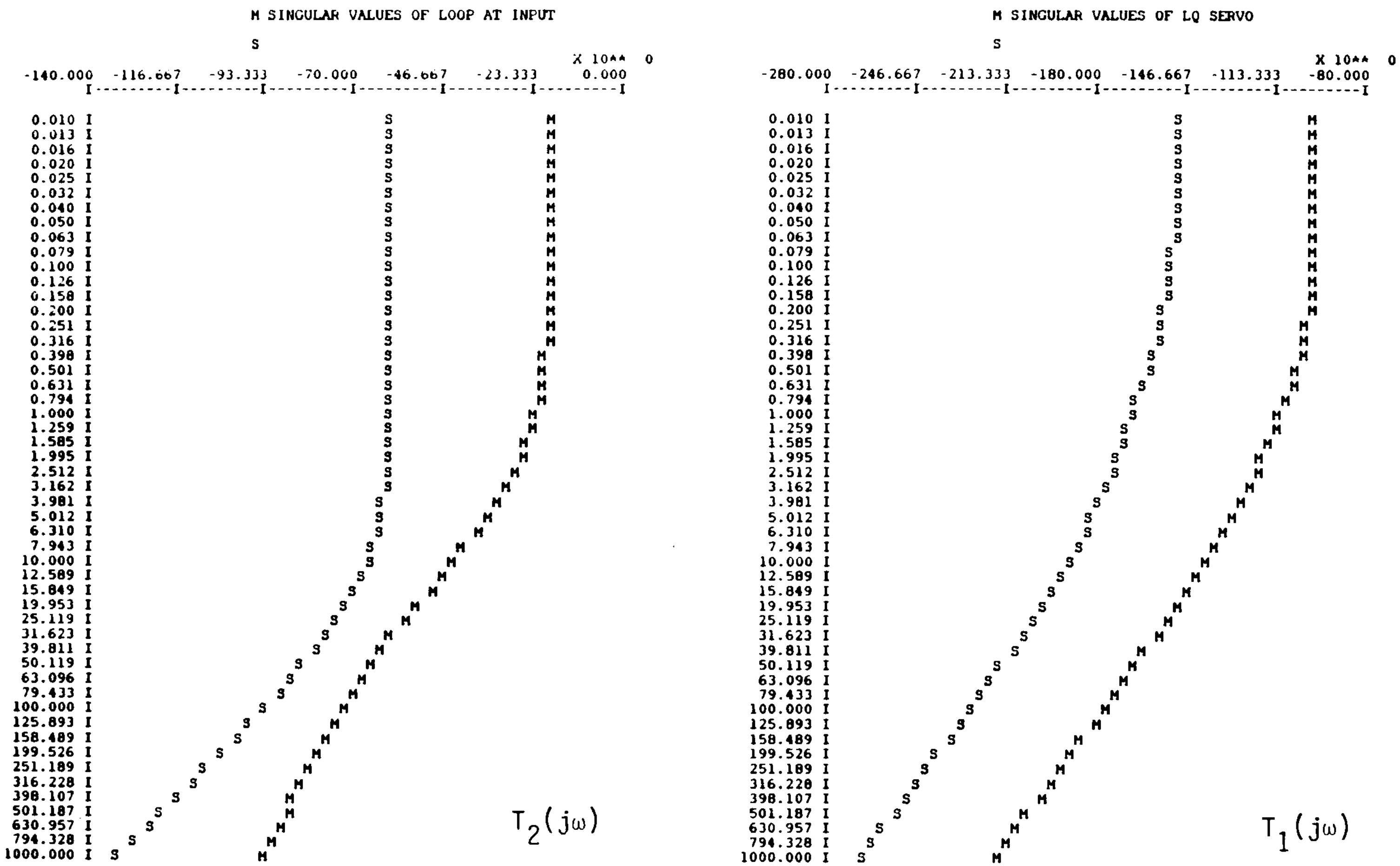

Figure 4.26. LQ regulator and LQ servo singular values - $\underline{R} = 10^{12}\underline{I}$.

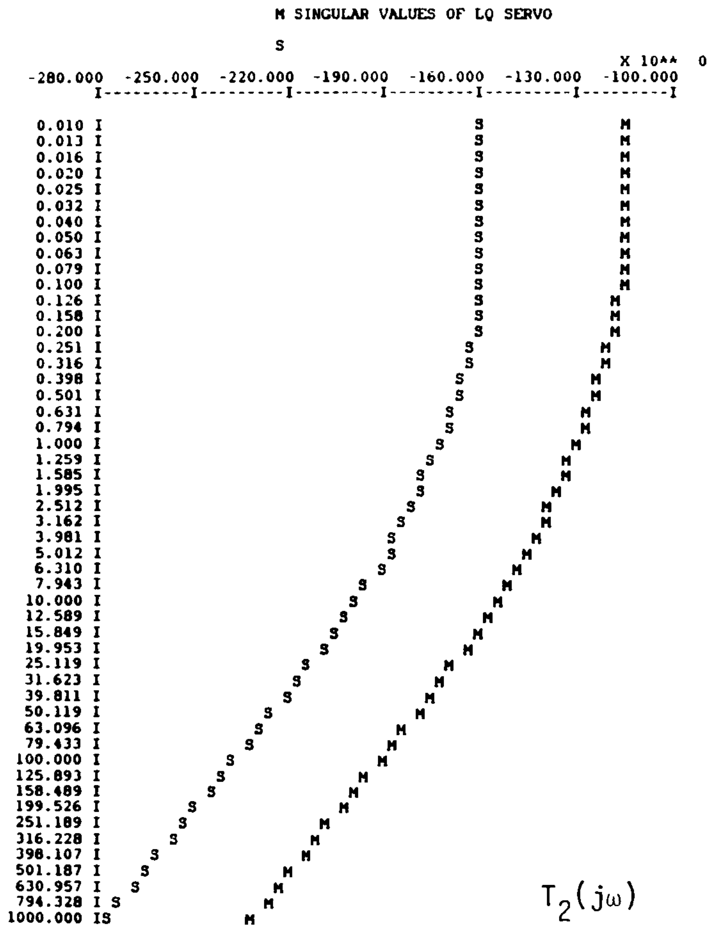

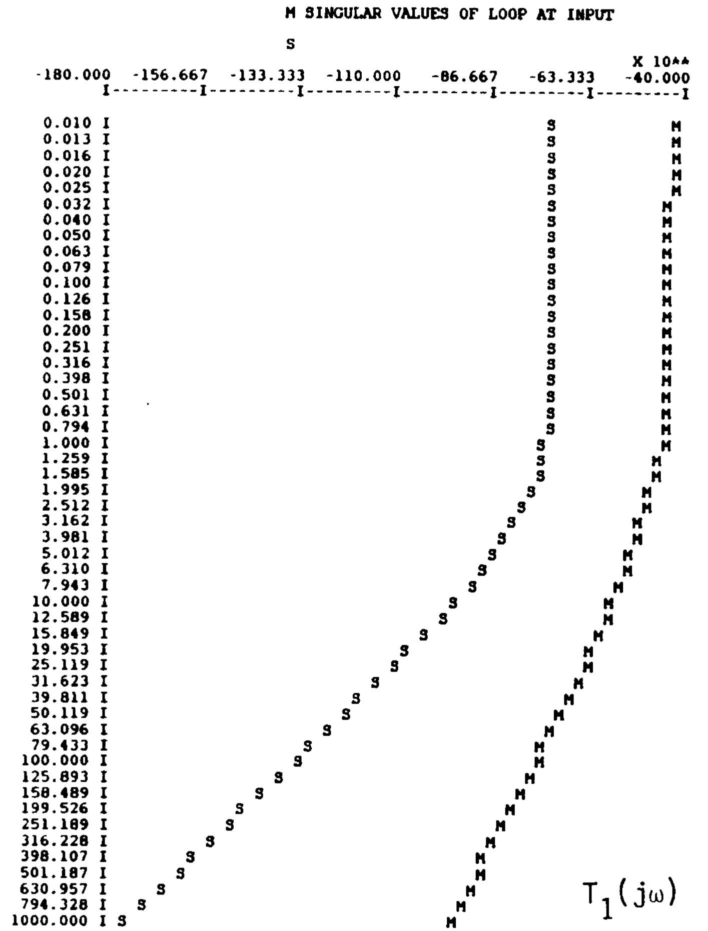

Figure 4.27. LQ regulator and LQ servo singular values - $\underline{R} = 10^{14}\underline{I}$.

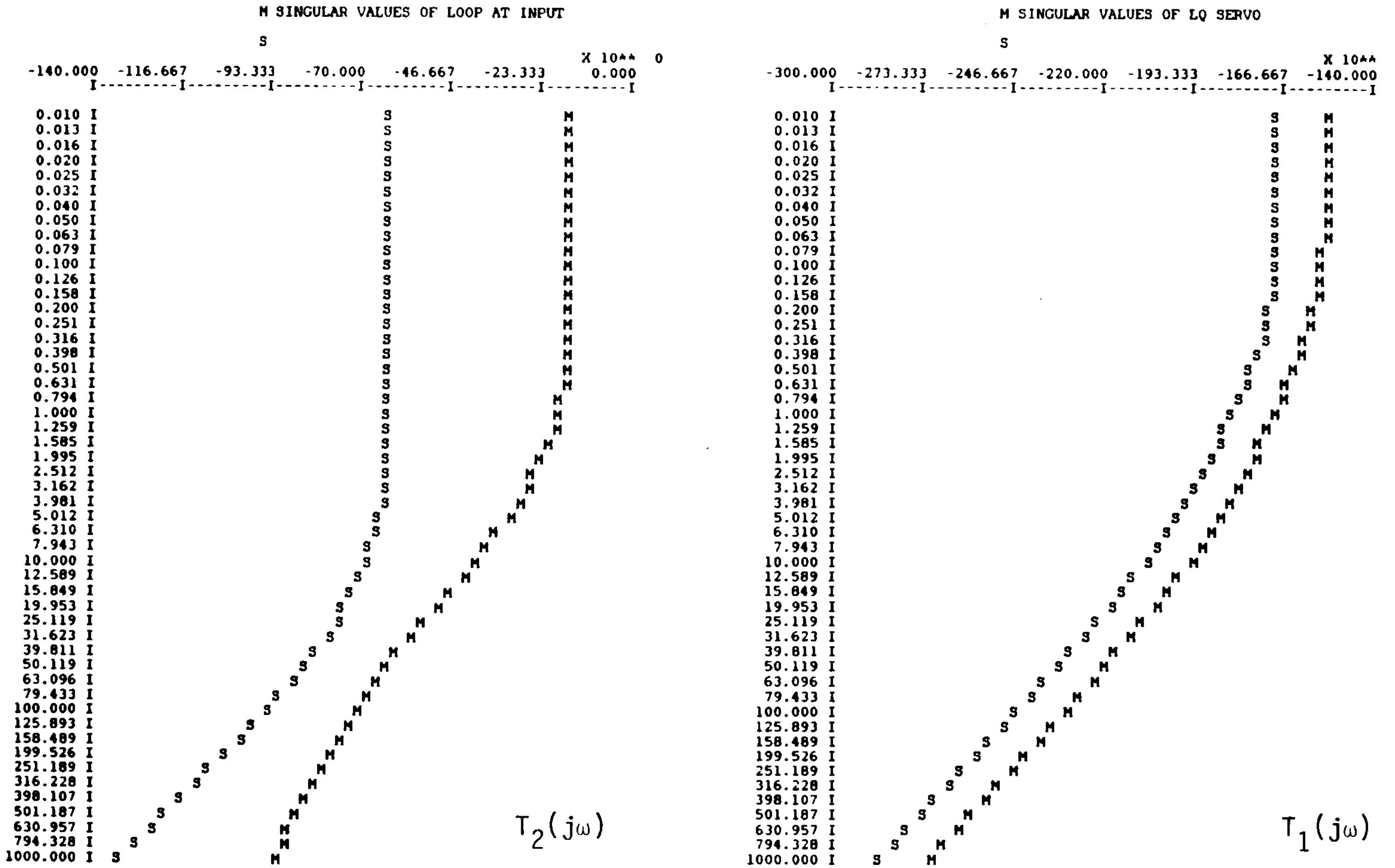

Figure 4.28. LQ regulator and LQ servo singular values - $\underline{R} = 10^{16}\underline{I}$.

1. The LQ servo appears to be remarkably effective in preserving a nearly constant distance between its maximum and minimum singular values (i.e., the condition number remains nearly constant), no matter what the singular values of the corresponding LQ regulator at the loop input happen to be doing. This particular characteristic could be a mixed blessing. Transfer functions with similar singular values at low frequencies will remain that way over a wide range of frequencies. Likewise, large spreads between maximum and minimum singular values tend to remain large over a wide range of frequencies. In particular, one generally would like to squeeze together the loop singular values at low frequencies, to ensure large enough low frequency gain for all loop elements to guarantee good command-following and disturbance rejection properties. Based on this unusual characteristic, additional work in the area of techniques for squeezing the LQ servo singular values in any frequency range appears to be potentially rewarding.
2. Rolloffs take place for both the LQ regulator and the LQ servo in the same general frequency ranges, although the LQ servo appears to transition more smoothly in all six of the cases studied.

3. With the exception of the case for $\underline{R} = 10^8 \underline{I}$, all of the maximum singular values for the LQ regulator approached a constant roll-off rate of - 20 db/decade at high frequencies. (See Table 4-1.) In contrast, the LQ regulator minimum singular values approached ~ 40 db/decade roll-off rate at high frequencies. Both the maximum and minimum singular values for the LQ servo rolled off at ~ 40 db/decade. To this author's knowledge, the open literature does not contain any references to theoretical relationships in this area. One-pole roll-off could be expected in the one-state (scalar) case, due to the dominance of w in the $(jw\underline{I} - \underline{A})^{-1}$ term, but evidently this result does not carry over to the multivariable case. Additional study would be welcomed here also.

4. Any unusual behaviors in the LQ regulator, such as large "pinches" between maximum and minimum singular values, are not necessarily demonstrated by the LQ servo in the same frequency ranges.

5. Perhaps the strongest conclusion to be drawn is that, as predicted by the LQ servo theory, the transfer functions $\underline{T}_1(jw)$ and $\underline{T}_2(jw)$ are not equivalent. Even though there are some familial relationships as outlined above, there are a large number of differences between the behavior of the

Table 4.1

Comparison of Calculated Rolloff Rates (db/decade) of Maximum and Minimum Singular Values - LQ Regulator and LQ Servo

	$\underline{R} = 10^6\,\underline{I}$	$\underline{R} = 10^8\,\underline{I}$	$\underline{R} = 10^{10}\,\underline{I}$	$\underline{R} = 10^{12}\,\underline{I}$	$\underline{R} = 10^{14}\,\underline{I}$	$\underline{R} = 10^{16}\,\underline{I}$
LQ Regulator						
Rolloff Rate for Maximum Singular Value	-20.05 (1 pole)	-33.88 (?)	-19.95 (1 pole)	-20.54 (1 pole)	-19.97 (1 pole)	-21.22 (1 pole)
Rolloff Rate for Minimum Singular Value	-39.29 (2 pole)	-20.20 (1 pole)	-37.5 (2 pole)	-39.42 (2 pole)	-40.0 (2 pole)	-39.03 (2 pole)
LQ Servo						
Rolloff Rate for Maximum Singular Value	40.0 (2 pole)	40.0 (2 pole)	40.0 (2 pole)	40.0 (2 pole)	40.0 (2 pole)	40.0 (2 pole)
Rolloff Rate for Minimum Singular Value	39.9 (2 pole)	40.0 (2 pole)	40.0 (2 pole)	40.0 (2 pole)	40.0 (2 pole)	39.9 (2 pole)

two transfer functions. The designer who modifies the LQ regulator for command following and disturbance rejection would be well advised to check his design by examining the calculated LQ servo singular values as a function of frequency.

E. CHAPTER SUMMARY

In this chapter, we have developed a specific numerical example, beginning with two parallel 3-state cascades, which, when interconnected and redrawn in state-space representation, provided us with a moderately complex base-case model.

After a brief look at this state-space model's open-loop dynamic behavior, we then devised and tested a series of six LQ regulators. These six LQ regulators were chosen to demonstrate a wide range of control actions by correspondingly wide choices of $\underline{R}$, the control weighting matrix.

We then compared the singular value plots for the LQ regulator and for the LQ servo. Based on these six test cases, a number of remarkable and unexpected behaviors were observed for the LQ servo.

We are now ready to develop some generalizations based on these specific cases and to summarize both the algebraic and the numerical analyses. These topics are developed in Chapter V, the concluding chapter of this work.

CHAPTER V

SUMMARY AND CONCLUSIONS

A. CHAPTER INTRODUCTION

In this chapter, we pull together all of the material in the previous chapters, so as to provide both a sense of perspective on past results and a sense of direction for future study.

The modification of the LQ regulator into the LQ servo is a vitally important ingredient in filling one of the last remaining voids in LQ theory for linear, time-invariant systems. It has been the goal of this work to at least begin some significant study of this unknown area. When the dynamic behavior of the LQ servo is completely understood, the control engineer can sit at a computer console and design systems correctly modified for command-following and disturbance rejection with a high degree of assurance that his designs will be stable, robust, and reliable.

B. SIGNIFICANT RESULTS

In Chapter I, we briefly outlined the historical developments of the mainstream of thought for linear quadratic control theory. At the same time, we addressed some of the major issues which have limited and continue to limit its application to real-world control problems. Indeed, much of the development work done over the last ten years has been directed toward solving some of these application problems.

Chapter II provided a mathematical basis for the remainder of the work. We illustrated the standard LQ formulation in a consistent set of notation and nomenclature. The singular value decomposition, together with some motivation for its use, was next developed.

The major topic of Chapter III was the LQ servo - a modified LQ regulator designed to include the real-world requirements of command following and output disturbance rejection. Once the LQ servo's basic structure had been described, we next attempted to develop theoretical techniques which would allow us to directly set the singular values of the LQ servo loop transfer function. The subsequent sections illustrated the value of complete algebraic analyses of some simple two-state and three-state LQ servos. In particular, we showed how the LQ regulator and the LQ servo will have similar dynamic structures, but with different pole and zero locations.

In Chapter IV, we developed a complete numerical example. We illustrated the state-space model itself and followed up with analyses of six test cases. Just as the results of Chapter III suggested, the displacement of the LQ servo open-loop eigenvalues from their LQ regulator position was small in all six cases. However, this result is strongly influenced by the structure of the $\underline{A}$ matrix, and should not be taken as a general result. LQ regulator and LQ servo singular value plots were next developed, and a number of unexpected behaviors were observed. Specifically, we saw how, to a remarkably high degree, the LQ servo tends to preserve the distance between the maximum and minimum singular values of the loop transfer function - at both low frequencies, and as the LQ servo singular values approach their ultimate - 40 db/decade roll-off rate.

C. DIRECTIONS FOR FUTURE STUDY

The following list is a compilation of the suggestions for future development that have arisen from this study:

1. All of this work has been directed toward continuous time systems. Before the LQ servo can be completely understood, it will be necessary to perform a companion study to this one for discrete time systems.
2. The LQ servo software described in this report was developed specifically for a very restricted class of systems - those with six states, two inputs, and two outputs. Perhaps the specific software described in Chapter IV could serve as a useful starting point for the development of more generalized routines.
3. The strong tendencies toward frequency independence demonstrated by the LQ servo should be investigated and exploited. In particular, if one could devise a means to squeeze the maximum and minimum singular values together at any one frequency, then the results of our six tests strongly suggest that the singular values would remain clustered at all frequencies, which would indeed be a valuable result for the control designer.

4. The limiting high-frequency roll-off behavior for the LQ regulator and the LQ servo is an area of control technology apparently in need of further development. Theoretical results which would allow the designer to reliably predict the ultimate high-frequency singular value behavior for multivariable control designs would be welcomed by the control community.

D. CHAPTER SUMMARY

We have developed a fairly complete description of LQ control theory as it applies in today's process control world. In addition, we have investigated in some detail an important extension of the previous theory - the LQ servo. We have also detailed a specific numerical example, and have uncovered several topics for additional future development work in this area.

At this point, the reader should have a fairly thorough and fundamental grasp of the current state of the art in modern control theory. The author thanks the reader for his interest and his time.

LIST OF REFERENCES

LIST OF REFERENCES

1. Bryson, A. E., Jr., "Some Connections Between Modern and Classical Control Concepts," ASME J. Dyn. Sys. Meas. Con., 101, 91 (1979).

2. Athans, M., "The Role and Use of the Stochastic Linear-Quadratic-Gaussian Problem in Control System Design," IEEE Trans. Auto. Con., AC-16, 529 (1971).

3. Athans, M., "The Discrete Time Linear-Quadratic-Gaussian Stochastic Control Problem," Ann. Econ. Soc. Meas., 1/4, 449 (1972).

4. Tomizuka, M., and D. M. Auslander, "About This Special Issue," ASME J. Dyn. Sys. Meas. Con., 101, 89 (1979).

5. Seborg, D. E., and D. G. Fisher, "Experience With Experimental Applications of Multivariable Computer Control," ASME J. Dyn. Sys. Meas. Con., 101, 108 (1979).

6. Edgar, T. F., and C. O. Schwanke, "A Review of the Application of Modern Control Theory to Distillation Columns," Proceedings of the JACC, 2, 1370 (1977).

7. Edgar, T. F., "Advanced Control Strategies for Chemical Processes: A Review," Chapter 4 in Computers Applied to Chemical Engineering, Ed. Squires, R. G., and G. V. Reklaitis, ACS Symposium Series, #124 (1980).

8. Pearson, R. K., "Modern Control: Why Don't We Use It?," In Tech, 47 (1984).

9. Ray, W. H., "Multivariable Process Control," Comp. and Ch.E., 7, 367 (1983).

10. Athans, M., and P. L. Falb, Optimal Control, McGraw-Hill, N.Y. (1966).

11. Sage, A. P., Optimum Systems Control, Prentice-Hall, N.J. (1968).

12. Bryson, A. E., Jr., and Y. C. Ho, Applied Optimal Control-Optimization, Estimation, and Control, Ginn, Waltham, Mass. (1969) [also John Wiley, N.Y. (1975) - revised printing].

13. Meditch, J. S., Stochastic Optimal Estimation and Control, McGraw-Hill, N.Y. (1969).

14. Anderson, B. D. O., and J. B. Moore, Linear Optimal Control, Prentice-Hall, N.J. (1971).

15. Kwakernaak, H., and R. Sivan, Linear Optimal Control Systems, Wiley-Interscience, N.Y. (1972).

16. Horowitz, I. M., Synthesis of Feedback Systems, Academic Press, N.Y. (1963).

17. Chen, C. T., Introduction to Linear Systems Theory, Holt Rinehart Winston, N.Y. (1970).

18. Saucedo, R., and E. E. Schiring, Introduction to Continuous and Digital Control Systems, Macmillan, N.Y. (1968).

19. Brogan, W. L., Modern Control Theory, Quantum Publishers, N.Y. (1974).

20. Kailath, T., Linear Systems, Prentice-Hall, N.J. (1980).

21. Gelb, A. (ed), Applied Optimal Estimation, MIT Press, Cambridge, Mass. (1974).

22. Jazwinski, A. H., Stochastic Processes and Filtering Theory, Academic Press, N.Y. (1970).

23. Bierman, A. B., Factorization Methods for Discrete Sequential Estimation, Academic Press, N.Y. (1977).

24. Sinha, N. K., and B. Kuszta, Modeling and Identification of Dynamic Systems, Van Nostrand, Reinhold, N.Y. (1983).

25. Brown, R. G., Introduction to Random Processes and Kalman Filtering, Wiley, N.Y. (1983).

26. Maybeck, Peter S., Stochastic Models, Estimation, and Control, Academic Press, N.Y. (1979).

27. Pontryagin, L. S., V. Boltyanskii, R. Gamkrelidze, and E. Mishchenko, The Mathematical Theory of Optimal Processes, Interscience, N.Y. (1962).

28. Bellman, R., Dynamic Programming, Princeton University Press, Princeton, N.J. (1957).

29. Kalman, R. E., "A New Approach to Linear Filtering and Prediction Problems," Trans. ASME Series D, J. Basic Eng., 82, 35 (1960).

30. Kalman, R. E., and R. S. Bucy, "New Results in Linear Filtering and Prediction Theory," Trans. ASME Series D, J. Basic Eng., 83, 95 (1961).

31. Kalman, R. E., and R. W. Koepcke, "Optimal Synthesis of Linear Sampling Control Systems Using Generalized Performance Indices," Trans. ASME Series D, J. Basic Eng., 80, 1820 (1958).

32. Joseph, P. D., and J. T. Tou, "On Linear Control Theory," Trans. AIEE (Appl. and Industry), 80, 193 (1961).

33. Gunckel, T. L., II, and G. F. Franklin, "A General Solution for Linear, Sampled Data Control," Trans. ASME Series D, J. Basic Eng., 85, 197 (1963).

34. Sandell, N. R., Jr., D. P. Looze, et al., LQGALPHA-User's Manual, Alphatech, Burlington, Mass. (1984).

35. Slater, G. L., "Perturbation Analysis of Optimal Integral Controls," ASME J. Dyn. Sys. Meas. Con., 106, 114 (1984).

36. Willsky, A. S., "A Survey of Design Methods for Failure Detection in Dynamic Systems," Automatica, 12, 601 (1976).

37. Harvey, C. A., "On Feedback Systems Possessing Integrity With Respect to Actuator Outages," in Recent Developments in the Robustness Theory of Multivariable Systems, N. R. Sandell, Jr. (ed.), LIDS Report LIDS-R-954, MIT, Cambridge, Mass. (1979).

38. Lehtomaki, N. A., N. R. Sandell, Jr., and M. Athans, "Robustness Results in Linear-Quadratic Gaussian Based Multivariable Control Designs," IEEE Trans. Auto. Con., AC-26, 75 (1981).

39. Wong, P. K., and M. Athans, "Closed-Loop Structural Stability for Linear-Quadratic Optimal Systems," IEEE Trans. Auto. Con., AC-22, 94 (1977).

40. Rosenbrock, H. H., and P. D. McMorran, "Good, Bad, or Optimal?," IEEE Trans. Auto. Con., AC-16, 552 (1971).

41. Wong, P. K., "On the Interaction Structure of Multi-Input Feedback Control Systems," M.S. Thesis, MIT, Cambridge, Mass. (1975).

42. Athans, M., "Model Based Compensators for Multivariable Control Synthesis and the LQG Algorithms - 6232/820308," "Model Based Compensators (MBC) and the Loop Transfer Recovery (LTR) Method - 6232/840404," "The Kalman Filter - 6232/830405," "How to Adapt LQ Regulator Designs to Command-Following and Output-Disturbance Rejection Feedback Control Systems - 6232/840418" course notes for MIT summer session on Multivariable Control System Design (1984).

43. MacGregor, J. F., "Optimal Discrete Stochastic Control Theory for Process Application," Can. J. Chem. Eng., 51, 468 (1973).

44. Makila, P. M., T. Westerlund, and H. T. Toivonen, "Constrained Linear Quadratic Gaussian Control With Process Applications," Automatica, 20, 15 (1984).

45. Toivonen, H. T., "Minimum Variance Control of First-Order Systems With a Constraint on the Input Amplitude," IEEE Trans. Auto. Con., AC-26, 556 (1981).

46. Toivonen, H. T., "Suboptimal Control of Discrete Stochastic Amplitude Constrained Systems," Int. J. Con., 37, 493 (1983).

47. Ross, D. W., and I. Flugge-Lotz, "Optimal Control of Systems Described by Differential Equations," Technical Report #177, Stanford University, Division of Engineering Mechanics (1967).

48. Larson, R. E., and C. H. Wells, "Combined Optimum Control and Estimation of Serial Systems With Time Delay," Proceedings of the JACC, Boulder, Colorado, 23 (1969).

49. Kwakernaak, H., "Optimal Filtering in Linear Systems With Time Delays," IEEE Trans. Auto. Con., AC-12, 169 (1967).

50. Ogunnaike, B. A., and W. H. Ray, "Incomplete State Feedback for Time Delay Systems: Observer Applications in Multidelay Compensation," AIChE Journal, 30, 717 (1984).

51. Kwakernaak, H., "Asymptotic Root Loci for Multivariable Linear Optimal Regulators," IEEE Trans. Auto. Con., AC-21, 378 (1976).

52. Harvey, C. A., and G. Stein, "Quadratic Weights for Asymptotic Regulator Properties," IEEE Trans. Auto. Con., AC-23, 378 (1978).

53. Stein, G., "Generalized Quadratic Weights for Asymptotic Regulator Properties," IEEE Trans. Auto. Con., AC-24, 559 (1979).

54. Moore, B. C., "On the Flexibility Offered by State Feedback in Multivariable Systems Beyond Closed Loop Eigenvalue Assignment," IEEE Trans. Auto. Con., AC-21, 689 (1976).

55. Francis, B. A., "The Optimal Linear-Quadratic Time-Invariant Regulator With Cheap Control," IEEE Trans. Auto. Con., AC-24, 616 (1979).

56. Kawasaki, N., and E. Shimemura, "Determining Quadratic Weighting Matrices to Locate Poles in a Specified Region," Automatic, 19, 557 (1983).

57. Gopal, M., and P. Pratapachandran, "Sensitivity-reduced Optimal Discrete Regulator With Prescribed Closed-Loop Eigenvalues," IEE Proceedings Part D, 132, 18 (1985).

58. Rosenbrock, H. H., "Design of Multivariable Control Systems Using the Inverse Nyquist Array," Proc. IEE, 116, 1929 (1969).

59. MacFarlane, A. G. J., and I. Postlethwaite, "The Generalized Nyquist Stability Criterion and Multivariable Root Loci," Int. J. Con., 25, 81 (1977).

60. Zames, G., "On the Input-Output Stability of Time-Varying Non-linear Feedback Systems. Part I: Conditions Using Concepts of Loop Gain, Conicity, and Positivity," IEEE Trans. Auto. Con., AC-11, 228 (1966).

61. Zames, G., "On the Input-Output Stability of Time-Varying Non-linear Feedback Systems. Part II: Conditions Involving Circles in the Frequency Plane and Sector Nonlinearities," IEEE Trans. Auto. Con., AC-11, 465 (1966).

62. Safonov, M. G., Stability and Robustness of Multivariable Feedback Systems, MIT Press, Cambridge, Mass. (1980).

63. Safonov, M. G., A. J. Laub, and G. L. Hartmann, "Feedback Properties of Multivariable Systems: The Role and Use of the Return Difference Matrix," IEEE Trans. Auto. Con., AC-26, 47 (1981).

64. Doyle, J. C., "Robustness of Multiloop Linear Feedback Systems," Proc. 1978 IEEE Conf. on Decision and Control, 12 (1978).

65. Doyle, J. C., and G. Stein, "Robustness With Observers," IEEE Trans. Auto. Con., AC-24, 607 (1979).

66. Doyle, J. C., and G. Stein, "Multivariable Feedback Design: Concepts for a Classical/Modern Synthesis," IEEE Trans. Auto. Con., AC-26, 4 (1981).

67. Lehtomaki, N. A., "Practical Robustness Measures in Multivariable Control Systems Analysis," Ph.D. Thesis, MIT, Cambridge, Mass. (1981).

68. Kappos, E., "Robust Multivariable Control for the F100 Engine," M.S. Thesis, MIT, Cambridge, Mass. (1983).

69. Athans, M., P. Kapasouris, E. Kappos, and H. Austin Spang, III, "Multivariable Control for the F100 Engine Using the LQG/LTR Methodology," AIAA Guid. Con. Conf., Seattle Wash. (1984).

70. Kapasouris, P., "Gain-Scheduled Multivariable Control for the GE-21 Turbofan Engine Using the LQR and LQG/LTR Methodologies," M.S. Thesis, MIT, Cambridge, Mass. (1984).

71. Pfeil, W. H., "Multivariable Control for the GE T700 Engine Using the LQG/LTR Design Methodology," M.S. Thesis, MIT, Cambridge, Mass. (1984).

72. Bergh, L. G., and J. F. MacGregor, "Robustness of Linear-Quadratic Controllers," 34th Canadian Chem. Eng. Conf. (1984).

73. Garcia, C., and M. Morari, "Internal Model Control. I: A Unifying Review and Some New Results," Ind. Eng. Chem. Proc. Des. Dev., 21, 308 (1982).

74. Moore, B. C., "Principal Component Analysis in Linear Systems: Controllability, Observability, and Model Reduction," IEEE Trans. Auto. Con., AC-26, 17 (1981).

75. Klema, V. C., and A. J. Laub, "The Singular Value Decomposition: Its Computation and Some Applications," IEEE Trans. Auto. Con., AC-25, 164 (1980).

76. Golub, G. H., and C. Reinsch, "Singular Value Decomposition and Least Squares Solutions," Numer. Math., 14, 403 (1970).

77. Stewart, G. W., Introduction to Matrix Computations, Academic Press, N.Y. (1973).

78. Forsythe, G. E., and C. B. Moler, Computer Solution of Linear Algebraic Systems, Prentice-Hall, N.J. (1967).

79. Forsythe, G. E., M. A. Malcolm, and C. B. Moler, Computer Methods for Mathematical Computations, Prentice-Hall, N.J. (1977).

80. Lawson, C. L., and R. J. Hanson, Solving Least Squares Problems, Prentice-Hall, N.J. (1974).

81. Nyquist, H., "Regeneration Theory," Bell Syst. Tech. J. (1932).

82. Bode, H. W., Network Analysis and Feedback Amplifier Design, Van Nostrand, N.J. (1945).

83. Kuo, B. C., Automatic Control Systems (2nd ed.), Prentice-Hall, N.Y. (1967).

84. Noble, B., and J. W. Daniel, Applied Linear Algebra (2nd ed.), Prentice-Hall, N.Y. (1977).

85. Kalman, R. E., "When is a Linear System Optimal?," Trans. ASME Series D, J. Basic, Eng., 86, 51 (1964).

86. Safonov, M. G., and M. Athans, "Robustness and Computational Aspects of Nonlinear Stochastic Estimators and Regulators," IEEE Trans. Auto. Con., AC-23, 717 (1978).

87. Doyle, J. C., "Guaranteed Margins for LQG Regulators," IEEE Trans. Auto. Con., AC-23, 756 (1978).

88. Bryson, A. E., "Random Problems in Control Theory," Stanford University, Rep. SUDAAR 447 (1972).

89. Kwakernaak, H., "Optimal Low-Sensitivity Linear Feedback Systems," Automatica, 5, 279 (1969).

90. Kwakernaak, H., and R. Sivan, "The Maximally Achievable Accuracy of Linear Optimal Regulators and Linear Optimal Filters," IEEE Trans. Auto. Con., AC-17, 79 (1972).

91. Joseph, B., and C. B. Brosilow, "Inferential Control of Processes," AIChE J., 24, 485 (1978).

92. Garcia, C. E., and M. Morari, "Internal Model Control. I: A Unifying Review and Some New Results," Ind. Eng. Chem. Proc. Des. Dev., 21, 308 (1982).

VITA

James Edward Doss was born in Roanoke, Virginia, on May 24, 1948. He attended elementary schools in that city and was graduated from Patrick Henry High School in 1966. The following September, he entered Virginia Polytechnic Institute where he graduated in June 1970 with a Bachelor of Science degree in chemical engineering.

After a period of active duty in the Marine Corps, he entered The University of Tennessee, Knoxville, in January 1971 and received the Master of Science degree with a major in chemical engineering in August 1973. Upon receiving the Doctor of Philosophy degree in chemical engineering in August 1974, he began employment with Tennessee Eastman Company in Kingsport, where he currently serves as Manager, Control Systems Engineering Department. He received the Master of Science degree in electrical engineering in December 1985.

He is married to the former Marian Joyce Jones, and they are the parents of two lovely children.